

NORTHWESTERN UNIVERSITY

Peptoids as Monodisperse, Multivalent Scaffolds for End-Labeled Free-Solution Electrophoresis (ELFSE) and Magnetic Resonance Imaging (MRI)

A DISSERTATION

SUBMITTED TO THE GRADUATE SCHOOL
IN PARTIAL FULFILLMENT OF THE REQUIREMENTS

for the degree

DOCTOR OF PHILOSOPHY

Field of Chemistry

By

Russell Dean Haynes

EVANSTON, ILLINOIS

June 2008

© Copyright by Russell Dean Haynes 2008
All rights reserved

ABSTRACT

Peptoids as Monodisperse, Multivalent Scaffolds for End-Labeled Free-Solution Electrophoresis (ELFSE) and Magnetic Resonance Imaging (MRI)

Russell Dean Haynes

The need for readily synthesized scaffold architectures to build monodisperse, high molar mass mobility modifiers or “drag-tags” in end-labeled free solution electrophoresis (ELFSE) led to the development of a novel class of multivalent molecular tools. Poly-*N*-substituted glycines (peptoids) were created with evenly spaced amino groups as branching points along the scaffold backbone. These molecules are comprised primarily of poly-*N*-(methoxyethyl)glycine (*N*meg) residues, as this side chain imparts many favorable properties such as water solubility, ease of synthesis in good yield and purity, and high chemical stability.

The initial scaffold design allowed for the attachment of five carboxylate-terminated branches of varying lengths *via* peptide bond forming reactions. Optimization of conditions and reagents resulted in near quantitative yield and complete grafting at all five reaction sites. Most importantly, the product could be chromatographically purified to complete monodispersity, an essential criterion for an ELFSE drag-tag. Specifically, a 30mer poly(*N*meg) backbone with five amino (*N*-Lysine) groups was appended with tetramer- and octamer-*N*meg branches; these comb-like conjugates along with an unbranched 30mer (acetylated amino groups) were attached to short DNA primers and evaluated as drag-tags. The important result of this study was that electrophoretic “drag”

or “?” scaled somewhat linearly with molecular weight, demonstrating that increased mass is the key design parameter for this class of drag-tags.

The octamer-branched drag-tag was further employed in a number of other studies, including multiplexed genotyping, DNA modified at both ends, and as the first example of DNA sequencing using a completely synthetic molecule. In the latter case, the seventy-monomer peptoid sequenced 80-100 bases of DNA in 16 minutes, close to the result achieved using a native protein (streptavidin), which is roughly eight times larger.

A similar scaffold and synthetic strategy was further used to construct a multivalent contrast agent for magnetic resonance imaging (MRI). A molecule containing eight branching points for gadolinium ligands was successfully synthesized, metallated, and subsequent relaxivity values were calculated. The relaxivity value per gadolinium ion (Gd III) was $10.7 \text{ mM}^{-1} \text{ s}^{-1}$ at 60 MHz as indicated by inductively coupled plasma (ICP), which corresponded to a relaxivity of $86 \text{ mM}^{-1} \text{ s}^{-1}$ per fully derivatized molecule. This relatively high relaxivity value is impressive, especially given that the multivalency of the molecule will allow for the inclusion of additional functionalities that may make the contrast agent even more useful. Further study and syntheses of this class of multivalent molecules could potentially lead to drag-tags capable of sequencing hundreds of bases of DNA and contrast agents that possess therapeutic relevance. Such strategies are discussed in the final chapter.

Acknowledgements

I would like to thank my research advisor, Professor Annelise Barron, for her continuing assistance and support. Loyalty, perfection and hard work are things I have learned whilst working under Professor Barron's supervision, the ingredients for success in professional and personal life. My past and present committee members: Professors Frederick Lewis, Olke Uhlenbeck, Richard Silverman, and Michael Wasielewski, who have all offered support and many great ideas. I am honored to have had the opportunity to interact with such great scientists.

Thank you to past and present Barron lab members for making the lab a fun and interesting place to work, especially to Dr. Robert J. Meagher, with whom I was fortunate to work closely with on the ELFSE project. Special thanks go to Professors Gary Slater and Jong-In Won, Jennifer Coyne, and Jennifer Lin, who are also on the ELFSE project and have helped me a lot both practically and intellectually. I would also like to thank my collaborators, Professor Tom Meade, Dr. Steve Bull and Lindsey Karfeld for their assistance with the development of the peptoid-based MRI contrast agents.

I am lucky to have incredibly supportive parents: my Mum and Roger and my Dad and Ann who have always been there for me. Most of all I need to extend thanks to my wife Binh, who has been both my partner and my cheerleader in this endeavor, every step of the way. And finally, I need to thank our two wonderful children Azura and Redmond, who just by being themselves are an endless source of inspiration.

Table of Contents

ABSTRACT	3
Acknowledgements	5
List of Figures, Tables, and Schemes	10
Chapter 1. Multivalent scaffolds – Background and significance	15
1.1 Multivalent inspiration.....	15
1.2 Multivalent scaffold selection.....	16
1.3 Multivalent architectures.....	17
1.4 Linear polyfunctional (multivalent) scaffolds.....	19
1.5 Peptidomimetics.....	19
1.6 Poly- <i>N</i> -substituted glycines or “peptoids”.....	20
1.7 End-labeled free-solution electrophoresis (ELFSE)	24
1.8 Magnetic resonance imaging (MRI) contrast agents	28
1.9 Challenges addressed in the present work	31
Chapter 2. Comb-like, monodisperse polypeptoid drag-tags for DNA separations by end-labeled free-solution electrophoresis (ELFSE)	32
2.1 Introduction.....	33
2.2 Experimental.....	42
2.2.1 General methods and materials	42
2.2.2 Reversed-phase high-performance liquid chromatography (RP-HPLC).....	42
2.2.3 Polypeptoid “backbone” (Compound 1).....	43
2.2.4 Tetramer “branch” (Compound 2)	44
2.2.5 Octamer “branch” (Compound 3).....	45
2.2.6 Backbone acetylation (Compound 4).....	45

2.2.7	Backbone grafting reactions (Compounds 5 & 6)	45
2.2.8	Sulfo-SMCC conjugation.....	49
2.2.9	Preparation of PCR products	50
2.2.10	Free-solution capillary electrophoresis	52
2.3	Results and discussion	53
2.3.1	Branched drag-tag design and synthesis	53
2.3.2	Backbone synthesis	55
2.3.3	Branch syntheses.....	57
2.3.4	Grafting of oligomeric branches to the polymeric backbone	60
2.3.5	Sulfo-SMCC activation.....	63
2.3.6	DNA reduction and conjugation to polypeptoids	63
2.3.7	Free-solution capillary electrophoresis analysis of DNA–drag-tag conjugates and the determination of α values.....	64
2.3.8	Separation of PCR products	70
2.4	Conclusions	75
Chapter 3. Theoretical and practical uses of high molar mass branched drag-tags		
76		
3.1	Applications for branched drag-tags in ELFSE studies	76
3.2	Free-solution electrophoresis of DNA modified with drag-tags at both ends ..	77
3.2.1	Introduction.....	78
3.2.2	Theory of end-effects in ELFSE	80
3.2.3	Materials and methods	85
3.2.4	Results – analysis of dsDNA conjugates	89
3.2.5	Discussion.....	95

3.3	Multiplexed p53 mutation detection by free-solution conjugate capillary and microchannel electrophoresis with polyamide drag-tags.....	98
3.4	Conclusions	104
Chapter 4. ELFSE DNA sequencing using a chemically synthesized drag-tag.. 105		
4.1	Introduction.....	105
4.1.1	Background	105
4.1.2	Theoretical analysis	107
4.2	Experimental procedures.....	110
4.2.1	Drag-tag-DNA conjugation.....	110
4.2.2	Sequencing reaction.....	110
4.3	Results and discussion	111
4.3.1	Capillary electrophoresis.....	111
4.3.2	Calculation of ?	115
4.4	Conclusions	118
Chapter 5. Multivalent, high relaxivity magnetic resonance imaging (MRI) contrast agents..... 119		
5.1	Magnetic resonance imaging (MRI).....	119
5.1.1	Background, contrast, and relaxivity	119
5.1.2	Gadolinium-based (GdIII) contrast agents – parameters for optimization	122
5.1.3	Current status of multivalent Gd(III) contrast agents	125
5.1.4	Multivalent Gd(III) contrast agents based on peptoid scaffold architectures	126
5.2	Experimental.....	127
5.2.1	Materials	127
5.2.2	Reversed-phase high-performance liquid chromatography (RP-HPLC)...	127

5.2.3	Synthesis of Gd(III) chelating ligand: pentanoic acid DO3A (Compound 1) 128	
5.2.4	Polypeptoid “backbone” synthesis (Compounds 2 and 4).....	131
5.2.5	Grafting reactions (Compounds 3 and 5).....	132
5.2.6	Deprotection and metallation with GdCl ₃ (Compound 6)	134
5.2.7	Relaxivity determination.....	134
5.3	Results and Discussion	135
5.3.1	Initial scaffold with two DO3A attachment sites.....	135
5.3.2	Subsequent 8-site 30mer scaffold design.....	136
5.3.3	Relaxivity data	139
5.4	Conclusions	140
Chapter 6.	Additional drag-tag designs, progress, and future directions	142
6.1	Hydroxy drag-tags.....	142
6.1.1	Rationale for use of a new, extremely hydrophilic drag-tag side chain in peptoid scaffold sequences.....	142
6.1.2	Hydroxy side chain design and synthesis	143
6.2	Positively-charged drag-tags.....	147
6.2.1	Rationale for including charge in drag-tag design	147
6.2.2	Drag-tag synthesis and preliminary results	148
6.3	Larger drag-tag designs.....	154
6.3.1	Doubling the size of the octamer-branched drag-tag.....	154
References.....	158
Appendix A	169

List of Figures, Tables, and Schemes

Figure 1.2 a) Peptide and peptoid structures and b) submonomer method for solid-phase peptoid synthesis	23
Figure 1.3 Drag-tag DNA conjugate structure [65].	26
Table 2.1. <i>N</i> -Substituted glycine (peptoid) side chains.	38
Scheme 2.1 The sub-monomer solid-phase polypeptoid synthesis protocol. Structure is predominantly poly- <i>N</i> -methoxyethyl glycine (<i>N</i> meg) residues with five evenly spaced <i>N</i> -aminobutyl (<i>N</i> abg) monomers included within. The final structure of “backbone” is shown with amino attachment sites deprotected.	40
Scheme 2.2 Chemical structures of the tetramer (a) and octamer (b) “branches.” They are oligo- <i>N</i> -methoxyethyl glycine (<i>N</i> meg) peptoids with reactive terminal glutamic acid residues.	41
Scheme 2.3 Solution-phase coupling protocol for the synthesis of branched and unbranched drag-tags (4-6) via grafting of oligopeptoids onto the backbone molecule (1).	47
Figure 2.1. MALDI-TOF data. Mass spectrometry was done at the Analytical Services Laboratory at Northwestern University ? -cyano-4-hydroxycinnamic acid (ACCA) as the matrix. Resulting spectra and lists of the major peaks for the Fmoc-protected drag-tag molecules (4-6) are given below:	48
Table 2.2 Oligonucleotide sequences used as primers for PCR products of 50, 75, 100, and 150 bp. In the forward primer sequence, X1 refers to a 5' thiol linker (C6 disulfide), and X2 refers to an internal fluorescein-dT base.	51
Table 2.3 Peptoid structures, molecular mass confirmation and crude purities.	56
Figure 2.2 RP-HPLC chromatogram of the crude products of the grafting reaction between the tetramer branches (2) and the backbone molecule (1). HPLC: C18 250 mm Vydac column, 58 °C, with 10-60% acetonitrile–water (0.1 % TFA) over 50 minutes.	59
Table 2.4 Drag-tag structures, molecular mass confirmation and alpha (?) values.	62
Figure 2.3 Free-solution capillary electrophoresis analysis of 20-base fluorescently labeled oligonucleotide conjugated to (a) an “unbranched” or acetylated 30mer drag-tag (4), (b) a tetramer-branched drag-tag (5), and (c) an octamer-branched drag-tag (6). Separations were carried out on a BioRad BioFocus capillary electrophoresis instrument at 40°C. The running buffer was 50 mM Tris, 50 mM TAPS, 2 mM	

EDTA, 7 M urea, pH 8.5, mixed with a 3% (v/v) aqueous dilution of a POP5 solution as a wall coating agent. The fused silica capillary had an inner diameter of 25 μm , and a total length of 25 cm (20.6 cm inlet to detector). Samples were introduced by hydrodynamic injection with a pressure-time constant of 5 psi*sec. The electric field was 10 kV (400 V/cm), with a typical current of 2.8 μA . The fluorescent label was excited at 488 nm, with emission detected at 520 nm. 67

Figure 2.4 Free-solution capillary electrophoresis analysis of 30-base fluorescently labeled oligonucleotide conjugated to acetylated, tetramer-branched, and octamer-branched drag-tags. Separations were carried out on a BioRad BioFocus capillary electrophoresis instrument at 40°C. Conditions similar to Figure 3. The SMCC-activated drag-tags were reacted with freshly reduced 5'-thiolated 30-base DNA primers. 68

Figure 2.5 Plot of hydrodynamic drag or “ ζ ” against molecular weight for the 20-base and 30-base DNA–drag-tag conjugates (for all three drag-tags, 4-6)..... 69

Figure 2.6 a). ELFSE separation of 50-, 75-, 100- and 150-base PCR products (and residual DNA impurities) conjugated to the octamer-branched drag-tag. Samples were denatured in formamide prior to injection. Analysis was performed in free solution on an ABI Prism 3100 instrument with a 36-cm long capillary array (55 μm i.d. capillaries) at 55°C. The buffer was 50 mM Tris, 50 mM TAPS, 2 mM EDTA, 7 M urea, pH 8.5, mixed with a 3% (v/v) aqueous dilution of a POP5 solution as a wall coating agent. An electrokinetic injection of ~ 22 V/cm for 2 seconds was used. The electric field during the run was ~ 320 V/cm, with a typical current of ~ 8.5 μA per capillary. The inset is a plot of $(\mu_0/\mu - 1)$ for each of the major peaks, versus the number of DNA bases N (4). b) Analysis of the reduced, thiolated PCR products (from the same reaction as part (a)) on an Agilent 2100 Bioanalyzer, using the DNA 1000 sizing kit. Each sample lane includes 15 bp and 1500 bp markers. 73

Table 3.1 Structures and code names for the six different dragtag molecules used in this study. P1–169 and P2–127 drag-tags had maleimide functionalites added to their N-termini by activation with sulfosuccinimidyl 4-N-maleimidomethyl cyclohexane-1-carboxylate (Sulfo-SMCC), as described in [22]. 84

Table 3.2 Oligonucleotides used as PCR primers for producing dsDNA conjugates with drag-tags at one or both ends. 88

Figure 3.1 Example electropherograms of dsDNA conjugated to a drag-tag. (A) 100-bp PCR product with forward primer thiolated, (B) 100-bp PCR product with both primers thiolated, (C) 200-bp PCR product with forward primer thiolated, and (D) 200-bp PCR product with both primers thiolated. Analysis conditions were the same as Fig. 2, except the run temperature was 25 °C and the injection was 1 kV for 20 s. Peaks labeled 0, 1, and 2 refer to DNA species with zero, one, or two drag-tags, respectively. 93

- Table 3.3 Apparent frictional parameter a for dsDNA with one or two drag-tags, averaged for all sizes of DNA..... 94
- Table 3.4. Design of primers for multiplexed SBE-FSCE. The branched, polyNmeg peptoid is conjugated to exon 5, locus 144-1..... 101
- Figure 3.2. Four-color electropherogram showing the FSCE separation of the products of a 16plex SBE genotyping reaction with a wildtype p53 template. Separations were performed in free aqueous solution on an ABI 3100 CE instrument using a capillary array with an effective length of 36 cm. The buffer was 89 mM Tris, 89 mM TAPS, 2 mM EDTA with 7 M urea. The run temperature was 55 °C. Samples were injected electrokinetically at 44 V/cm for 20 s. The field strength for the separation was 312 V/cm, with a current of 11 μ A per capillary. Each peak is labeled with the corresponding p53 locus and genotype. 102
- Figure 3.3. (A,B) Four-color FSCE electropherograms showing the analysis of 16plex SBE reactions using PCR amplicons of two different p53 variants as templates, with the mutated loci highlighted, including two heterozygotes confirmed by re-sequencing of the mutant template in (B). Separation conditions are the same as described for Figure 1. 103
- Table 4.1. Peptoid drag-tag structure and properties including the experimental sequencing results and theoretical prediction using Equation (2). In the branch portion of the drag-tag chemical structure, *N*-(methoxyethyl)glycine peptoid residues are abbreviated as “NMEG.” 109
- Figure 4.1 Four-color DNA sequencing performed using an M13 sequencing primer linked to the octamer-branched polypeptoid drag-tag. The ABI SNaPshot kit was used, with different amounts of dNTPs added to generate different sequencing read lengths. In (A), no dNTPs were added, giving a single-base extension. In (B) and (C), 20 μ M and 200 μ M of each dNTP were used, generating a short (B) or longer (C) read. Separations were performed with the ABI 3100, with injections performed at 1 kV for 10 or 30 seconds. 113
- Figure 4.2 4-color sequencing electropherogram obtained with 70mer branched drag-tag, with manual base calls of the M13mp18 sequence. The DNA fragment sizes (M_c) are shown at the top of each panel, and a red “X” around $M_c = 52$ bases marks an unexpected “G” peak. For purposes of presentation, the “C” and “T” signals have been scaled by a factor of 2 to give peak heights comparable to the “G” and “C” traces, and the data has been smoothed to reduce high-frequency noise, possibly due to a small bubble in the fluid path. 114
- Figure 4.3 A fit of experimentally measured mobilities (μ_0/μ) versus DNA fragment size $1/M_c$, according to a rearranged version of Equation (1), with a slope of $\gamma = 18.0$ for the octamer-branched drag-tag. Different symbols are used to represent fragments

with G, C, A, or T terminations, which reveals no terminator-specific deviation from model behavior.....	117
Figure 5.1 Gd(III) chelators DOTA and DO3A, where DO3A allows for the chelator to be attached to a macromolecular structure as a pendant group.....	124
Scheme 5.1 Synthesis of Gd(III) Chelator pentanoic acid DO3A (Compound 1). Hydrogenation-labile deprotection was used to reveal the reactive carboxylic acid group for further reaction with amino groups on multivalent scaffolds. Once grafting is complete the acid-labile tert-butyl groups can be removed allowing for Gd(III) chelation.	130
Scheme 5.2. To test the possibility of densely grafting DO3A pentanoic acid chelators onto a polyNmeg peptoid scaffold, Compound 2 was synthesized. 2.1 Equivalents of Compound 1 were used along with 2.5 Eq PyBroP and DIEA in dry NMP.	133
Scheme 5.3 Modified version of previously published grafting protocol.	137
Scheme 5.4 Deprotection of the DO3A side-chains followed by metalation using GdCl ₃	138
Scheme 6.1. Synthesis of 22-mer polyNmeg/hydroxy drag-tag using TBS-protected 2-(2-Aminoethoxy)ethanol as a peptoid submonomer.	145
Figure 6.1 MALDI-TOF/MS and analytical RP-HPLC trace of Compound 3.....	146
Figure 6.2. Schematic representation of 30-mer drag-tag design with five octamer branches containing positive charges near to the branching junction on the peptoid scaffold backbone.	148
Figure 6.3 a) Compound 4 is a positively charged octamer “branch.” The design included a Boc-protected short ethylamino group (in red) and was acetylated at the <i>N</i> -terminus. The terminal glutamic acid residue had an unprotected carboxylate group (in blue) that served as the peptide bond-forming functionality. b) Compound 5 represents the molecule that was actually isolated due to poor quality acetic anhydride that was used in the penultimate synthesis step prior to cleavage from the solid-phase resin.	151
Scheme 6.2. Synthesis of a 5+ and 10+ branched drag-tag following literature grafting procedures.	152
Figure 6.4 MALDI-TOF/MS spectra of Compounds 5 and 6. The trifluoroacetic acid in the MALDI matrix solution resulted in varying degrees of the acid-labile Boc-protecting group deprotection.	153

Figure 6.5. Structure of 15mer polyNmeg “branch” for attachment to an 8-site 30mer scaffold..... 156

Figure 6.6 Analytical RP-HPLC trace of 15mer polyNmeg “branch.” So far 300mg of this pure material has been amassed for further attachment to 30mer polyNmeg scaffold. Phenomenex Jupiter analytical (150 mm × 2 mm, 5 μm, 300 Å) C18 column, conditions: 5-40% Acetonitrile/water (0.1% TFA) over 50minutes. Black trace is 220nm absorbance and blue trace is 260nm. 157

Chapter 1. Multivalent scaffolds – Background and significance

1.1 Multivalent inspiration

Macromolecular structures that are multivalent typically have multiple functionalities and branching points that can be exploited for a myriad of different uses and applications. Allowing for the display or attachment of pendant groups greatly increases a macromolecule's usefulness as a diagnostic tool or therapeutic device. These appendages could be biologically active, or they may provide imaging, separation, solubility improvements, or increases in molar mass, as presented in this dissertation.

Nature uses multivalent arrangements of ligands to achieve affinity and selectivity for the corresponding receptors. This facet is of crucial importance in many biological processes, such as recruitment of leukocytes during inflammation, cancer progression and metastasis, embryogenesis, etc [1]. These examples have inspired new multivalent synthetic systems that aim to understand and intervene in biological processes at the molecular level.

Proteins commonly possess numerous functional groups that are keys to their uses biologically. Synthetic mimicry of natural proteins and enzymes is one of the most exciting and challenging pursuits in modern science. The literature in this field focuses mainly on mimicking secondary and tertiary structures found in native molecules [2-5]. A more facile approach to incorporating different functions into single molecule typically involves the use of a simple scaffold type backbone to which functional appendages may

be attached. Applying the idea of a multivalent model to problems in a wide range of scientific research fields offers potential solutions that are embodied in a single drug or molecular tool. For instance, a multivalent drug delivery system might entail using a scaffold with branches that can a) solubilize b) target and c) deliver a drug to a specific site. This system might entail appending a solubilizing group, thereby facilitating the use of sparingly soluble active molecules, and then a targeting group, to get the molecule in the desired target vicinity, and then a cleavable linker, so that the drug may be released and delivered at the target site.

The coupling of low molecular-weight anticancer drugs to polymers through a cleavable linker has been an effective method for improving the therapeutic index of clinically established agents, and the first candidates of anticancer drug-polymer conjugates are being evaluated in clinical trials. Other systems may simply require control over the chemistry in such a way that multiple different groups can be added to enhance the usefulness and characterizability of a given diagnostic molecule or probe. An example of this is a macromolecular MRI contrast agent that must include at least one paramagnetic metal center, a fluorescent dye, and possibly other targeting moieties.

1.2 Multivalent scaffold selection

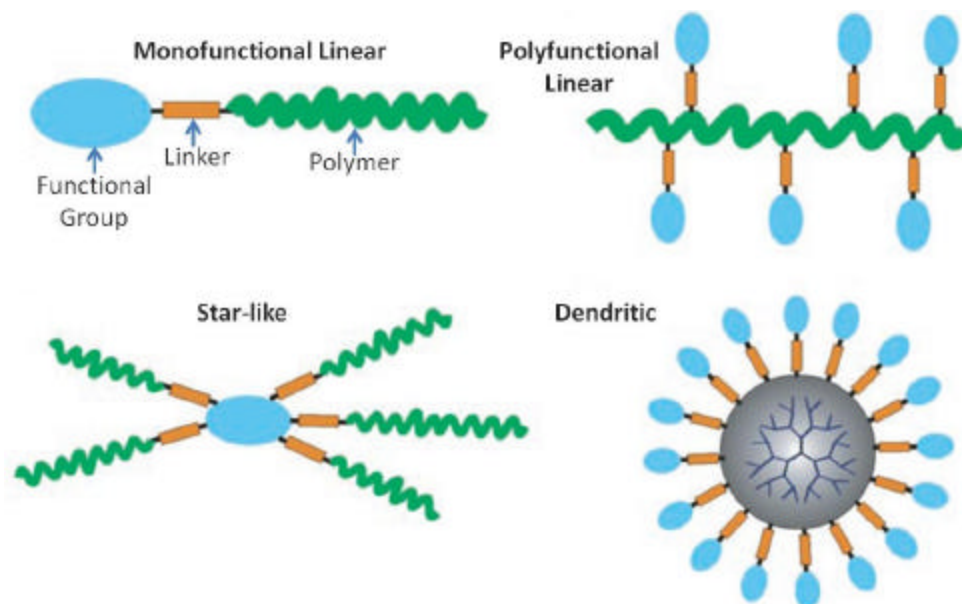
Functional groups such as targeting moieties, fluorescent tags, and solubilizing agents vary widely based on the desired application. The properties of a multivalent scaffold are dictated by the functional groups needed for a given application. Most scaffolds can be described at least in part as being polymers of some kind, whether they

are native molecules such as proteins and viruses, polysaccharides, synthetic peptides and peptidomimetics, or synthetic polymers. Narrowing this list down, only peptidomimetics and synthetic polymers offer both ease of synthesis and complete control over chemical design and diversity of function.

1.3 Multivalent architectures

Figure 1 shows a simplified view of the spectrum of scaffolds for the synthesis of multivalent molecules, including A) monofunctional linear, B) polyfunctional linear, C) star-like, and D) dendritic structures which are all currently being investigated [6]. In each example, the functional group, linker, and polymer portions of these molecules could be any number of a wide range of chemical species. These general architectures represent the main choices at the disposal of the chemist wishing to design multivalent macromolecular conjugates. Although all examples are viable options, the linear polyfunctional scaffold offers many desirable qualities. Firstly, the design allows for complete control over the backbone length and the number of branching points. Secondly, orthogonally protected side chains can be incorporated, thereby increasing the number of different functionalities possible for incorporation. A drawback of monofunctional linear designs is that transformations may only occur at one end of the molecule. With the other architectures, it is commonly quite difficult to isolate completely monodisperse products. This is due to the exponential increases in grafting sites with dendrimers as well as grafting densities, particularly with the star-like examples, resulting in steric repulsions that work against complete derivatization of the core unit.

Figure 1.1 Reproduced in part and adapted from a recent review by Haag *et al* [6]. The figure illustrates A) linear, B) polyfunctional linear, C) star-like, and D) dendritic architectures.



1.4 Linear polyfunctional (multivalent) scaffolds

Both peptides/peptidomimetics and synthetic polymers have excellent types of synthetic strategies to create linear molecules with a diverse multivalent character along a linear backbone. Of these, peptides and peptidomimetics offer complete control over the placement of functionality, so in this respect, they may be considered a superior choice with regards to applications that require discreet molecular structures. However, peptides are known to be susceptible to instability, short shelf life, and rapid *in vivo* degradation. Synthetic polymers are typically easier to synthesize in large quantities, but the control over purity and placement of functionality is very low compared to monomer or submonomer strategies found in peptidomimetic synthesis.

1.5 Peptidomimetics

Peptides are short, amino-acid containing oligomers that are ubiquitous in nature, and smaller than their larger polypeptide or protein counterparts. Peptides span an amazing range of biological functions, not including the advances in synthetic peptide chemistry, which have generated innumerable other sequences tailored to a wide range of biological or even non-biological applications. Interestingly, the functions and characteristics of peptides are largely dependent on their adopted secondary structure rather than their amino-acid-specific sequences. The attractiveness of peptides lies in the ease of synthesis using automated equipment, but hydrophobic or complex sequence synthesis and purification can become quite cost-prohibitive on a large scale. However, as discussed, peptides suffer from short shelf

life, low bioavailability due to *in vivo* degradation, and the possible risk of immune response.

Non-natural peptidomimetics are thus currently being researched and developed in an attempt to mimic the function of therapeutic peptides, but offer the additional advantages of bioavailability, non-immunogenicity, and cost-effectiveness [2, 7, 8]. These molecules are often designed to obtain secondary structures similar to those of peptides. Some examples of such families of molecules are β -peptides, γ -peptides, oligopyrrolinones, and poly-*N*-substituted glycines [9, 10]. Indeed, it was discovered that these peptidomimetics are capable of folded structure, and can mimic the therapeutic functions of peptides. For instance, β -peptides have been shown to successfully mimic the activity of helical, facially amphipathic antibacterial peptides, oligopyrrolinones have been used to mimic the inhibitory activity of HIV-1 protease, and poly-*N*-substituted glycines can be used to mimic peptide ligands, antibacterial peptides, and lung surfactant proteins [11].

As protein- and peptide-based multivalent scaffolds are being actively pursued in the research community, it may seem as only natural that non-natural peptidomimetic variants be explored as viable scaffold architecture options.

1.6 Poly-*N*-substituted glycines or “peptoids”

Poly-*N*-substituted glycines, or peptoids, possess a peptide backbone wherein the side chains are appended to the amide nitrogen rather than the α -carbon in the backbone sequence (Figure 1.1) [10, 12]. They are easily and inexpensively synthesized on automated equipment, with the ability to include a diverse range of

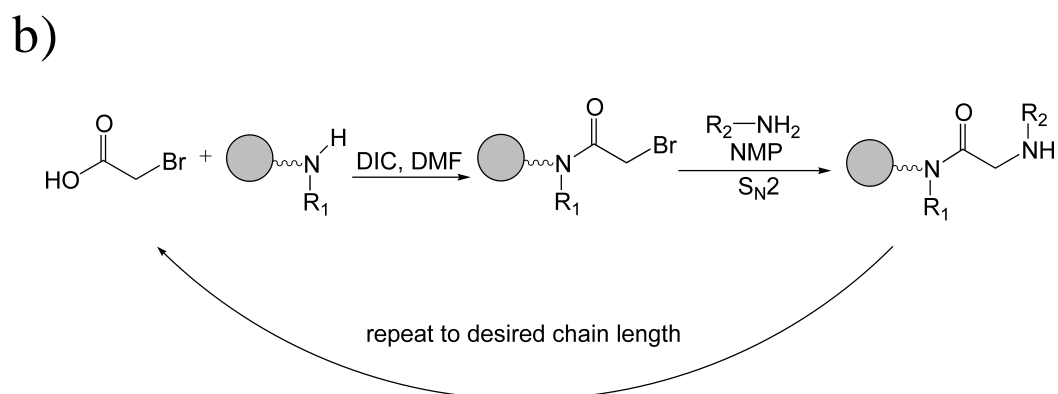
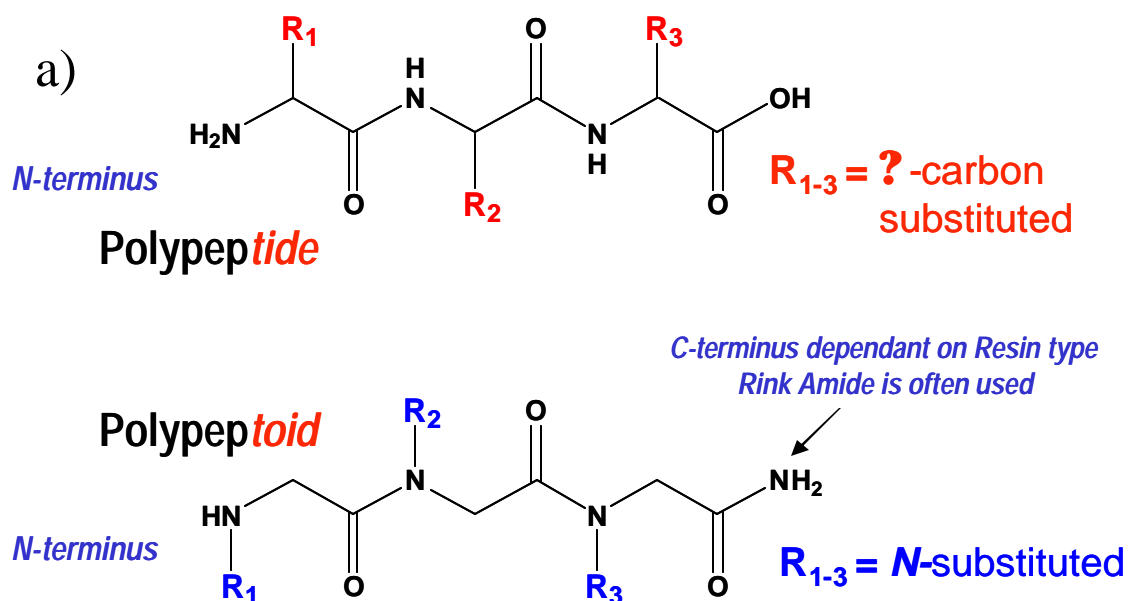
chemical functionalities or *N*-substituted ‘side chains.’ Peptoids can be precisely and strictly controlled in terms of sequence-specific design, just as peptides, and it has been previously demonstrated that various oligomers, ranging from 3 to 22 monomers in length, exhibit a variety of interesting biological activities [11, 13-15].

Peptoids exhibit a unique advantage in comparison to a number of other non-natural oligomers under investigation for a variety of applications [2, 7, 8, 16]. The high monomer coupling efficiencies that can be attained, and the low cost of production from inexpensive and readily available starting reagents make peptoids distinct from other non-natural peptidomimetics. Sequence-specific peptoids of up to at least 50 residues in length can be synthesized in high yield using a solid-phase protocol and an automated peptide synthesizer [17]. Peptoids are synthesized using the submonomer approach developed by Zuckermann *et al.* shown in Figure 1.2 [12]. A solid scaffold support is used for extension of the oligomer. In the first step of the submonomer approach, bromoacetic acid is used to acylate a secondary amine on the resin, leaving a good S_N2 reaction substrate. In the second step a primary amine is added to the oligomer *via* an S_N2 reaction. These steps are repeated until an oligomer of the desired length is obtained. This novel synthetic route gives access to a diversity of functionalized peptoids at modest cost and effort, and average submonomer coupling efficiencies are comparable to those attained in Fmoc peptide synthesis (> 98.5%).

Peptoids can also be synthesized following a monomer protocol, whereby activated Fmoc-protected monomers are coupled [18-21]. One can alternate between submonomer and monomer protocols within a single automated solid-phase synthesis,

enabling the creation of peptoid-peptide chimerae. This allows the simultaneous optimization of bioactivity and biodegradation rate.

Figure 1.2 a) Peptide and peptoid structures and b) submonomer method for solid-phase peptoid synthesis



The *N*-substituted structural design also results in an achiral backbone, as well as an absence of backbone hydrogen bond donors. Although peptoids cannot form backbone-backbone hydrogen bonds to stabilize secondary structure, structural studies have shown that peptoid sequences with chiral side chains form stable helical structures with a chiral handedness, similar to peptide polyproline helices [9]. Peptoid helices have a helical pitch of approximately 6 Å and a periodicity of 3 residues per turn, and are stabilized primarily by steric and electronic repulsions [22]. CD spectra for peptoids containing chiral, aromatic side chains exhibit two minima near 204 and 218 nm and a maximum near 190 nm, similar to those seen in the spectra of a peptide 3^{10} helix or an α -helix, while CD spectra for peptoids containing chiral, aliphatic side chains exhibit two shallow minima near 200 and 225 nm and one maximum near 210 nm, similar the spectra of a peptide polyproline helix [15]. Crystallography of a pentamer containing chiral, aliphatic side chains reveal the same 3 residues per turn periodicity, but a looser pitch of 6.7 Å [15].

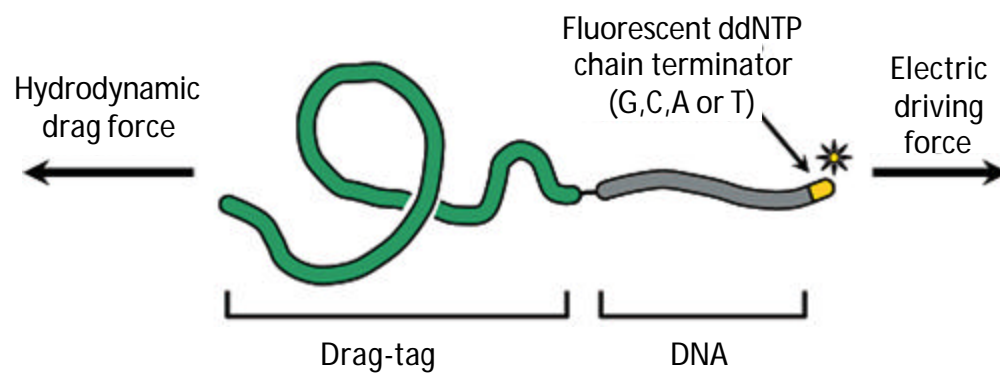
1.7 End-labeled free-solution electrophoresis (ELFSE)

The completion of a high-accuracy, finished sequence of the human genome (announced April 14, 2003) was made possible by the development and commercialization of high-throughput capillary array electrophoresis instruments. Capillary electrophoresis (CE) is an automated, microscale analytical technique that separates species by applying voltage across buffer-filled capillaries. CE is generally used for separating ions (esp. DNA), which move at different speeds depending on their size and charge. These instruments and other developments helped drive down

the cost of sequencing significantly. Further decreases in the cost of DNA sequencing, however, will require novel approaches to surpass fundamental limits inherent in existing technologies. Microfluidic devices, or microchips, currently under development already have shown higher throughput than even the best capillary results. Some challenges remain, however, including the loading of viscous DNA separation gels into small microchannels, which is either very slow or requires very large pressure gradients.

A novel approach is to change the way sequencing is done by eliminating the need for a gel, and instead, to perform sequencing in free solution using an approach called End-Labeled Free-Solution Electrophoresis (ELFSE) (Figure 3). Attaching a perturbing entity or "drag-tag" such as a protein to a DNA molecule breaks the symmetry between charge and friction, an approach first conceived by Noolandi [23]. In practice a "drag-tag" is covalently attached to a single end of a DNA molecule, altering the free-solution electrophoretic mobility of the DNA molecule in a regular, size-dependent fashion. By attaching identical "drag-tags" to all of the DNA molecules in an ensemble of differently sized ssDNA molecules, such as is generated in the Sanger cycle-sequencing reaction [24], separation of the sequencing ladder can be achieved. In principle, this requires only that the entities are monodisperse and have a different ratio of charge to friction than DNA.

Figure 1.3 Drag-tag DNA conjugate structure [65].



The physical mechanism behind ELFSE is quite simple, and was derived by Slater and coworkers [25]. Consider a DNA molecule with N monomers, conjugated to a drag-tag having a net free-flow mobility equal to μ/μ_0 times that of DNA in free solution (μ_0), and a total hydrodynamic drag equivalent to λ bases of DNA. Based on the theory for the electrophoresis of polyampholytes developed by Long and coworkers [26], the equation for the mobility of DNA attached to an electrostatically neutral drag-tag is:

$$\frac{\mu}{\mu_0} = \frac{1}{1 + \lambda/N} \quad (1)$$

In principle, ELFSE eliminates the limitations on read length imposed by sieving matrices. In addition, the electrophoretic mobility of DNA is much higher in free solution, and thus ELFSE potentially could be much faster than sequencing in gels. It also removes any inconvenience with loading gels, or tradeoffs between viscosity and performance. This method could provide faster separations and/or longer read lengths than matrix electrophoresis, and is particularly well suited for use in microchips.

Poly(ethylene glycol) (PEG) and related molecules are potentially ideal drag-tags. Its backbone $(\text{CH}_2\text{CH}_2\text{O})_n$ is amphiphilic, non-adsorptive to glass, hydrophilic and uncharged. Unfortunately, techniques used to prepare PEG, even those of fairly low relative molecular mass such as 3400, involve a poorly controlled polymerization step. Resultant PEG molecules are polydisperse and hence unsuitable for ELFSE.

Polypeptoids are a class of molecules that could be formulated as suitable ELFSE drag-tags. Capable of combining the advantages of both PEG and polypeptides (precise length, convenient high-yielding synthesis), polypeptoids, or poly-*N*-substituted glycines, are non-natural sequence-specific polymers based on a polyglycine backbone [21]. Polypeptoids with side chains containing methoxy groups display PEG-like properties but also are monodisperse. Polypeptoids can be conjugated to polypeptides at specific sites, such as the ϵ -amino side chains of lysine or the carboxyl groups of glutamic acid residues along the polypeptide backbone. Attached as comb-like appendages, polypeptoids will increase protein water solubility and will reduce interactions with the microchannel walls. So-called comb-like copolymers with densely grafted side chains in a good solvent can adopt a wormlike cylindrical brush configuration, with the side chains stretched normal to the backbone [27, 28], making them ideal drag-tag architectures.

1.8 Magnetic resonance imaging (MRI) contrast agents

Magnetic resonance imaging (MRI) is a widely used diagnostic tool in radiology that generates high resolution images of living tissue. This non-invasive technique thus allows for three-dimensional visualization of the body's biological structures, processes, and functions at cellular resolution [29-31]. MRI relies on the NMR signal of protons of mostly water, and signal intensity in a given volume element is therefore a function of water concentration and proton relaxation times. The resulting signal intensity variations generate image contrast, permitting differentiation between various tissue types and stages of disease. High contrast is very desirable for

imaging, as it increases the diagnostic capabilities of MRI in the clinical environment. There are many different mechanisms for creating contrast in an image, where an imaging sequence can be weighted to display differences in proton relaxation rates, chemical shifts, water diffusion, blood flow effects, or magnetization transfer techniques [32].

MRI signal intensity is derived from the local value of the longitudinal relaxation rate of water protons, $1/T_1$, and the transverse rate, $1/T_2$. Signal tends to positively correlate with $1/T_1$ and inversely correlate with $1/T_2$. T_1 -weighted pulse sequences are hence those that emphasize changes in $1/T_1$, and oppositely for T_2 -weighted scans. In T_1 -weighted imaging, a more intense signal is observed in regions where the longitudinal relaxation rate $1/T_1$ is fast, *i.e.*, where T_1 is short. The longitudinal relaxation rate of water protons can be further enhanced by the addition of paramagnetic metal complexes. These complexes, termed MRI contrast agents [33], afford increased image contrast in regions where the complex localizes.

Thus, the administration of MRI contrast agents in patients significantly expands the scope of imaging capabilities available to doctors and researchers. Several compounds are currently approved for clinical use, and more are undergoing clinical trials. Initial contrast agents were developed to distribute to plasma and extracellular space [34], while later efforts focused on targeting the liver and bodily fluids [35]. The current, pre-clinical development of contrast agents hones in on improvements in “molecular imaging” [36].

Exogenous contrast agents employ paramagnetic metal ions, and most function by shortening the local T_1 , or increasing $1/T_1$, of solvent water protons, thus providing

increased contrast. Depending on their nature and the applied magnetic field, contrast agents increase both $1/T_1$ and $1/T_2$ to varying extents. Agents such as gadolinium in its +3 oxidation state, Gd(III), increase both $1/T_1$ and $1/T_2$. Because the long electron spin relaxation time and high magnetic moment of Gd(III) make it an efficient perturbant of T_1 , this agent is best visualized using T_1 -weighted images, as the percentage change in $1/T_1$ in tissue is much greater than that in $1/T_2$. Advances in MRI have primarily favored T_1 agents, thus the widespread use of Gd(III) [33].

Relaxivity is defined as the ability of a complex to enhance the relaxation rate of the solvent, denoted r , (Equation 1), with units of $\text{mM}^{-1}\text{s}^{-1}$, where $\Delta 1/T_1$ is the change in the solvent relaxation rate after contrast agent addition at metal concentration $[M]$:

$$r = \frac{\Delta 1/T_1}{M} \quad (1)$$

High relaxivity thus translates to the increased ability of the contrast agent to be detected at lower concentrations, which may allow the imaging of low concentration molecular targets. Highly paramagnetic metal ions with a large spin number, S , are preferred, provided that electronic relaxation is slow. Therefore, again, complexes of Gd(III) [37] are commonly used as contrast agents because the metal center has seven unpaired electrons. However, current clinically used contrast agents have low relaxivities ($3\text{--}7 \text{ mM}^{-1}\text{s}^{-1}$) and must be used at high concentrations for the MRI signal enhancement to be useful [38].

1.9 Challenges addressed in the present work

The aim of the present research is to develop multivalent scaffolds for electrophoretic and MRI applications. The work described in Chapters 2-4, and 6 focuses on using poly N meg peptoid scaffolds as drag-tags for the ELFSE project. Chapter 5 describes the development of peptoid-based MRI contrast agents.

The work described in Chapter 2 shows that drag scales linearly with molar mass for branched poly N meg drag-tags of varying size.

Chapter 3 describes the use of drag-tags in theoretical and practical applications using ELFSE. In one instance, DNA is doubly modified with a drag-tag at both ends to provide experimental evidence for the idea that drag increases more than two-fold over singly modified DNA. In another instance, sixteen drag-tags, include peptoid variants, were employed in multiplexed genotyping to locate mutations in sixteen hotspots of the p53 gene.

Chapter 4 presents the first instance of DNA sequencing using a completely synthetic drag-tag. Up to 100 bases are resolved in 16 minutes.

Chapter 5 outlines the development of poly N meg-containing sequences as multivalent scaffolds for MRI contrast agents. Specifically, a 30mer peptoid was modified with a derivatized DOTA chelator and metalated with Gd(III), which resulted in one of the highest relaxivity values reported for a discrete macromolecular contrast agent.

Further work to better design drag-tags for ELFSE sequencing is described in Chapter 6. These efforts involve the inclusion of aminoxy side chains to enhance hydrophilicity in the drag-tag, positive charges to increase drag, and synthetic strategies to generate molecules with larger molecular mass.

Chapter 2. Comb-like, monodisperse polypeptoid drag-tags for DNA separations by end-labeled free-solution electrophoresis (ELFSE)

Reproduced with the permission from *Bioconjugate Chemistry*, **16** (4), 929 –938, **2005**.

Copyright 2005, American Chemical Society.

The development of innovative technologies designed to reduce the cost and increase the throughput of DNA separations continues to be important for large-scale sequencing and genotyping efforts. We report research aimed at the further development of a free-solution bioconjugate method of DNA size-separation by capillary electrophoresis (CE), in particular the determination of an optimal molecular architecture for polyamide-based “drag-tags.” We synthesized several branched, poly-*N*-methoxyethyl glycines (poly(*N*megs), a class of polypeptoids) as novel friction-generating entities for end-on attachment to DNA molecules. A 30mer poly(*N*meg) “backbone,” comprising five evenly spaced, reactive α -amino groups, was synthesized on solid phase, cleaved and purified to monodispersity by RP-HPLC. Three different comb-like derivatives of this backbone molecule were created by: (1) acetylating the α -amino groups, or (2) appending small, monodisperse *N*meg oligomers (a tetramer, and an octamer). Grafting of the oligo*N*megs was done using solution-phase amide bond-formation chemistry. Once purified to total monodispersity, the three different

drag-tags were studied by free-solution electrophoresis to observe the effect of branching on their hydrodynamic drag or “ ζ ,” and hence their ability to separate DNA. Drag was found to scale linearly with total molecular weight, regardless of branch length. The octamer-branched drag-tag–DNA conjugate was used to separate ssDNA products of 50, 75, 100 and 150 bases in length by free-solution CE, in less than 10 minutes. Hence, the use of branched or comb-like drag-tags is both feasible and an effective way to achieve high frictional drag, allowing the high-resolution separation of relatively large DNA molecules by free-solution CE without the need to synthesize very long polymers.

2.1 Introduction

The development of novel and improved technologies for DNA separation and analysis continues to be driven by a societal need to make sequencing and genotyping more cost effective. Capillary electrophoresis (CE) and capillary array electrophoresis (CAE) enable high-throughput DNA sequencing and genotyping separations by allowing the use of higher electric fields and greater automation than was possible with the traditional slab gel format. Both CE and CAE require the use of highly viscous polymer solutions (*e.g.*, entangled solutions of linear polyacrylamide) as intracapillary DNA size-separation matrices. In addition to their expense, these polymer solutions require the application of high pressure to be loaded into narrow capillaries, and generally DNA sequencing read lengths, with even the best polymers and CAE instruments, are limited to about 800 bases at best.

DNA separation cannot normally be achieved by electrophoresis in free solution, *i.e.*, in the absence of polymer networks, because the electrophoretic mobility of DNA molecules is independent of their chain length [39]. It was theorized in 1992 that DNA could be separated by free-solution electrophoresis, if one attached a monodisperse perturbing entity or “drag-tag” to DNA fragments of varying size [23]. That is, it was predicted that the charge-to-friction ratio of DNA can be rendered size-dependent if a monodisperse drag-tag is covalently attached to one end of the DNA molecules to be separated, allowing the DNA chains to be separated by microchannel electrophoresis in a regular, size-dependant fashion. This approach, called End-Labeled Free-Solution Electrophoresis (ELFSE), has been under development for the past 10 years as a promising bioconjugate method of DNA sequencing and genotyping that could eliminate the need for viscous polymer solutions in capillary and chip electrophoresis of DNA [25, 40, 41]. Experimentally, ELFSE with various types of drag-tags has been used to separate short oligonucleotides with high resolution [42, 43] as well as long double-stranded DNA fragments [44]. For DNA sequencing applications, ELFSE promises to provide faster separations and longer read lengths than matrix-based electrophoresis, and should be particularly well suited for use in microfluidic devices [1, 41, 45].

The amount of drag created by the drag-tag can be characterized in terms of the parameter “ ζ ,” which has the units of the hydrodynamic drag of a single base of ssDNA [25]. In circumstances and conditions likely to be present in this study, recent theoretical treatments of the electrophoretic mobilities of composite molecules from the Slater group [42, 46] interpret ζ in terms of hydrodynamic “blobs.” The effective

friction coefficient ζ for a drag-tag can be estimated experimentally by measuring (simultaneously) the electrophoretic migration times of unconjugated, “free” DNA, and that of a drag-tag–DNA conjugate comprising of the same DNA. The parameter ζ can then be calculated with the equation:

$$\zeta = N \frac{\mu_0}{\mu} \quad (2.1)$$

for a conjugate molecule consisting of N bases of DNA, and a charge-neutral drag-tag with friction equivalent to ζ bases of ssDNA, having the electrophoretic mobility μ , and where μ_0 is the electrophoretic mobility of unlabeled DNA (about 2.5×10^{-4} cm²/V·s for the conditions herein) [25].

High-resolution ELFSE separations of DNA require the ideal drag-tag to be: (i) totally monodisperse, (ii) of high enough molecular weight to impart sufficient drag to separate DNA analytes of varying size, (iii) water-soluble and polar, but essentially charge-neutral [47], and (iv) resistant to non-specific (band broadening) interactions with microchannel walls. Taken together, the various and in some cases contradictory design criteria make drag-tag design and synthesis a challenging problem in molecular engineering.

Natural proteins and viruses have been proposed as candidate drag-tags [23, 25]. This prediction was validated by the successful sequencing of *ca.* 110 DNA bases in 18 minutes by free-solution CE with the use of the protein streptavidin as a drag-tag [48]. This result, although remarkable, highlighted some significant drawbacks of using natural proteins as drag-tags. For instance, the results indicated a problem with obtaining streptavidin in a truly monodisperse preparation, and also showed that even

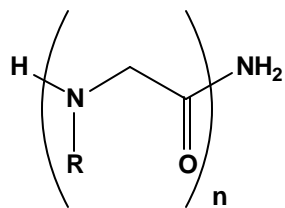
a virtually charge-neutral protein can suffer from strong adsorptive interactions with the microchannel wall. These interactions result in band broadening and a decrease in peak resolution. Streptavidin is a tetrameric protein [49] (4 x 13 kDa, totaling 536 amino acid residues) that has numerous biochemical applications [50], but despite its relatively large size, it adopts a compact, globular conformation, resulting in a relatively low drag, equal to approximately thirty bases of DNA. This was the primary factor limiting read length in the study by Slater and Drouin.

Synthetic polymers have also been examined for use as ELFSE drag-tags. Poly(ethylene glycol) (PEG) is water-soluble, relatively non-adsorptive to glass, hydrophilic and uncharged – all potentially ideal molecular properties for ELFSE. However, even PEGs with a low molecular mass such as 3400 g/mol [51], with an ultra-low polydispersity index (M_w/M_n) of 1.01, are not sufficiently monodisperse for DNA sequencing or genotyping applications [42].

Poly-*N*-substituted glycines (polypeptoids) are non-natural, sequence-specific polymers based on a polyglycine backbone [10]. This class of molecules may be synthesized on solid phase in high yield using a “submonomer approach,” to include a myriad of different side-chain functionalities [52, 53]. After cleavage from the solid phase, they can be purified to monodispersity by reversed-phase high-performance liquid chromatography (RP-HPLC).

Vreeland *et al.* successfully employed a family of linear, poly-*N*-methoxyethyl glycine peptoids (poly(*N*meg)s) with PEG-like side chains (Table 1) as drag-tags for the ELFSE separation of short DNA oligonucleotides. Poly(*N*meg) drag-tags ranging in size from 10 to 60 monomers in length were used to separate 20- and 21-base

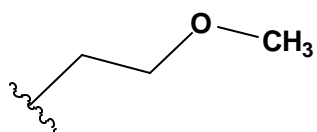
ssDNAs [42] as well as single-base extension (SBE) reaction products between 19 and 24 bases in length [54]. The longest polypeptoids used in these studies were sixty monomers in length, and were obtained in only modest yields by the divergent solid-phase peptide synthesis techniques used.

Table 2.1. *N*-Substituted glycine (peptoid) side chains.

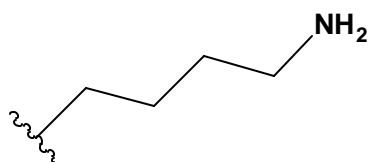
N-substituted glycine oligomer,
or *peptoid*

R = Side chain

Designator



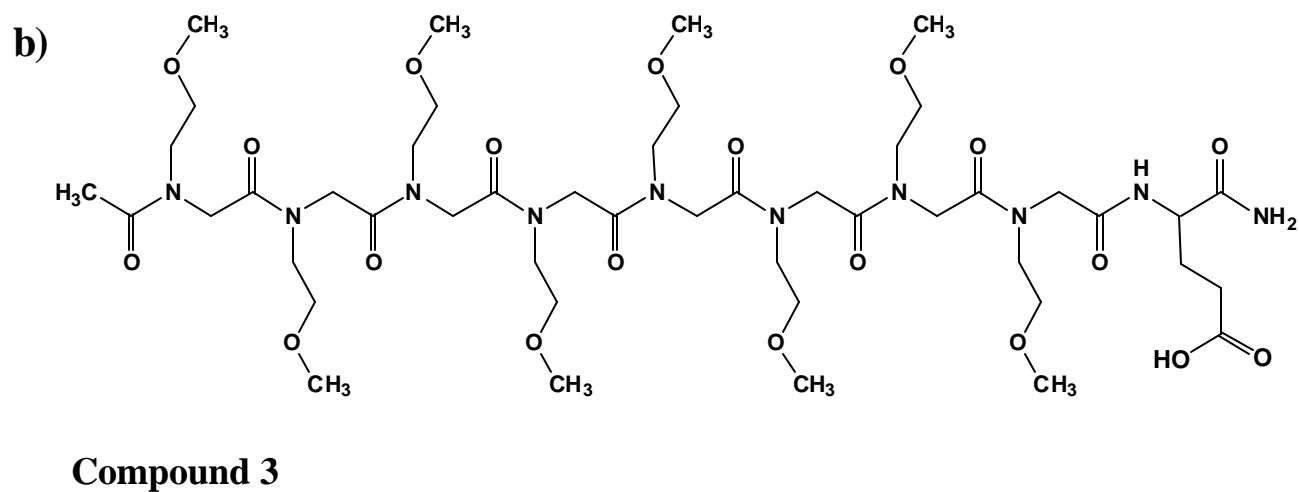
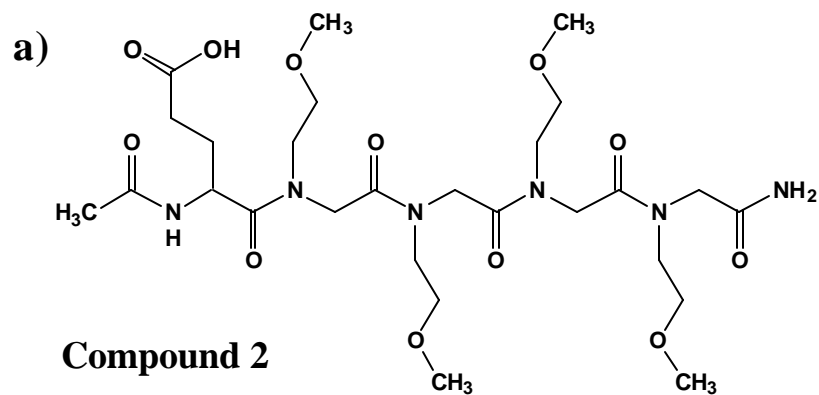
Nmeg = *N*-(methoxyethyl) glycine



Nabg = *N*-(amino butyl) glycine

Aiming to improve upon this work, we hypothesized that the grafting of “branch” molecules onto a “backbone” would be an efficient convergent strategy for the synthesis of monodisperse, high-molecular weight drag-tags that could allow the separation of larger DNA. To test this idea we designed a 30mer poly(*N*meg) “backbone” (Scheme 1), with five evenly spaced α -amino sites, to be grafted *via* a peptide bond-forming reaction with tetramer (**2**) and octamer (**3**) oligo(*N*meg) peptoids possessing a terminal carboxylic acid (Scheme 2). The amino groups arrayed along the backbone of **1** could also be acetylated, yielding a set of three drag-tags with increasing branch length. We anticipated that the testing of these three different molecules as drag-tags for DNA separation by free-solution CE would provide valuable information regarding the relationship between chain architecture, molecular weight and hydrodynamic drag (ζ). Grafting reactions could in theory be performed whilst the backbone molecule (**1**) is still on the solid-phase resin; however, in order for the coupling methodology to be more widely applicable for various classes of backbone molecules, we chose a solution-phase grafting strategy. In this research article, we describe how unbranched (acetylated), tetramer-branched, and octamer-branched comb-like poly(*N*meg) peptoid drag-tags were synthesized, characterized, and evaluated. These drag-tags were attached to both 20- and 30-base DNA primers, and free-solution CE was used to analyze the electrophoretic mobilities of the bioconjugate molecules. We were able to observe and quantify the ζ values for each of these drag-tags. We also demonstrate the use of one of these drag-tags for the efficient separation of differently sized DNA fragments up to 150 bases long, by CE in free solution.

Scheme 2.2 Chemical structures of the tetramer (a) and octamer (b) “branches.” They are oligo-N-methoxyethyl glycine (Nmeg) peptoids with reactive terminal glutamic acid residues.



2.2 Experimental

2.2.1 General methods and materials

The “sub-monomer” synthesis of the poly-*N*-substituted glycines or “polypeptoids” used in this work has been described previously [10]. Scheme 1 depicts the protocol that was used to synthesize the polypeptoid molecules made for this study. All reactions were carried out on an ABI 433A automated peptide synthesizer (Applied Biosystems, Foster City, CA). All reagents used were purchased from Aldrich (Milwaukee, WI), unless stated otherwise. The mass spectra were recorded by MALDI-TOF (Figure 1) (Voyager Pro DE, Perseptive Biosystems, Framingham, MA) and ESI (Waters Micromass Quattro II, Milford, MA).

2.2.2 Reversed-phase high-performance liquid chromatography (RP-HPLC)

Analytical RP-HPLC was performed on a column with C18 packing (Vydac, 5 μm , 300 \AA , 2.1 x 250 mm). The following conditions were employed, unless otherwise stated: a linear gradient of 10-40 % B in A was run over 50 min at a flow rate of 0.5 mL/min (solvent A = 0.1 % TFA in water, solvent B = 0.1 % TFA in acetonitrile) at 58 $^{\circ}\text{C}$; analytes were detected by UV absorbance at 220 nm and/or 260 nm. Preparative HPLC was performed on a Vydac C18 column (Vydac, 15 μm , 300 \AA , 22 x 250 mm) using the same solvent and detection systems; analytes were eluted with a linear gradient of 10-40 % B in A over 50 min at 12 mL/min.

2.2.3 Polypeptoid “backbone” (Compound 1)

Synthesis details: Fmoc-Rink amide resin (Nova Biochem, San Diego CA. 0.30 mmol scale) was deprotected by treatment with piperidine in dimethylformamide (DMF) (20 % v/v; 2 x 7 mL) in two consecutive 15-min treatments. The oligomer chain was then assembled with alternating cycles of the bromoacetylation step and amine displacement of the alkyl bromide moiety. Bromoacetylation was achieved by mixing the resin with bromoacetic acid (BAA) (1.2 M; 4.3 mL) in DMF and diisopropylcarbodiimide (DIC) (1 mL; 9.9 mmol). The mixture was vortexed for 45 min, the liquid drained, and the resin rinsed with DMF (4 x 7 mL). The resin was then mixed and vortexed (45 min) with either methoxyethylamine (1.0 M; 4 mL) or mono-Boc protected diaminobutane (1.0 M; 4 mL) [55] in *N*-methylpyrrolidone (NMP) to introduce the *N*-methoxyethyl (*N*meg) or *N*-aminobutyl (*N*abg) side chain moieties (Table 1). The liquid was drained, and the resin rinsed with DMF (4 x 7 mL). These two reaction cycles were alternated until the polypeptoid was of the desired sequence and length. Finally, an Fmoc protecting group was installed on the amine terminus while the polypeptoid was still on the resin. This was achieved by adding Fmoc-Glycine and DIC under the same conditions as used for the bromoacetylation step.

Finally, the polypeptoid was cleaved from the solid support by treatment with 95:2.5:2.5 trifluoroacetic acid (TFA):triisopropylsilane (TIS):water for 10 min. The polypeptoid was filtered through a fritted glass vessel to remove the solid support, diluted with water (50 mL), frozen (-80 °C) and then lyophilized. The product of the solid-phase synthesis was evaluated by analytical RP-HPLC. Preparative RP-HPLC was

subsequently performed and appropriate fractions were combined to afford the desired product (1) in pure preparation.

2.2.4 Tetramer “branch” (Compound 2)

Using the same methods described above, this oligopeptoid was synthesized using the “sub-monomer” approach [10] on a 0.30 mmol scale on Fmoc-Rink amide resin (Scheme 2a). Following procedures outlined above, four additions of the *N*-methoxyethyl glycine monomer were followed by the addition of an *N*- α -Fmoc-L-glutamic acid α -*t*-butyl ester (Fmoc-Glu(OtBu)-OH) residue, which involves the coupling of the amino acid to the terminal secondary amine. This coupling was achieved by dissolving the amino acid in NMP (1.0 M; 4 mL) with PyBroP (1.2 M) and DIEA (1.2 M). The Fmoc group at the *N*-terminus of the glutamic acid residue was subsequently removed using (20% v/v) piperidine in DMF, and the resultant primary amine was capped with acetic anhydride. This was achieved by immersing the resin in fresh acetic anhydride (neat) (Applied Biosystems, Foster City, CA), followed by agitation with occasional venting for 15 minutes. The resin was filtered and cleaved, as previously described. For the branch molecules, cleavage from the resin also resulted in deprotection of the *t*-butyl protected glutamic acid side chain functionality, revealing the carboxylic acid group. The oligopeptoid was cleaved from the solid support, frozen and lyophilized, as previously described. The product of the solid-phase synthesis was evaluated by analytical RP-HPLC. Preparative RP-HPLC was performed and appropriate fractions were combined to afford the desired tetramer (2). The product was identified by ESI mass spectrometry and analyzed by RP-HPLC.

2.2.5 Octamer “branch” (Compound 3)

The octamer branch molecule (Scheme 2b) was synthesized by pre-loading the Rink amide resin with Fmoc-Glu(OtBu)-OH as the first step using standard peptide chemistry. The Fmoc group on the glutamic acid residue was subsequently removed using (20 % v/v) piperidine in DMF, followed by the addition of eight monomers of *N*-methoxyethyl glycine. The terminal secondary amine was acetylated and the oligopeptoid was then cleaved from the solid support, frozen and lyophilized, as previously described. Preparative RP-HPLC was performed and appropriate fractions combined to afford compound 3. The product was identified by ESI mass spectrometry and was analyzed by RP-HPLC.

2.2.6 Backbone acetylation (Compound 4)

An “unbranched” 30mer drag-tag was synthesized by the addition of neat acetic anhydride (1 mL) to the purified backbone molecule 1 (5.0 mg, 1.3 μ mol) (Scheme 3). Excess acetic anhydride was removed *in vacuo*, quenched with water (10 mL), frozen (-80 $^{\circ}$ C) and lyophilized. Preparative RP-HPLC was performed and appropriate fractions were combined to afford 4. The product was identified by MALDI-TOF mass spectrometry and was analyzed by RP-HPLC.

2.2.7 Backbone grafting reactions (Compounds 5 & 6)

Typical synthesis protocol: Tetramer 2 (25.5 mg, 39 μ mol) and PyBroP (24.85 mg, 39 μ mol) were added to a cooled solution (0 $^{\circ}$ C ice-bath) of backbone 1 (5.0 mg, 1.3

μmol) in NMP (1 mL). The resultant mixture was stirred under nitrogen for 5 minutes. The reaction mixture was stirred vigorously and diisopropylethylamine (DIEA) (5 mg, 39 μmol) was added dropwise *via* cannula under a positive nitrogen atmosphere. The reaction mixture was allowed to warm to room temperature and the reaction to proceed for 3 hrs. NMP was then removed *in vacuo*, and the solution was diluted with deionized water (12 mL), frozen, and lyophilized. The grafting reaction was monitored by analytical RP-HPLC using a slightly different method than previously stated: A linear gradient of 10-60 % B in A was run over 50 min at a flow rate of 0.5 mL/min (solvent A = 0.1 % TFA in water, solvent B = 0.1 % TFA in acetonitrile) at 58 °C on C18 packing (Vydac, 5 μm , 300 Å, 2.1 x 250 mm); analytes were detected by UV absorbance at 220 and 260 nm. Preparative HPLC was performed on a Vydac C18 column (Vydac, 15 μm , 300 Å, 22 x 250 mm) using the same solvent and detection systems; analytes were eluted with a linear gradient of 10-60 % B in A over 50 min at 12 mL/min. Preparative RP-HPLC was performed and appropriate fractions combined. Compound 5 was then treated with 20 % (v/v) piperidine in methanol (1 mL), to remove the terminal Fmoc protecting group, and stirred for 20 minutes. The solvent was then removed *in vacuo* and the resulting material was re-purified by RP-HPLC as previously described. The same conditions were used, and similar results were obtained for the grafting reaction with the octamer branch to produce compound 6 (Scheme 3).

Scheme 2.3 Solution-phase coupling protocol for the synthesis of branched and unbranched drag-tags (4-6) via grafting of oligopeptoids onto the backbone molecule (1).

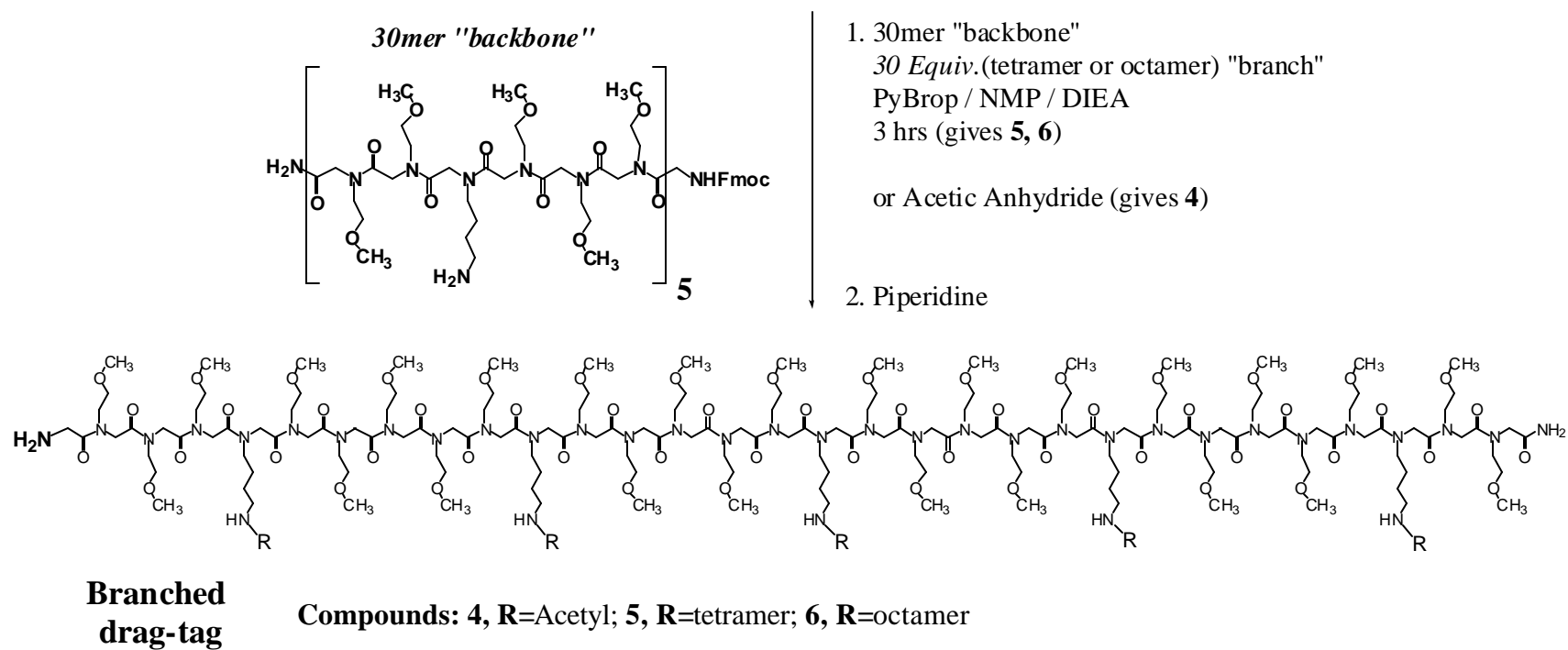
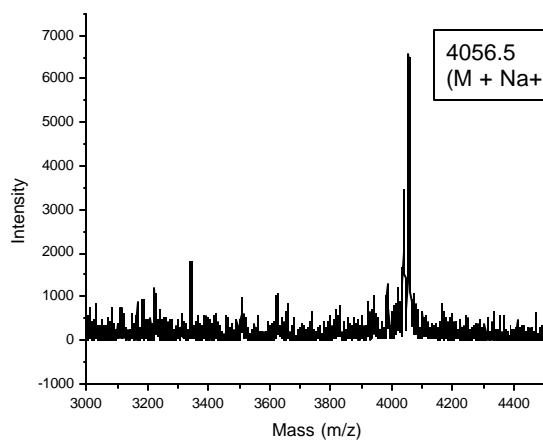
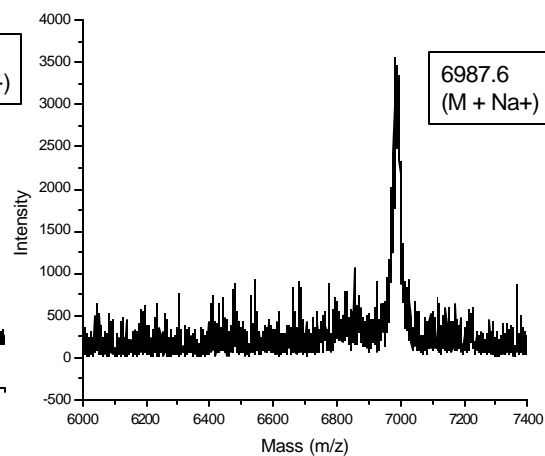


Figure 2.1. MALDI-TOF data. Mass spectrometry was done at the Analytical Services Laboratory at Northwestern University ?-cyano-4-hydroxycinnamic acid (ACCA) as the matrix. Resulting spectra and lists of the major peaks for the Fmoc-protected drag-tag molecules (4-6) are given below:

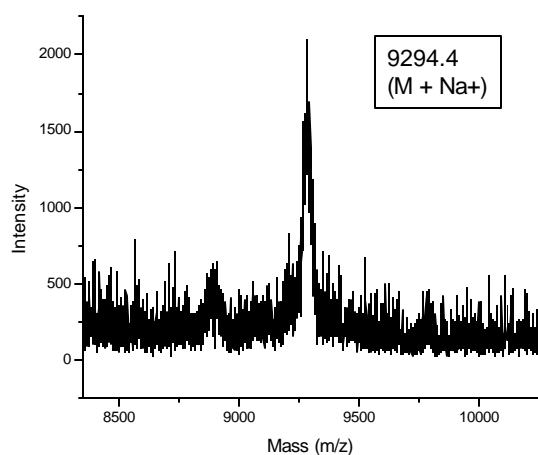
(Fmoc) Acetylated drag-tag (4)



(Fmoc) Tetramer-branched drag-tag (5)



(Fmoc) Octamer-branched drag-tag (6)



2.2.8 Sulfo-SMCC conjugation

The drag-tags (**4-6**) – displaying a free amine at the *N*-terminus – were dissolved in 0.1 M sodium phosphate buffer, 0.15 M sodium chloride, pH = 7.18. Sulfo-SMCC (Sulfosuccinimidyl 4-[*N*-maleimidomethyl] cyclohexane-1-carboxylate) (Pierce Scientific, Rockford, IL) (10 mg/mL in water) was added to the drag-tag/buffer solution. This reaction mixture was agitated at room temperature for 1 hour. The reaction was quenched by the addition of water (2 mL), and then purified by preparative HPLC using the conditions described above. The appropriate fractions were then combined.

Drag-tag – DNA Conjugation

Sulfo-SMCC-activated polypeptoid drag-tags were each, individually, conjugated to 5'-thiolated, fluorescently labeled DNA oligonucleotides of lengths 20 and 30 bases (Integrated DNA Technologies, Coralville, IA). The 20- and 30-base DNA sequences were: [5'-**X₁**G**TX₂**TTCCCAGTCACGACGTT-3'] and [5'-**X₁**CC**X₂**TTTAGGGTTTTCCCAGTCACGACGTTG-3'], where **X₁** was a 5' thiol modifier (C6 disulfide), and **X₂** was an internal fluorescein-labeled dT base. Both sequences are designed to be used as primers for an M13mp18 template; the 30-base sequence includes six non-hybridizing bases at the 5' end. The thiol linkers were reduced by incubating 125 pmol of thiolated DNA with 5000 pmol of tris(2-carboxyethylphosphine) hydrochloride (TCEP) (Acros Organics, Morris Plains, NJ) in a total volume of 10 μ L of sodium phosphate buffer (100 mM, pH 7.2) at 40°C for 110 minutes.

Reduced DNA was conjugated to Sulfo-SMCC-activated polypeptoids by mixing 500 pmol of polypeptoid with 12.5 pmol of the reduced DNA mixture (containing 500

pmol of TCEP) in a volume of 5-7 μ L of sodium phosphate buffer (100 mM, pH 7.2). Conjugation reactions proceeded in the dark at room temperature for approximately 6 hours before CE analysis.

2.2.9 Preparation of PCR products

The 30-base thiolated, fluorescently labeled M13 oligonucleotide described above [5'-X₁CCX₂TTTAGGGTTTTCCCAGTCACGACGTTG-3'] was used as a forward primer. Four different 20-base oligonucleotides (Table 2) were purchased from IDT (Coralville, IA) and served as M13 reverse primers for generating PCR products of 50, 75, 100, and, 150 bp in length. M13mp18 ssDNA obtained from Amersham Biosciences (Piscataway, NJ) was used as a template. PCR reactions using *Thermus aquaticus* (*Taq*) DNA polymerase were performed using an MJ Research DNA Thermal Cycler with 30 cycles of 95 °C for 1 min (denaturing), 55 °C for 1 min (annealing), and 72 °C for 2 min (elongation). The size of each PCR product (dsDNA) was confirmed via 3 % agarose gel electrophoresis. The PCR products (with no additional purification) were reduced with Tris(2-carboxyethyl)phosphine (TCEP) and conjugated to drag-tags as described above for the DNA primers.

Table 2.2 Oligonucleotide sequences used as primers for PCR products of 50, 75, 100, and 150 bp. In the forward primer sequence, X1 refers to a 5' thiol linker (C6 disulfide), and X2 refers to an internal fluorescein-dT base.

Primer	DNA sequence
M13 forward	5'-X ₁ CCX ₂ TTTAGGGTTTTCCCAGTCACGACGTTG-3'
M13- 50 reverse	5'-TGGCACTGGCCGTCGTTTTA-3'
M13- 75 reverse	5'-GAGTCGACCTGCAGGCATGC-3'
M13- 100 reverse	5'-GAGCTCGGTACCCGGGGATC-3'
M13- 150 reverse	5'-GCGGATAACAATTCACACA-3'

2.2.10 Free-solution capillary electrophoresis

DNA-polypeptoid conjugates were analyzed by capillary electrophoresis with laser-induced fluorescence detection, using either a BioRad BioFocus 3000 single-capillary instrument (BioRad, Hercules, CA) or an Applied Biosystems Prism 3100 capillary array instrument (Applied Biosystems, Foster City, CA).

Oligonucleotide primers conjugated to polypeptoid drag-tags were analyzed by free-solution electrophoresis using the BioRad BioFocus instrument at 40-55 °C in 25- μ m inner-diameter, fused silica capillaries (Polymicro Technologies, Phoenix, AZ) cut to a total length of 25 cm (20.4 cm from inlet to detector). The running buffer was 1X TTE with 7 M urea (50 mM Tris, 50 mM TAPS, 2 mM EDTA, 7 M urea, pH = 8.5). Typical DNA sequencing conditions were used, to keep the DNA in an unstructured state (7 M urea and a run temperature of 55 °C). The internal surface of the capillary was coated with an adsorbed layer of POP5 polymer (Applied Biosystems, Foster City, CA), using a low-viscosity, 3 % (v/v) aqueous dilution of the commercially available POP5 solution, to reduce electroosmotic flow to negligible levels. Immediately prior to sample injection, the injection end of the capillary was dipped into deionized water to remove any residual buffer salts on the outer surface of the capillary. The samples were introduced into the capillary by pressure injection, with pressure-time constants of 5-15 psia-sec. Electrophoresis was conducted at 400 V/cm until all peaks had eluted, with typical currents of 2.8 μ A. Detection of the analytes was accomplished by excitation of the fluorescent label on the DNA using the 488 nm line of an Argon-ion laser, with emission detected at 520 nm.

Electrophoretic analysis of PCR products conjugated to polypeptoids was carried out in free solution using the Applied Biosystems Prism 3100 Genetic Analyzer, with an array of fused silica capillaries of length 36 cm and inner diameter 50 μM . Analysis conditions were identical to those described above for the BioFocus experiments, except the electric field was 320 V/cm, and samples were introduced by an electrokinetic injection of 22 V/cm for 2 seconds. The PCR product-polypeptoid conjugates were diluted in deionized formamide (Applied Biosystems, Foster City, CA) and denatured at 95 °C for 5 minutes prior to electrophoretic analysis to yield single-stranded DNA-drag-tag conjugates.

2.3 Results and discussion

2.3.1 Branched drag-tag design and synthesis

Attaching large molecules onto a scaffold containing multiple grafting sites, and achieving full coverage, is a challenging proposition [56]. For ELFSE applications the grafting linkages need to be stable enough to withstand further conjugation reactions, purification steps, wide pH ranges, and the high temperatures used in thermal cycling. For this reason we decided on peptide-bond linkages. We designed the backbone (**1**) to have regularly spaced, pendant α -amino groups as attachment sites for tetramer (**2**) and octamer (**3**) branch molecules with terminal carboxylic acid groups. This is an attractive strategy as it allows for the convergent reaction between large molecules that have been pre-purified to monodispersity. Although the resolving power of RP-HPLC could potentially allow for a subsequent removal of the incompletely grafted side-products,

complete grafting is a desired outcome, as even slight impurities in the drag-tag are exposed by CE analysis and will limit its usefulness.

Indeed, early attempts in our lab to graft polyamide oligomers onto lysine-containing polypeptides resulted in a ladder of partially grafted products that ultimately proved too difficult to purify to monodispersity [57]. In the present work we have used poly-*N*-methoxyethyl glycines and their derivatives for both the backbone and branch structures, and were able to produce highly monodisperse components in high yield. The structure of poly(*N*meg) is consistent with recently proposed rules for creating chemical surfaces that are resistant to adsorption of proteins from solution. Specifically, it was found that surfaces presenting groups that are polar but uncharged, hydrophilic, and contain hydrogen-bond acceptors (but not hydrogen-bond donors) are inert to adsorption of proteins from solution [58]. We hypothesized that poly(*N*meg), which has all of these structural features, would be resistant to adsorption from solution onto surfaces. This is a critical feature for capillary electrophoresis, where wall-analyte interactions are a major source of band broadening. Indeed, in previous ELFSE separations using streptavidin as a drag-tag, the interaction between streptavidin and the capillary wall was the primary factor limiting separation efficiency at high electric field strengths [48].

We had to design the drag-tag for two stages of conjugation: a grafting reaction that introduced the monodisperse branches, and then a conjugation to DNA. To achieve this, the backbone molecule (**1**) was designed with a glycine group at the *N*-terminus (Scheme 1), and this resulted in a terminal amine protected with 9-fluorenylmethyloxycarbonyl (Fmoc). The Fmoc protecting group is orthogonal to the *tert*-butyloxycarbonyl (Boc)-protected *N*-butylamine (*N*abg) α -amino groups along the

backbone, and when removed (after grafting), exposes a free *N*-terminal amine for DNA conjugation. Cleavage from the resin using trifluoroacetic acid (TFA) also conveniently cleaves the Boc groups on the side chains without affecting the Fmoc-protected amino terminus.

The terminal Fmoc-glycine residue also facilitates purification. The increased hydrophobicity afforded by the inclusion of the Fmoc group dramatically increases the HPLC retention time, thus helping separate the desired product from impurities. Also, the UV absorbance of the Fmoc moiety allows for facile identification of the product peak at 260 nm by RP-HPLC. The Fmoc amino group can then be easily deprotected at a later point for conjugation to DNA prior to ELFSE analysis.

2.3.2 Backbone synthesis

The backbone (**1**) was synthesized (Scheme 1) using commercially available materials and mono-Boc protected diaminobutane, the latter synthesized and purified in-house according to literature procedures [55]. RP-HPLC analysis revealed a single major product peak, approximately 77 % by area (Table 3) (greater than 99% coupling efficiency per monomer residue). Compound 1 was obtained in pure form by preparative RP-HPLC, and its correct mass was confirmed by ESI mass spectrometry.

Table 2.3 Peptoid structures, molecular mass confirmation and crude purities.

Compound	peptoid oligomer	monomer sequence (amino-to-carboxy)	molar mass calcd:found	purity, ^a %
1	30mer <i>backbone</i>	FmocGly[(<i>N</i> meg) ₃ (<i>N</i> abg)(<i>N</i> meg) ₂] ₅ NH ₂	3818.2 : 3819.3	77
2	Tetramer <i>branch</i>	AcGlu(OH)(<i>N</i> meg) ₄ NH ₂	648.3 : 648.8	96
3	Octamer <i>branch</i>	Ac(<i>N</i> meg) ₈ Glu(OH)NH ₂	1108.6 : 1109.1	95

^a As estimated by analytical reversed-phase HPLC of crude product. All compounds were purified to > 99 % homogeneity before conjugation reactions.

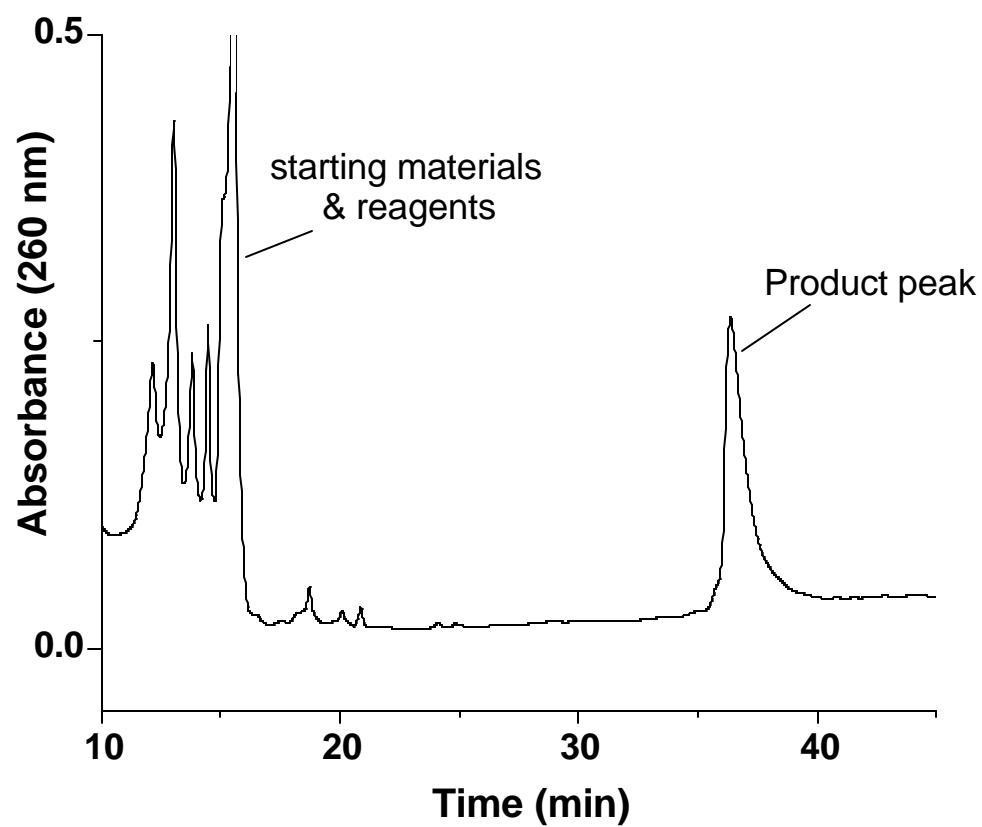
2.3.3 Branch syntheses

The tetramer and octamer branches were both synthesized in excellent yield (Table 3) and purified to monodispersity by RP-HPLC. They were designed as oligo-*N*-methoxyethyl glycine peptoids with terminal glutamic acid (peptide) functionalities. Previous, unsuccessful attempts in our lab to make similar tetramer and octamer branches suitable for high-yielding grafting involved using a terminal glycine unit to provide the reactive carboxylic acid group. Specifically, we had synthesized tetramer and octamer oligo-*N*-methoxyethyl glycine peptoids on pre-loaded glycine Wang resin that revealed a *C*-terminal carboxylate upon cleavage. However, the carboxylate groups on these glycine-terminated drag-tags were apparently too sterically hindered for high-yielding grafting reactions. In our hands, they failed to react efficiently with the γ -amino groups along the backbone. Attempts to graft with these branch molecules resulted in incomplete coverage and hence relatively low yields of the desired, fully derivatized drag-tags (<30% crude yield). The tetramer-branched drag-tag obtained using this strategy was successfully isolated in sufficient quantity for conjugating to DNA, but in low overall yield. Hence, the glycine-terminated branch design was abandoned in favor of glutamic acid-terminated branches; as described below, grafting of the backbone with these oligomers yields conjugates with the correct, accurate masses.

With the intention of improving the coupling efficiency of the grafting reaction, glutamic acid-terminated oligomer branches were designed with the carboxylic acid functionality at the end of a longer, more flexible side chain. We designed the tetramer (**2**) to have the glutamic acid at the *N*-terminus and the octamer (**3**) with that group at the *C*-terminus (Scheme 2), since we did not know *a priori* which strategy was best or

whether this would make a difference. Synthetically, the two branch designs differ only slightly, but potentially enough to affect the monodispersity, since the acetic anhydride capping of **1** takes place on a primary amine, while the capping of **2** occurs on a secondary amine. For both branch molecules, however, synthetic yields were high: RP-HPLC analysis revealed a single major product peak; yields were approximately 95 % by area for both designs (Table 3). In addition, highly efficient grafting was achieved with both designs as described below (Figure 2).

Figure 2.2 RP-HPLC chromatogram of the crude products of the grafting reaction between the tetramer branches (2) and the backbone molecule (1). HPLC: C18 250 mm Vydac column, 58 °C, with 10-60% acetonitrile-water (0.1 % TFA) over 50 minutes.



2.3.4 Grafting of oligomeric branches to the polymeric backbone

The “unbranched,” or *N*-acetylated drag-tag (**4**) was synthesized by the addition of acetic anhydride to a solution of the backbone (**1**) in methanol. Removal of the solvents *in vacuo*, followed by RP-HPLC purification, afforded a single, pure product. The Fmoc protecting group was then removed from the isolated product using piperidine; analysis of the products of this deprotection reaction gave a single peak by RP-HPLC. Compound **4** was collected as a white solid.

One of the most challenging aspects of this synthesis was to achieve complete reaction at all five amino sites on the backbone molecule with the tetramer and octamer branches. In order to generate a completely monodisperse product, we had to find the best way to couple several large molecules together whilst forming bonds that are extremely stable. Peptide-bond linkages can be formed efficiently and were found to be sufficiently stable to withstand the further manipulations needed to make the drag-tag useable.

Finding the appropriate reagents and conditions to form five simultaneous peptide bonds in one reaction initially proved difficult. Solvents including NMP and DMF were examined. Several peptide bond-forming coupling reagents including PyBOP, HATU and PyBroP were examined [59-61]. Optimum results with respect to the efficiency of coupling were obtained utilizing a combination of NMP and PyBroP with DIEA. The use of freshly lyophilized chemicals and Aldrich “sure-seal” packaging (where available) and the employment of rigorous Schlenk techniques under a positive nitrogen atmosphere were found to be highly important factors in the achievement of complete grafting coverage of the backbone. The backbone molecule was found to be especially sensitive

to air, as it possesses five free amines, which may react with carbon dioxide. After optimization of the reaction conditions, the RP-HPLC chromatograms for the analysis of the crude products of the grafting reactions show a single product peak, later identified by mass spectrometry to be the fully grafted comb-like polymer. Under the described reaction conditions, the grafting reaction is highly efficient and goes to completion in only a few hours. Using six equivalents of branch molecule per amino site on the backbone (thirty equivalents overall) was found to be sufficient to achieve complete grafting of all five sites. Preparative HPLC fractions were collected and lyophilized to afford a white solid. This protocol does expend a large quantity of the branch reagent, but to assure that the reaction goes to completion (due to the strict monodispersity needs for ELFSE applications), the expense is deemed acceptable.

Isolated yields for the synthesis of these branched drag-tags are difficult to accurately quantitate since on the scale we performed them (5 mg of backbone), the masses of final product are low (*ca.* 1 mg). The crude yield as determined by RP-HPLC is ? 97 % (Figure 2). However, in order to assure complete monodispersity, only the product appearing in the central area of the RP-HPLC peak was carried on. The drag-tag conjugate molecules were found to have the correct masses by MALDI-TOF mass spectrometry (Table 4). As described above, the derivatized (branched) molecules were then treated with piperidine and further purified to afford drag-tags with free (and unique) primary amino groups at the N-terminus. These molecules were then ready for sulfo-SMCC activation to enable their conjugation to oligonucleotide primers.

Table 2.4 Drag-tag structures, molecular mass confirmation and alpha (?) values.

Compound	Drag-tag	molar mass calcd:found	? (20-base DNA – drag-tag conjugate)	? (30-base DNA – drag-tag conjugate)
4	Acetylated	4023.2 : 4023.5	7.9	7.9
5	Tetramer-branched	6964.9 : 6964.6	12.5	13.7
6	Octamer-branched	9266.1 : 9271.4	16.4	17.2

2.3.5 Sulfo-SMCC activation

The free-amine terminated drag-tags were reacted with the heterobifunctional linker sulfo-SMCC. This reagent consists of two reactive groups: a sulfo-NHS group (reactive toward primary amines), and a maleimide (reactive toward thiols), connected by a cyclohexyl-containing aliphatic linker. The primary amino terminus of the drag-tags reacts with the sulfo-NHS end of the linker. RP-HPLC was then used to remove excess sulfo-SMCC from the reaction mixture, resulting in a high yield (> 95 %) of drag-tag with a reactive maleimide, for subsequent conjugation to thiolated oligonucleotides.

2.3.6 DNA reduction and conjugation to polypeptoids

The 5'-thiolated DNA is obtained as the disulfide dimer, which must be reduced to yield free sulfhydryl groups. Complete reduction of the DNA is essential for obtaining a high yield of the desired conjugate molecule. DNA reduction conditions, involving a 40:1 molar ratio of tris(2-carboxyethyl)phosphine (TCEP) to thiolated DNA, incubated at 40 °C for at least 90 minutes, were found to reliably reduce picomole amounts of disulfide-modified DNA with yields in excess of 80 %. Dithiothreitol (DTT) may also be used for reduction at slightly alkaline pH, although in our experience a larger excess of DTT must be used with a significantly longer incubation at 40 °C to achieve a comparable level of reduction with these very small amounts of thiolated DNA. Solid-phase reducing agents (resin-bound DTT or TCEP) have given us inconsistent results. Literature reports as to the reactivity of TCEP toward maleimides are varied [62-64]. We have found that the presence of excess TCEP does seem to reduce the efficiency of the

conjugation of thiolated DNA to maleimide-activated polypeptoids, and addition of maleimide-activated polypeptoid in slight excess relative to TCEP appears to give optimal conjugation yields (data not shown). Since the polypeptoids in this case are available in large quantities relative to the tiny amounts of DNA required for capillary electrophoresis analysis, the removal of excess TCEP by gel filtration or dialysis was not necessary. Conjugation yields were approximately 70 % for polypeptoids conjugated to the 20-base DNA, and closer to 95 % for polypeptoids conjugated to 30-base DNA.

2.3.7 Free-solution capillary electrophoresis analysis of DNA–drag-tag conjugates and the determination of α values

Capillary electrophoresis with laser-induced fluorescence detection is a powerful and sensitive analytical technique in which charged analytes are separated on the basis of differences in their charge-to-friction ratios, or electrophoretic mobilities. Separations are carried out in narrow fused silica capillaries, which allow efficient heat removal and thus enable the use of higher electric fields than can be maintained in conventional slab gel electrophoresis. DNA separations are typically carried out in 50- or 75- μm inner diameter capillaries filled with a viscous polymer solution or sieving matrix. In this study, modifying DNA oligonucleotides with the drag-tags allowed the separation of DNA in free solution, with no viscous polymer solution. The elimination of the polymer solution simplifies CE operations, and allows the use of narrower capillaries (as small as 25 μm in inner diameter), which afford improved resolution.

The highly negatively charged DNA oligomer component of the drag-tag–DNA conjugates endows each of the bioconjugate molecules with a strong electromotive force

during electrophoresis. The polypeptoid portion gives each molecule an additional amount of hydrodynamic drag. The analysis of the drag-tag-DNA conjugates by free-resolution electrophoresis allows the determination of the frictional parameter ζ of the drag-tag, as described in the introduction (Equation 1).

The results of the electrophoretic analyses of the drag-tags conjugated to the 20-base and 30-base oligonucleotide are shown in Figures 3-4, and ζ values calculated from the experiments are shown in Table 4. The acetylated 30mer **4** gives an ζ of 8, whereas the addition of tetramer and octamer branches increases ζ to about 13 and 17, respectively. Note that the 536-residue protein streptavidin gives a ζ value which is only twice that of the octamer-branched drag-tag (**6**), which comprises only 70 monomers. A high degree of monodispersity is a key property for drag-tags, and these drag-tags display excellent purity (> 99 % by area). Extremely monodisperse drag-tags are necessary for ELFSE analysis because impurities lead to multiple peaks for each size of DNA. Such extra peaks would confound the results of sequencing or other ELFSE separations demanding high resolution. These results give us good confidence in the viability of making high molar mass peptoids for ELFSE applications.

Interestingly, the relationship between ζ and the molecular weight of the drag-tag for these poly-*N*-methoxyethyl glycine-based molecules was found to be essentially linear (Figure 5). Table 4 shows the relative molecular weights and averaged ζ value for each of these drag-tag conjugates with two DNA primers of different length. This study shows that hydrodynamic drag is not simply a function of the length of the backbone. Rather, drag scales linearly with the total molecular weight, or the total number of monomer units. This is in line with previous observations for linear polypeptoids [42]),

and suggests that the polypeptoids, whether branched or linear, adopt an “expanded” conformation in aqueous solution such that all of the monomer units are hydrodynamically exposed to the solvent during electrophoresis.

Figure 2.3 Free-solution capillary electrophoresis analysis of 20-base fluorescently labeled oligonucleotide conjugated to (a) an “unbranched” or acetylated 30mer drag-tag (4), (b) a tetramer-branched drag-tag (5), and (c) an octamer-branched drag-tag (6). Separations were carried out on a BioRad BioFocus capillary electrophoresis instrument at 40°C. The running buffer was 50 mM Tris, 50 mM TAPS, 2 mM EDTA, 7 M urea, pH 8.5, mixed with a 3% (v/v) aqueous dilution of a POP5 solution as a wall coating agent. The fused silica capillary had an inner diameter of 25 μm , and a total length of 25 cm (20.6 cm inlet to detector). Samples were introduced by hydrodynamic injection with a pressure-time constant of 5 $\text{psi}\cdot\text{sec}$. The electric field was 10 kV (400 V/cm), with a typical current of 2.8 μA . The fluorescent label was excited at 488 nm, with emission detected at 520 nm.

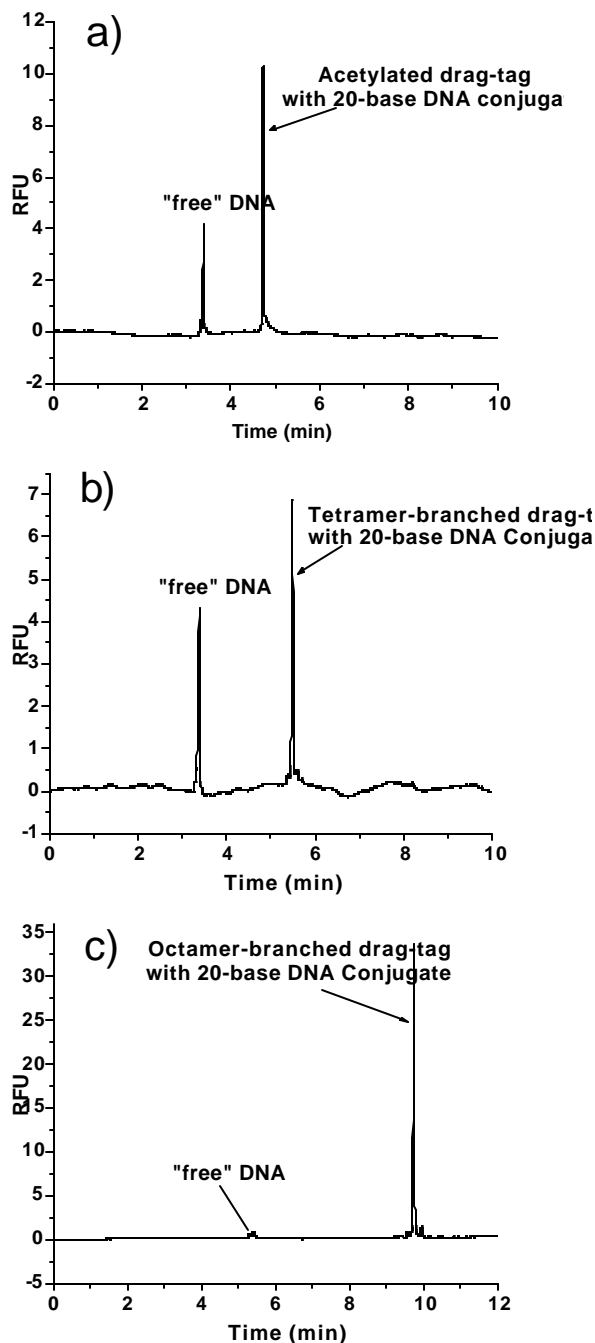


Figure 2.4 Free-solution capillary electrophoresis analysis of 30-base fluorescently labeled oligonucleotide conjugated to acetylated, tetramer-branched, and octamer-branched drag-tags. Separations were carried out on a BioRad BioFocus capillary electrophoresis instrument at 40°C. Conditions similar to Figure 3. The SMCC-activated drag-tags were reacted with freshly reduced 5'-thiolated 30-base DNA primers.

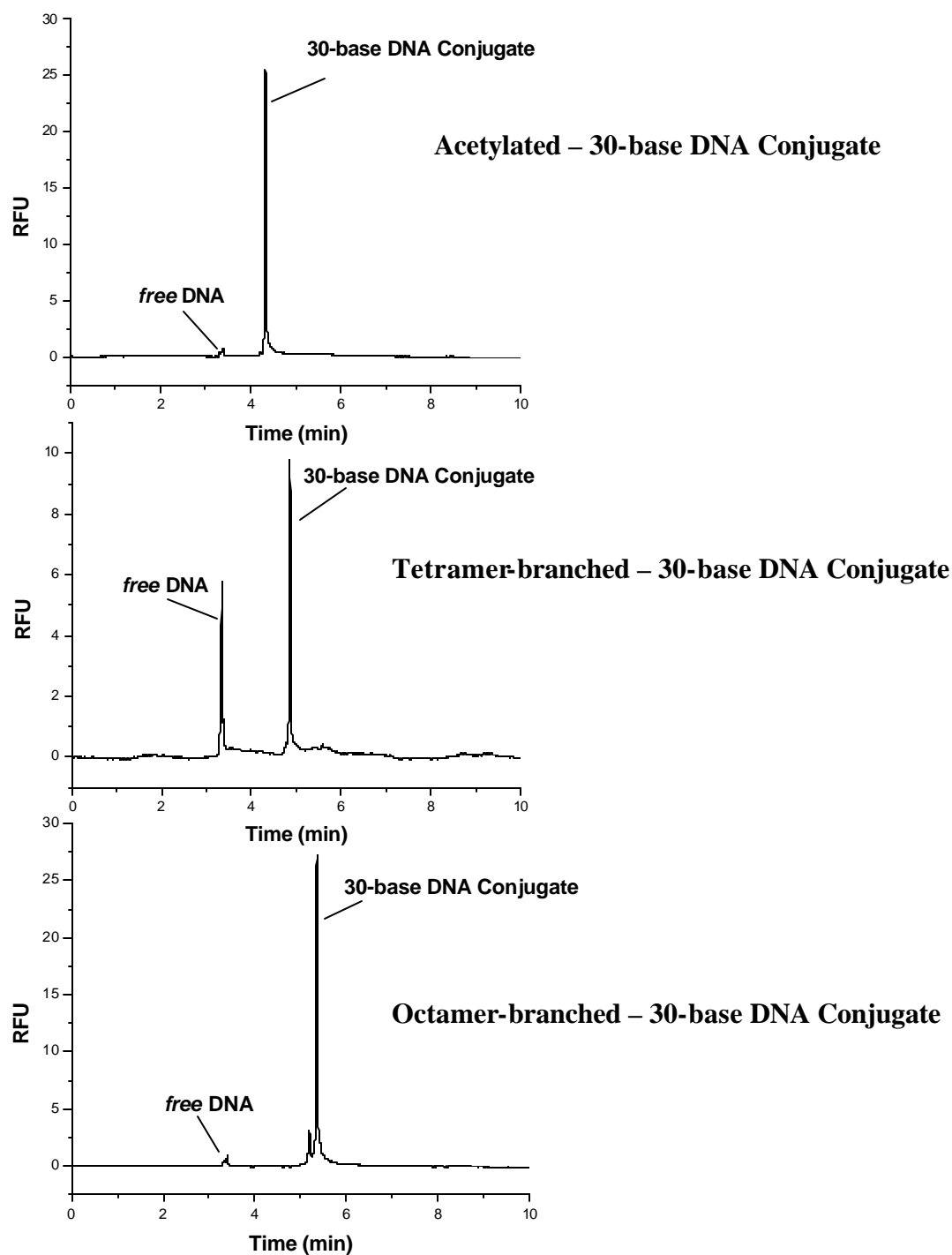
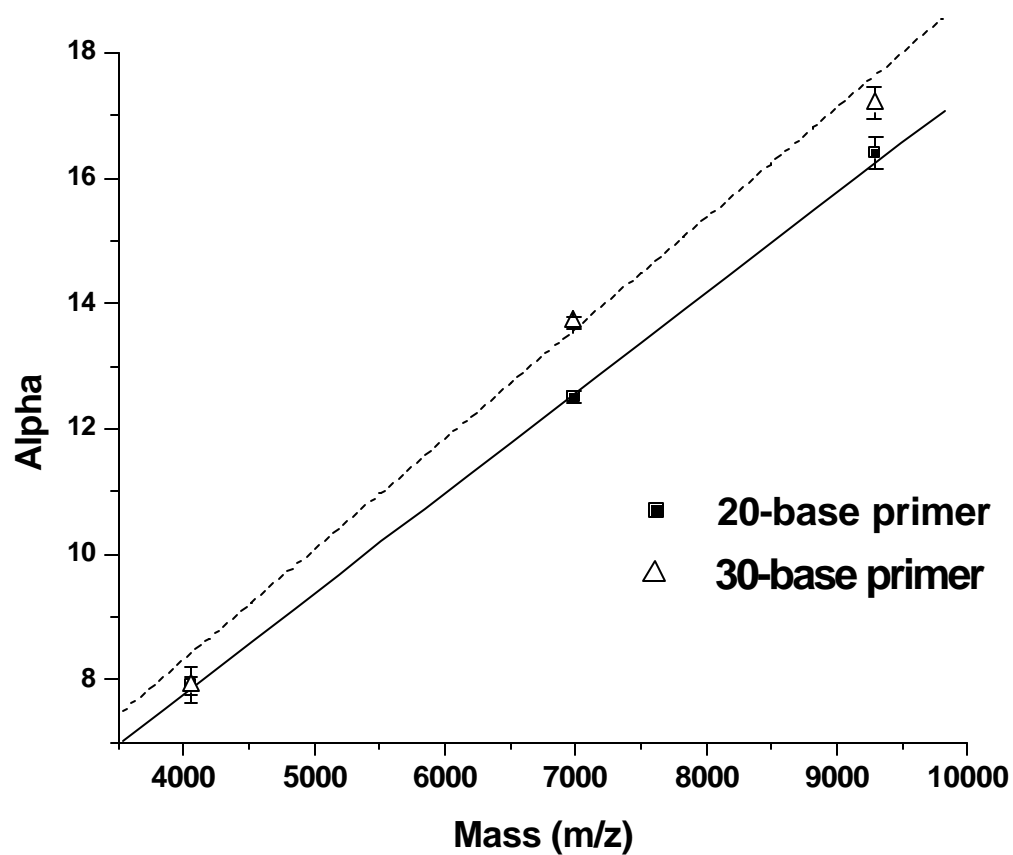


Figure 2.5 Plot of hydrodynamic drag or “?” against molecular weight for the 20-base and 30-base DNA–drag-tag conjugates (for all three drag-tags, 4-6)



2.3.8 Separation of PCR products

The octamer-branched drag-tag (**6**) was utilized in separating thiolated DNA products from a PCR reaction. PCR was used to generate double-stranded DNA fragments of 50, 75, 100, and 150 base pairs in size. The monodisperse, comb-like polymer drag-tag **6** was conjugated to each of the fragments following the PCR reaction, and these conjugate products were successfully separated by CE in free solution, as shown in Figure 6(a). The PCR products were denatured prior to analysis, and analyzed under denaturing conditions, so that the analysis represents single-stranded DNA-drag-tag conjugates. The PCR reaction products were not purified prior to analysis; hence there are some shorter products representing partially amplified PCR products shorter than 50 bases. We left these impurities in the mixture to demonstrate the ability of the drag-tag **6** to resolve small DNA with single-base resolution. The peaks for the 50-base and 75-base fragments are actually split into doublets, indicating the presence of two species (perhaps 50 and 51, and 75 and 76 bases). The reason for this could be due to the propensity of *Taq* polymerase to generate “stutter” or “shadow” bands, in this case possibly adding an extra base during the PCR reaction. Multiple closely spaced peaks are also present for “free” DNA (carrying no drag-tag). There are several different sizes of DNA present in the mixture, including some unreduced disulfide dimers, which may have slightly different mobilities, resulting in the spread of closely spaced peaks centered around 6.1 minutes. For comparison, the separation of these PCR products was performed using a chip-based electrophoresis system (the Agilent 2100 Bioanalyzer), with a polymer solution to provide size-based separation of DNA. The correct sizes of the PCR products were confirmed by comparison to DNA size standards (Figure 6b).

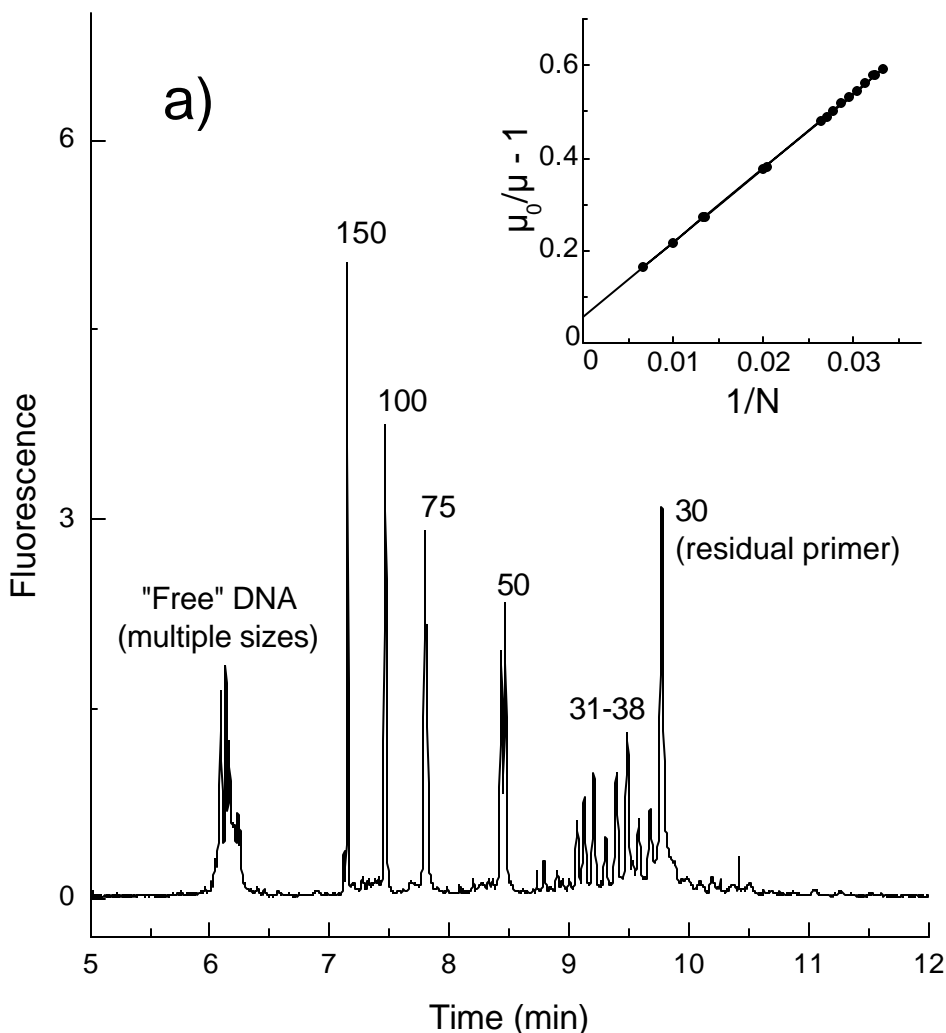
The DNA polydispersity around 50 bases correlates well with what was found using the ELFSE technique (compare Figures 5a and 5b).

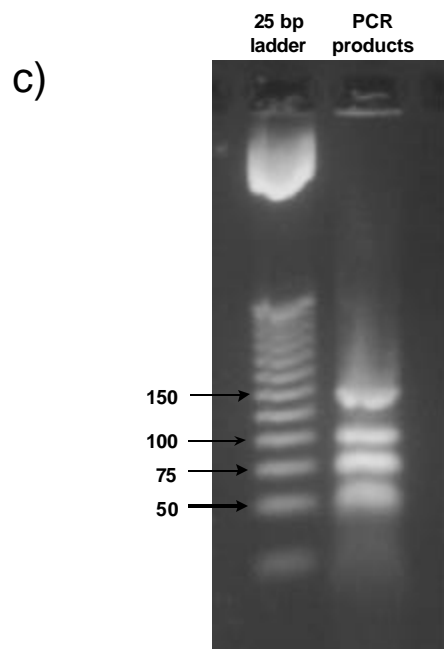
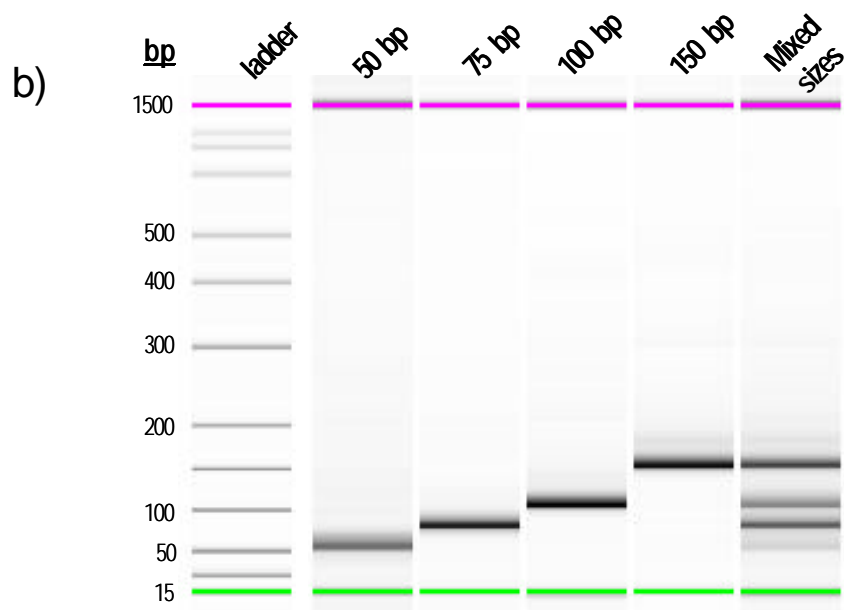
The inset of Figure 6 shows a plot of the mobility ratio $\mu_0/\mu - 1$ versus number of bases for each of the major peaks in Figure 6, including the residual primer and impurity peaks. The tallest of the “free” DNA peaks at 6.13 minutes was chosen as the reference peak for μ_0 . As can be observed by a simple rearrangement of Equation (1), this plot should yield a straight line with slope equal to β . The resulting plot is highly linear ($R^2 = 0.9997$), with a slope of 16.15, in good agreement with the β values calculated from the separations of the 20-base and 30-base oligonucleotides. The intercept is slightly offset from zero; this may be the result of the fluorescein label, which contains a negative charge, and thus slightly affects the electrophoretic mobility of both the conjugates (μ) and the free DNA (μ_0).

This separation of PCR products demonstrates the potential usefulness of branched polypeptoid drag-tags for a wide variety of genotyping or “DNA fingerprinting” applications that require size-based separation of DNA. The mixture shown here was intentionally not purified to demonstrate the resolving power of ELFSE for smaller oligonucleotides (the small impurities are easily separated with single-base resolution). This separation methodology could easily be adapted to analyze double-stranded PCR products as well. The highly monodisperse drag-tag and separation method used here offers excellent resolution and peak shape compared to the previous demonstrations of dsDNA separation by ELFSE using streptavidin [44], due to the true monodispersity and favorable chemical properties of these drag-tags. The octamer-branched drag-tag is likely too small for high-resolution separation of much larger PCR

products or DNA sequencing fragments, but a similar methodology may be employed to construct much larger branched molecules, *e.g.*, using larger branches and/or a longer backbone.

Figure 2.6 a). ELFSE separation of 50-, 75-, 100- and 150-base PCR products (and residual DNA impurities) conjugated to the octamer-branched drag-tag. Samples were denatured in formamide prior to injection. Analysis was performed in free solution on an ABI Prism 3100 instrument with a 36-cm long capillary array (55 μ m i.d. capillaries) at 55°C. The buffer was 50 mM Tris, 50 mM TAPS, 2 mM EDTA, 7 M urea, pH 8.5, mixed with a 3% (v/v) aqueous dilution of a POP5 solution as a wall coating agent. An electrokinetic injection of ~ 22 V/cm for 2 seconds was used. The electric field during the run was ~ 320 V/cm, with a typical current of ~ 8.5 μ A per capillary. The inset is a plot of $(\mu_0/\mu - 1)$ for each of the major peaks, versus the number of DNA bases N (4). b) Analysis of the reduced, thiolated PCR products (from the same reaction as part (a)) on an Agilent 2100 Bioanalyzer, using the DNA 1000 sizing kit. Each sample lane includes 15 bp and 1500 bp markers.





Slab gel analysis of reduced, thiolated PCR products prior to conjugation to the drag-tag. PCR products of different size were pooled prior to this analysis. The slab gel was 3% agarose with TBE buffer and ethidium bromide staining. The ladder (left lane) is a 25 bp DNA step ladder from Promega (Madison, WI).

2.4 Conclusions

In this work, we have developed methodology for creating totally monodisperse, comb-like, hydrophilic and water-soluble copolymers, which were successfully synthesized and characterized. The peptide bonds between the branches and the backbone were formed most efficiently using an excess of glutamic acid-terminated branches, and PyBroP as a coupling reagent. By conjugating the drag-tags to monodisperse DNA oligonucleotides 20 and 30 bases in length, these branched molecules were then evaluated by free-solution CE as ELFSE drag-tags in terms of their respective frictional parameters (ζ and τ). The octamer-branched molecule was also used to successfully separate ssDNA fragments of varying lengths, up to 150 bases.

The ELFSE studies of this family of branched drag-tag–DNA bioconjugates reveal a direct, linear relationship between molecular weight and hydrodynamic drag. This information will prove useful in the future design of drag-tags for applications in free-solution CE. Achieving significant hydrodynamic drag, for poly(*N*meg) peptoids, may be considered a direct function of molecular weight or the number of monomers, rather than simply the length of the backbone.

We intend to use this structural information about drag-tag design to generate drag-tags with tailored designs that allow the free-solution sequencing of hundreds of bases of DNA. A comb-like architecture appears to be an excellent design for drag-tags for the ELFSE technique.

Chapter 3. Theoretical and practical uses of high molar mass branched drag-tags

3.1 Applications for branched drag-tags in ELFSE studies

Previously described branched, poly*N*meg-containing peptoids [41] were found to have many desirable properties that made them ideal for use in multiple electrophoretic applications [65, 66]. In one study, the free-solution electrophoresis of dsDNA modified with synthesized branched peptoid drag-tags at both ends yielded 23% additional drag relative to end-on, singly modified DNA. This significant increase in drag superseded that obtained using linear poly*N*meg peptoids of increasing length. In a subsequent study, multiplexed p53 mutation detection by free-solution conjugate capillary array and microchannel electrophoresis was carried out using the synthesized branched peptoid and other polyamide drag-tags. Using a new bioconjugate approach, sixteen peptoid drag-tags of unique size were conjugated to primers designed to aid in the successful, simultaneous genotyping of sixteen mutation ‘hot spots’ on the p53 gene, exons 5-9. Genotyping was accurate in excess of 96%, with microchannel separation obtained in less than 70 s. These combined works demonstrate the multifunctional nature of these branched peptoids for their use in a variety of applications.

3.2 Free-solution electrophoresis of DNA modified with drag-tags at both ends

Reproduced in part with permission from *Electrophoresis* 2006, 27, 1702-1712, copyright WILEY-VCH Verlag GmbH & Co.

In end-labeled free-solution electrophoresis (ELFSE), DNA molecules are labeled with a frictional modifier or “drag-tag”, allowing their size-based electrophoretic separation in free solution. Among the interesting observations from early work with dsDNA using streptavidin as a drag-tag was that the drag induced by including a streptavidin label at both ends was significantly more than double that from a single streptavidin [44]. This finding was assumed to be in error, and subsequent work focused on experiments in which only a single drag-tag is appended to one end of the DNA molecule. Recent theoretical work [67] has examined the contribution of end-effects to the free-solution electrophoretic mobility of charged-uncharged polymer conjugates, reopening the question of enhanced drag from placing a drag-tag at both ends. In this study, this effect is investigated experimentally, using dsDNA PCR products generated with primers appropriate for the attachment of drag-tags at one or both ends. A range of sizes of drag-tags are used, including synthetic polypeptoid drag-tags as well as genetically engineered protein polymer drag-tags. The enhanced drag arising from labeling both ends has been confirmed, with 10–23% additional drag for the dsDNA arising from labeling both ends than would be expected from simply doubling the size of the drag-tag at one end. These experimental findings demonstrate the feasibility of

enhancing ELFSE separations by labeling both ends of the DNA molecule, leading to greater resolving power and a wider range of applications for this technique.

3.2.1 Introduction

Size-based separations of DNA for applications such as DNA sequencing and genotyping are frequently accomplished by electrophoresis in a polymeric sieving matrix, examples of which include crosslinked gels and highly entangled solutions of linear polymers[68]. Although this technique is a workhorse of modern molecular biology, the sieving matrix imposes limitations on the speed of separation, and electric field-induced band-broadening and molecular orientation effects lead to a reduced ability to separate larger DNA fragments [68-71]. Additionally, crosslinked gels and viscous polymer solutions are problematic to load into miniaturized microfluidic devices currently being developed for DNA sequencing, PCR product sizing, and other electrophoretic separations [72-76].

A variety of alternative DNA separation modes have been proposed for use in capillaries and microfluidic devices [77], including entropic trapping [78, 79], separation in ultradilute polymer solutions [80] or in microfabricated arrays of posts or other obstacles [81, 82]. One exciting approach that has received considerable attention is end-labeled free-solution electrophoresis (ELFSE) [23, 25, 44, 48, 83]. In this approach, DNA is modified end-on with an uncharged, monodisperse, polymeric end-label, or “dragtag” to create a charged-uncharged polymer conjugate. During electrophoresis in free solution, the drag-tag imparts the bioconjugate with a fixed amount of additional hydrodynamic friction. The additional friction modifies the electrophoretic mobility of

the DNA-drag-tag conjugates in a size-dependent fashion: Conjugates comprising small DNA fragments migrate more slowly than conjugates with large DNA fragments, and thus a size-based separation can be accomplished in the absence of a sieving matrix.

The theoretical principles and experimental demonstrations of ELFSE have been recently reviewed [83]. In the first experimental demonstration of ELFSE, streptavidin was used to label dsDNA restriction fragments that had been biotinylated at one or both ends [48]. The efficiency of this separation was limited primarily by the inherent polydispersity of the streptavidin label, as well as by interactions between the streptavidin and the capillary walls. One of the interesting results of this study, however, was that the amount of hydrodynamic drag associated with adding a streptavidin label to both ends of the DNA was observed to be significantly more than twice the friction for adding streptavidin to one end only. Whereas a single streptavidin provided friction equivalent to an additional 23 bp of DNA, two streptavidins provided the friction of an additional 54 bp, 17% greater than would be expected from simply doubling the amount of friction from a single streptavidin. The implications of this finding were not fully appreciated at the time, and, being attributed to experimental error, this effect was not explored further. In later work, a gel-purified streptavidin was used to label ssDNA sequencing fragments generated using a 5'-biotinylated primer [48]. Using the more homogeneous streptavidin as a drag-tag at the 5' end of the sequencing fragments, and employing a more effective wall-coating agent, approximately 110 bases of the four-color sequencing reaction were separated by ELFSE. Although these initial results were promising, the main limitation preventing the further use of ELFSE has been the lack of suitable large, water-soluble, monodisperse drag-tags with appropriate chemical functionality for unique attachment to

DNA. More recently, progress has been made with the development of novel drag-tags consisting of long, repetitive, genetically engineered polypeptides (or “protein polymers”) [84, 85], or linear or branched polyamides synthesized by solid-phase techniques [54, 86, 87]. A variety of these new drag-tags have been used in this study to revisit the potential for performing ELFSE separations of DNA molecules with drag-tags at each end.

3.2.2 Theory of end-effects in ELFSE

The standard theory of ELFSE was developed through investigations into the electrophoretic mobility of polymers with nonuniform charge distributions. For the case of the migration of a DNA-drag-tag conjugate, with a charged DNA segment consisting of M_C charged monomers and an uncharged drag-tag consisting of M_U uncharged monomers, the mobility μ is given by a weighted average of the electrophoretic mobilities of the charged and uncharged monomers:

$$\mu = \mu_0 \frac{M_C}{M_C + \alpha_1 M_U} \quad (1)$$

where μ_0 is the mobility of the charged monomers (*i.e.*, the free-solution mobility of DNA). (The uncharged monomers have zero electrophoretic mobility, and thus do not appear in the numerator of Eq. (1).) The parameter α_1 reweights the number of uncharged monomers M_U to reflect differences in persistence length and other hydrodynamic properties. The product $\alpha_1 M_U$, referred to as α , describes the total friction

provided by the drag-tag, in terms of the number of additional uncharged monomers of DNA that would add equivalent friction. Thus, in the experiments described previously [44], a single streptavidin drag-tag provided $\alpha = 23$, *i.e.*, an amount of friction equivalent to 23 uncharged bp of DNA, whereas two streptavidins gave $\alpha = 54$. Notably, Eq. (1) cannot adequately explain the more than doubling of α arising from using two drag-tags.

The weighting of the individual monomer units in constructing the average in Eq. (1) was recently re-examined theoretically [67]. Whereas previous theory assumed that each monomer unit (after rescaling the uncharged monomers by α) contributes equally to the electrophoretic mobility of the composite molecule, more recent theory has taken into account end-effects originally described by Long *et al.* [26]. According to this theory, monomer units near either end of the polymer chain have greater influence than monomer units near the middle in determining the electrophoretic mobility of the composite molecule. This can be expressed by including a weighting factor Ψ in the calculation of the mobility. For the case of ELFSE, with M_C charged monomers conjugated end-on to M_U uncharged monomers, and scaling M_U by the factor α such that the total number of monomers is effectively $N = M_C + \alpha M_U$, the weighted average mobility is expressed as

$$\mu = \frac{1}{N} \int_0^{M_C} \mu(n) \Psi\left(\frac{n}{N}\right) dn \quad (2)$$

where the index of integration, n , represents the position of a charged monomer unit in the chain. The ratio n/N , which appears as the argument of the weighting function Ψ , ranges from 0 to 1, and represents the relative position of a given monomer unit in the

chain. The limits of integration are written from 0 to M_C (rather than 0 to N) since the uncharged monomers ($n = M_C + 1 \dots N$) have zero electrophoretic mobility, and only the charged monomers contribute to the total. Making the further substitution that for charged DNA monomers, the mobility $\mu(n) = \mu_0$, and using the definition $N = M_C + \alpha_1 M_U$, the mobility of the composite molecule can be written as

$$\mu = \frac{\mu_0}{M_C + \alpha_1 M_U} \int_0^{M_C} \Psi\left(\frac{n}{M_C + \alpha_1 M_U}\right) dn \quad (3)$$

The normalized weighting function $\Psi(n/N)$ of a Gaussian polymer chain was found in [26] to be well represented by the following function:

$$\Psi\left(\frac{n}{N}\right) \approx -0.65 + 0.62\left(\frac{n}{N}\right)^{-\frac{1}{4}} + 0.62\left(1 - \frac{n}{N}\right)^{-\frac{1}{4}} \quad (4)$$

Equation (4) is a well behaved, easily calculated (and easily integrated) function for $0 < (n/N) < 1$, and is depicted in Fig. 1 of [88]. Using this functional form in Eq. (3) allows the straightforward calculation of the electrophoretic mobility for any composite molecule consisting of a DNA chain linked end-on to an uncharged drag-tag chain, provided that the scaling factor α_1 is known for a given set of experimental conditions. For the slightly more complicated case of a charged DNA chain with uncharged dragtags at *both ends* of the DNA chain, Eqs. (2) and (3) need only be modified by changing the limits of integration, and the total number of effective monomer units N . For the case of a DNA chain consisting of M_C charged monomers, with identical drag-tags consisting of M_U uncharged monomers at each end, the total number of effective monomers is now $N =$

$M_C + 2\alpha_1 M_U$. With this change, and inserting the appropriate limits of integration, the mobility becomes

$$\mu = \frac{\mu_0}{M_C + 2\alpha_1 M_U} \int_{\alpha_1 M_U}^{\alpha_1 M_U + M_C} \Psi\left(\frac{n}{M_C + 2\alpha_1 M_U}\right) dn \quad (5)$$

Besides providing a more complete analysis of the electrophoretic mobility of ELFSE conjugates, and improving the quantitative analysis of previous data from the molar mass profiling of PEG [89], the theory of end-effects makes useful predictions for enhancing the performance of DNA sequencing and other separations using ELFSE. The (n/N) function in Eq. (4) has its maxima near the ends of the molecule, indicating that the chain ends are weighted more heavily in determining the electrophoretic mobility of the composite molecule. The heavier weighting of the chain ends implies that adding an uncharged drag-tag to each end of a DNA molecule provides more than twice the drag of using a single drag-tag of the same size at one end of the DNA molecule. This is consistent with the initial experimental observations using streptavidin as a drag-tag [48]. Moreover, since the production of very large, totally monodisperse drag-tag molecules has thus far been problematic [47, 85], the effect might be exploited to provide sufficient drag for high-efficiency separations by using two smaller (and more monodisperse) drag-tags, rather than one larger drag-tag. In this study, we provide experimental confirmation of this effect using large dsDNA PCR products, with drag-tags of varying sizes at one or both ends of the DNA molecules.

Table 3.1 Structures and code names for the six different dragtag molecules used in this study. P1-169 and P2-127 drag-tags had maleimide functionalites added to their N-termini by activation with sulfosuccinimidyl 4-N-maleimidomethyl cyclohexane-1-carboxylate (Sulfo-SMCC), as described in [22].

Drag-tag	Structure
NMEG-20 NMEG-40 NMEG-44	
Branched NMEG-70	
P1-169	$\text{H}_2\text{N} - (\text{Gly Ala Gly Gln Gly Ser Ala})_{24} \text{Gly} - \text{COOH}$
P2-127	$\text{H}_2\text{N} - (\text{GAGTGSA})_4 - \text{GAGTGRA} - (\text{GAGTGSA})_7 - \text{GAGTGRA} - (\text{GAGTGSA})_5 - \text{G} - \text{COOH}$

3.2.3 Materials and methods

3.2.3.1 Chemicals

Tris(2-carboxyethylphosphine) (TCEP) and maleimide were purchased from Acros Organics (Morris Plains, NJ, USA). Sulfosuccinimidyl 4-*N*-maleimidomethyl cyclohexane-1-carboxylate (Sulfo-SMCC) was purchased from Pierce (Rockford, IL, USA). Buffer salts Tris (free base), *N*tris(hydroxymethyl)methyl-3-aminopropane-sulfonic acid (TAPS), and EDTA were purchased from Amresco (Solon, OH, USA). POP-6 polymer solution was purchased from Applied Biosystems (Foster City, CA, USA). All water was purified using an E-Pure system from Barnstead (Boston, MA, USA) to a minimum resistivity of 17.8 M Ω cm.

3.2.3.2 Drag-tag molecules

Six different drag-tag molecules were used in this study. Three were linear *N*-methoxyethylglycine (*N*meg) oligomers of length 20, 40, or 44 monomers, produced by a solid-phase submonomer synthetic protocol [12], capped with an *N*-terminal maleimide, and purified to monodispersity by RP-HPLC as described previously [86, 87, 89]. Another drag-tag used was a monodisperse branched molecule consisting of a 30mer poly(*N*meg) backbone with five octamer oligo(*N*meg) branches, also described previously [41]. The final two drag-tags were repetitive protein polymers of length 127 and 169 amino acids, produced using the controlled cloning technique [47], and activated at the *N*-termini using the heterobifunctional cross-linker Sulfo-SMCC by reacting the protein polymers with a ten-fold molar excess of Sulfo-SMCC for 1 h at room temperature and pH 7.2, and then removing excess cross-linker by gel filtration as

described previously [47, 85]. The structures and short names of the drag-tags are shown in Fig. 1. The large tags were used for the studies of dsDNA. All of the drag-tags used are hydrophilic, water-soluble molecules. Following the maleimide activation of the *N*-termini, the *N*meg drag-tags are charge-neutral, whereas the P1–169 has a net charge of –1 (from deprotonation of the C-terminus), and the P2–127 (with two cationic arginine residues) has a net charge of 11.

3.2.3.3 *Production of dsDNA conjugates*

Oligonucleotides used as PCR primers were purchased from Integrated DNA Technologies, and are shown schematically in Table 1. The oligonucleotides consist of an M13 forward primer with a 5'-thiol linker and an internal fluorescein-dT base, and a set of M13 reverse primers, with or without 5'-thiol linkers, designed to produce dsDNA products of 75, 100, 150, or 200 bp in size when used in a PCR reaction with the forward M13 primer.

PCR reactions were performed using Pfu Turbo polymerase (Stratagene, La Jolla, CA, USA). Eight reactions were carried out with 20 pmol of the fluorescently labeled, thiolated M13 forward primer, and 20 pmol of each of the M13 reverse primers shown in Table 1, in a total volume of 20 mL. M13mp18 control DNA from a sequencing kit (0.2 mL) (Amersham Biosciences, Piscataway, NJ, USA) was used as a template. The M13 template was PCR-amplified with 32 cycles of denaturation at 94°C for 30 s, followed by annealing at 54°C for 30 s and extension at 72°C for 60 s. Products were analyzed by 2.5% agarose gel electrophoresis to confirm the sizes of the dsDNA amplicons, and the products were stored at –20 °C until subsequent use.

Thiolated PCR products were reduced using a large excess of TCEP. To do this, 7 μ L of PCR product was mixed with 0.7 μ L of 1 M TCEP (in 1 M Tris buffer), plus an additional 0.35 μ L of 1 M Tris, resulting in a solution of pH \sim 5. This mixture was incubated for 2–2.5 h at 40 $^{\circ}$ C. Excess TCEP as well as PCR reaction components was removed using QIAquick PCR purification spin columns (QIAGEN, Valencia, CA, USA) according to the manufacturer's instructions, with elution of the purified DNA in 30 μ L of 100mM sodium phosphate buffer, pH 7.2.

The purified PCR products (with one or two reduced thiols, depending on the reverse primers used) were split into multiple aliquots, and treated with one of four maleimide- activated drag-tags: *N*meg-44, branched *N*meg-70, P1–169, or P2–127. The amounts of drag-tag were sufficient in most cases to produce significant quantities of DNA with one or two drag-tags. Additional aliquots were treated with excess maleimide, to simply cap the reduced thiols and prevent further reaction or dimerization.

Table 3.2 Oligonucleotides used as PCR primers for producing dsDNA conjugates with drag-tags at one or both ends.

Oligonucleotide	Sequence
M13-Forward	X ₁ CCX ₂ TTTAGGG TTTTCCCAGT CACGACGTTG
75-Reverse	GAGTCGACCT GCAGGCATGC
75-Reverse-T	X ₁ GAGTCGACCT GCAGGCATGC
100-Reverse	GAGCTCGGTA CCCGGGGATC
100-Reverse-T	X ₁ GAGCTCGGTA CCCGGGGATC
150-Reverse	GCGGATAACA ATTTACACA
150-Reverse-T	X ₁ GCGGATAACA ATTTACACA
200-Reverse	CCAGGCTTTA CACTTTATGC
200-Reverse-T	X ₁ CCAGGCTTTA CACTTTATGC

X₁, 5'-thiol linker with 6-carbon spacer; X₂, internal fluorescein-dT base

3.2.3.4 CE analysis of conjugates

Free-solution CE analysis was performed using an Applied Biosystems Prism 3100 Genetic Analyzer (Applied Biosystems), using an array of 16 fused-silica capillaries with inner diameter of 50 μ m and a total length of 47 cm (36 cm to the detector). The running buffer was 89 mM Tris, 89 mM TAPS, 2 mM EDTA, pH 8.5, and 1% v/v POP-6 polymer solution to act as a wall-coating agent, with the adsorbed poly(dimethylacrylamide) effectively suppressing the EOF [90]. (The resulting polymer concentration is very low, and does not lead to any size-based sieving of the DNA.) Samples were diluted in water prior to analysis, to provide signals of appropriate strength for the fluorescence detector. The dsDNA samples were analyzed at 25 °C to prevent denaturation. Samples were introduced into the capillaries by electrokinetic injection at 1 kV (22 V/cm) for 2–20 s. Separations were carried out at 15 kV (320 V/cm). The fluorescein label of the DNA was detected in the “G” channel of ABI Dye Set E5, with λ_{max} 530 nm.

3.2.4 Results – analysis of dsDNA conjugates

dsDNA conjugate molecules were produced by performing PCR using a thiolated forward primer and normal (unthiolated) reverse primer (for production of dsDNA conjugates with a drag-tag at one end only), or using thiolated forward and reverse primers (for production of dsDNA conjugates with drag-tags at both ends). A large excess of TCEP was used for reduction of the thiols after the PCR reaction. Since TCEP is supplied as an HCl salt, the use of a large excess results in an acidification of the PCR buffer. To compensate for this, and to prevent longterm exposure of the DNA to very

acidic conditions, additional 1 M Tris was added to the reduction mixture, resulting in a more acceptable pH. Following the reduction, the PCR products were purified using QIAquick spin columns, which effectively remove residual buffer salts, surfactants, enzyme, and reducing agents left over from the PCR reaction and reduction, which might otherwise interfere with reaction with the drag-tags.

The drag-tags used for the dsDNA conjugates were two moderately large synthetic polypeptoids (linear *Nmeg-44* and branched *Nmeg-70*), and two protein polymers produced by genetic engineering of *Escherichia coli*. The branched *Nmeg-70* and the P1–169 drag-tags have been described previously for the separation of denatured (single-stranded) PCR products of sizes similar to those described here [41, 85]. In this study, CE analysis was performed at room temperature with no denaturants in the buffer, ensuring that the DNA remained in its double stranded state. Keeping the DNA in its double-stranded state allows for the easy incorporation of a drag-tag at both ends, which was expected to generate more than twice the drag of a single drag-tag, allowing the separation of a wider size range of dsDNA molecules.

The concentration of the DNA purified with the QIAgen spin column was too low for accurate measurement of absorbance at 260 nm, and thus the molar ratios of DNA to drag-tag are not known precisely. The amounts of drag-tag were generally sufficient to produce significant amounts of product with zero and one drag-tag (for products with only the forward primer thiolated), and zero, one, and two drag-tags (for PCR products with both primers thiolated). Typical electropherograms for two sizes of DNA (100 bp and 200 bp) with the P2–127 protein polymer are shown in Fig. 2. In each case, the migration time of the “free” DNA (with no drag-tag) is around 6.2 min. In panels (A)

and (C), which show PCR products generated with only a thiolated forward primer, the free DNA peak is followed by a single peak, corresponding to DNA with a single drag-tag. In panels (B) and (D), which show PCR products generated with both forward and reverse thiolated primers, there is an additional peak 1–2 min later, corresponding to DNA with a drag-tag at both ends. Note also in panels (B) and (D) that, for the products generated with both primers thiolated, there are two closely spaced peaks migrating around the same time as the product with one drag-tag in panels (A) and (C). The exact cause of this phenomenon is unknown, but it was observed for all sizes of dsDNA with all of the dragtags, and may result from slight differences in electrophoretic mobility arising from labeling at either end of the DNA molecules.

The P1–169 and P2–127 protein polymers used here as drag-tags were not entirely monodisperse [85], leading to some additional peak broadness. The additional broadness is most noticeable with the smaller sizes of DNA, and is more pronounced for the species with two drag-tags. Both of these effects are as expected. Sharper peaks for larger sizes of DNA conjugated to impure drag-tags (including P1–169) were reported in [85], and are also in line with theory presented in [42]. The conjugation of a polydisperse drag-tag to both ends of a DNA molecule leads to a large number of possible combinations, each with slightly different electrophoretic mobility, which is apparent as additional peak broadness. The *N*meg-44 and branched *N*meg-70 drag-tags, both of which were purified to near monodispersity by RP-HPLC, generate cleaner, sharper peaks than the protein polymer dragtags.

Alpha values were calculated from the peak migration times of each species. In previous ELFSE literature, the relative mobilities of unlabeled and labeled DNA (α_0/α) would be

plotted with respect to $1/M_C$, resulting in a straight line with slope η [44, 48]. This approach neglects the end-effects theory, which predicts η different overall value of η for each size of DNA. In this case, such plots are still essentially linear (not shown), and can be used to give an average apparent value of η for each drag-tag, as given in Table 2. (Note that the average η values determined by the linear fit of η_0/η vs. $1/M_C$ are not necessarily equal to the arithmetic average of the individual η values calculated for each size of DNA.) As indicated by the right-most ("Ratio") column in Table 2, the average η for two drag-tags is noticeably greater (10–23%) than twice η for a single-drag-tag, for these dsDNA species.

Figure 3.1 Example electropherograms of dsDNA conjugated to a drag-tag. (A) 100-bp PCR product with forward primer thiolated, (B) 100-bp PCR product with both primers thiolated, (C) 200-bp PCR product with forward primer thiolated, and (D) 200-bp PCR product with both primers thiolated. Analysis conditions were the same as Fig. 2, except the run temperature was 25 °C and the injection was 1 kV for 20 s. Peaks labeled 0, 1, and 2 refer to DNA species with zero, one, or two drag-tags, respectively.

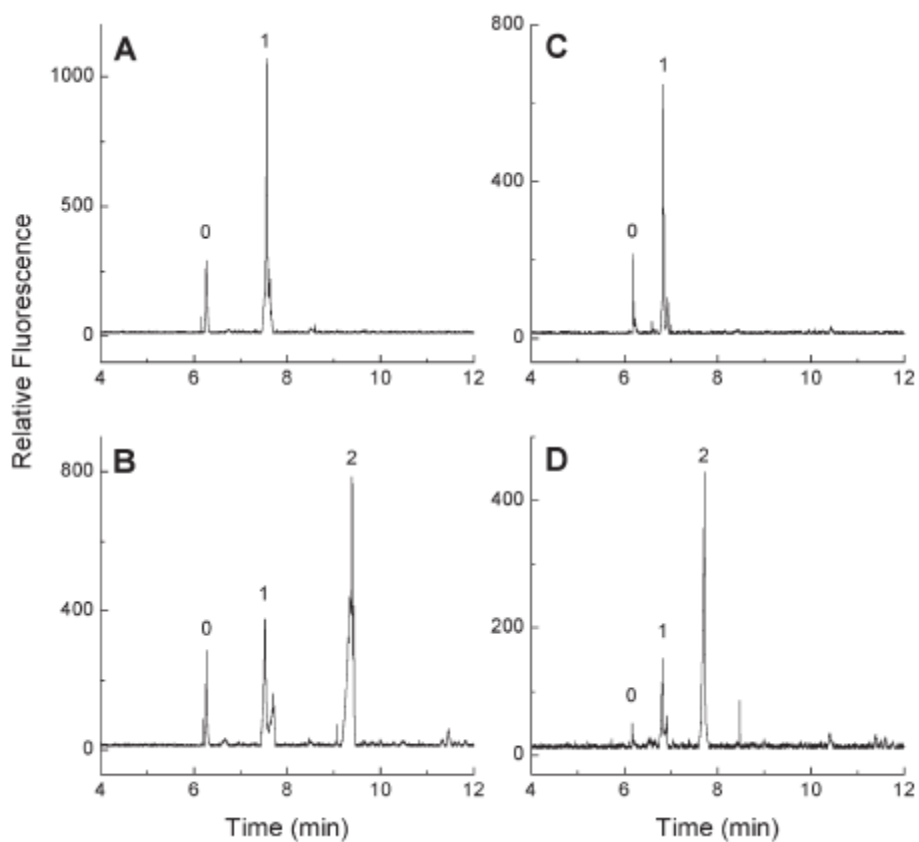


Table 3.3 Apparent frictional parameter a for dsDNA with one or two drag-tags, averaged for all sizes of DNA

Drag-tag	Average α	Ratio ($\alpha_{(2)}/2\alpha_{(1)}$)
NMEG-44 (one)	12.7	1.10
NMEG-44 (two)	28.0	
Branched NMEG-70 (one)	17.0	1.22
Branched NMEG-70 (two)	41.6	
P1-169 (one)	27.2	1.13
P1-169 (two)	61.7	
P2-127 (one)	19.9	1.23
P2-127 (two)	48.8	

Final column gives the ratio of the drag for a tag at each end vs. the expected drag for a single tag of twice the size.

3.2.5 Discussion

The quantitative end-effect theory is not directly applicable to the dsDNA data presented here. Although the dsDNA products are significantly longer, dsDNA is also considerably stiffer than ssDNA. Thus, even the longer dsDNA products are more likely to resemble stiff rods or cylinders, rather than random coils. Even with such a geometry, there is still likely an end-effect, which is dramatically illustrated by the experimental measurements of a presented in Table 2. Since the dsDNA-drag-tag conjugates are not likely to even approximate Gaussian coils, application of the theory used for ssDNA conjugates is not appropriate.

The drag enhancement for placing a drag-tag at each end of dsDNA is noticeably larger than was observed for placing a drag-tag at each end of ssDNA (ssDNA data not shown). This could simply be a function of the specific sizes of DNA and drag-tags that were chosen for study, but it may also be the result of the stiff rod-like structure of the dsDNA. Because the dsDNA molecules studied here are relatively short, the ends of the dsDNA molecule are more often on the “outside” of the chain, as opposed to a true Gaussian coil for which the chain ends may occupy positions in the interior of the coil. In addition, there may be a greater degree of hydrodynamic segregation between the rod-like dsDNA and the random coil drag-tags. Detailed theoretical analysis is required to determine if these simple arguments can explain the larger end-effect observed for dsDNA in these experiments.

The enhanced drag arising from placing a drag-tag at both ends of DNA leads to interesting new possibilities for sequencing and genotyping by ELFSE. The separation capacity of ELFSE is tied directly to the amount of friction generated by the drag-tag, and

previous efforts have been focused on creating larger drag-tags to generate more friction. The possibility of including a drag-tag at both ends extends the range of separations that are possible with existing drag-tags. This is particularly important as the production of very large, totally monodisperse protein polymer drag-tags has proven difficult [47, 85]. The direct application of this technique to DNA sequencing would be difficult with current commercially available dye terminator chemistry, which presents no convenient functional group for attaching a second drag-tag at the 3'-end of the sequencing fragment. The application of labeling both ends to the separation of dsDNA generated by PCR is more straightforward than ssDNA, given the wide availability of custom-synthesized DNA primers with a variety of functional groups and linkers that can be incorporated at the 5'-end.

This study has provided verification of an important and interesting prediction of the new theory of end-effects in ELFSE separations. Using larger dsDNA products generated by PCR, labeled at one or both ends with a variety of drag-tags, it has been shown that the drag induced by labeling both ends is more than double the drag arising from a single drag-tag at one end, and is also larger than the drag that would arise from a single drag-tag of twice the size at one end. The effect is significant, with drag (?) enhanced 10–23% for the dsDNA in the size range tested with the available drag-tags. Specifically, the *Nmeg-70* branched drag-tag yielded the close to the largest amount of drag of the dsDNA conjugates, and exhibited cleaner, sharper peaks in the electropherograms than protein polymers due to its near monodispersity. Monodispersity was improved due to the *Nmeg-70* branched drag-tag being conjugated to DNA using sulfo-SMCC which is less prone to hydrolysis. This enhanced drag from double end-

labeling could potentially be useful for various types of ELFSE separations such as DNA sequencing, if a suitable experimental approach can be developed for incorporating a drag-tag on each end of the DNA prior to analysis.

3.3 Multiplexed p53 mutation detection by free-solution conjugate capillary and microchannel electrophoresis with polyamide drag-tags

Reproduced in part with permission from *Analytical Chemistry* **2007**, 79, 1848-1854.

Copyright 2007. American Chemical Society.

A new, bioconjugate approach was used to perform highly multiplexed single-base extension (SBE) assays, which was demonstrated by genotyping a large panel of point mutants in exons 5-9 of the p53 gene. A series of monodisperse polyamide “drag-tags,” including a branched drag-tag, was created using both chemical and biological synthesis and used to achieve the high-resolution separation of genotyping reaction products by microchannel electrophoresis without a polymeric sieving matrix. A highly multiplexed SBE reaction was performed in which 16 unique drag-tagged primers simultaneously probe 16 p53 gene loci, with an abbreviated thermal cycling protocol of only 9 min. The drag-tagged SBE products were rapidly separated by free-solution conjugate electrophoresis (FSCE) in both capillaries and microfluidic chips with genotyping accuracy in excess of 96%. The separation requires less than 70 s in a glass microfluidic chip, or about 20 min in a commercial capillary array sequencing instrument.

The SBE-FSCE technique allows the simultaneous genotyping of 16 mutation “hot-spots” in p53 exons 5-9, using the 16 different primers described in Table 1, which

range in size from 17 to 23 bases. Each primer was conjugated to a monodisperse polyamide drag-tag of unique size, chosen from a set of drag-tags that included 14 different lengths of linear poly(*N*-methoxyethylglycine) (poly(NMEG)), one branched poly(NMEG), and one genetically engineered protein polymer. The 15th drag-tag was a branched polypeptoid, consisting of a 30mer poly(NMEG) backbone derivatized with five 8mer oligo-(NMEG) branches, activated at the *N*-terminus with sulfosuccinimidyl 4-(*N*-maleimidomethyl)-1-cyclohexane carboxylate (Sulfo-SMCC).

A multiplexed SBE reaction with fluorescent ddNTPs extends the primer-drag-tag conjugates by one base, and rapid, high-resolution separation of the bioconjugates by free-solution microchannel electrophoresis allows unambiguous determination of the genotypes simply by the observation of the color of each product peak. Figure 1 shows a typical separation of the wild-type p53 SBE products, achieved using a commercial CE sequencing instrument. The CE separation gives 16 sharp, well-resolved peaks of different colors, each of which corresponds to the wild-type genotypes shown in Table 1. We confirmed the identity of each peak and the yield of the conjugation reaction by separate CE analysis of individual drag-tag-primer conjugates (data not shown).

In samples with a point mutation at one or more loci, the corresponding peak(s) change color from those observed for the wild-type sample. For example, in Figure 2A, the sixth peak is green rather than black, indicating a C-to-A substitution mutation at locus 249-3. Other templates displayed mixed genotypes at certain loci, as in Figure 2B, which illustrates peaks of 2 colors at 2 loci. This sample heterozygosity was confirmed by direct sequencing. Notably, these dual genotypes were typically a mixture of wild-

type and the expected mutation, indicating that the original sample cell lines must contain mixed populations of wild-type and mutant cells.

Of 16 loci across 22 mutant templates (352 loci total), SBE-FSCE correctly and reproducibly genotyped 325 loci. Twenty-seven loci reproducibly gave genotypes that were different from those that we expected on the basis of direct sequencing that had been done by our collaborators at NIST, including 10 apparent heterozygotes. When the original NIST genetic samples were then re-sequenced at Northwestern University, 14 of the 27 unexpected genotypes were confirmed to be accurate, including 5 of the 10 apparent heterozygotes; hence, SBE-FSCE more accurately identified these heterozygotes than the original direct sequencing done at NIST. Ten of the remaining unexpected SBE-FSCE genotypes could not be confirmed because the scarce samples could not be sufficiently amplified for re-sequencing. We expect, however, on the basis of the other results, that many of these SBE-FSCE results are correct for these samples as well. Overall, 339 of the 352 loci could be confirmed to be correctly genotyped, representing a confirmed accuracy of 96.3% for SBE-FSCE. Accuracies in excess of 99% have been reported for other SBE-based assays, 42 and the molecular biology of the SBE reaction is seemingly not affected by the drag-tag's presence.

Table 3.4. Design of primers for multiplexed SBE-FSCE. The branched, polyNmeg peptoid is conjugated to exon 5, locus 144-1.

Table 1. Design of Primers for Multiplexed SBE-FSCE^a							
exon	locus	strand	sequence	drag-tag size	migration order	wild-type	
9	328-1	-	AAG ACT TAG TAC CTG AAG GGT GA	8	1	A	
5	128-1	+	CCT TCC TCT TCC TAC AGT ACT CC	12	2	C	
9	330-2	-	GGT CCC AAG ACT TAG TAC CTG A	16	3	A	
6	198-1	-	ACT CCA CAC GCA AAT TTC CTT	20	4	C	
6	196-2	-	ACA CGC AAA TTT CCT TCC ACT	24	5	C	
7	249-3	-	GTG ATG ATG GTG AGG ATG GG	28	6	C	
6	196-1	+	CCC CTC CTC AGC ATC TTA TC	32	7	C	
7	245-1	+	TAA CAG TTC CTG CAT GGG C	36	8	G	
8	273-1	+	ACG GAA CAG CTT TGA GGT G	40	9	C	
8	273-2	-	CCA GGA CAG GCA CAA ACA	44	10	C	
5	173-1	+	CAG CAC ATG ACG GAG GTT	48	11	G	
6	221-3	+	TGT GGT GGT GCC CTA TGA	52	12	G	
5	149-1	+	GTG CAG CTG TGG GTT GAT	56	13	T	
5	175-2	+	GAC GGA GGT TGT GAG GC	60	14	G	
5	144-1	+	CCA AGA CCT GCC CTG TG	70 ^a	15	C	
5	173-2	+	AGC ACA TGA CGG AGG TTI	127 ^{**a}	16	T	

^a The drag-tags are all linear poly-N-methoxyethylglycines made by solid-phase synthetic methods, except for a branched 70mer NMEG (*)³⁰ and a linear 127mer genetically engineered protein polymer (**).

Figure 3.2. Four-color electropherogram showing the FSCE separation of the products of a 16plex SBE genotyping reaction with a wildtype p53 template. Separations were performed in free aqueous solution on an ABI 3100 CE instrument using a capillary array with an effective length of 36 cm. The buffer was 89 mM Tris, 89 mM TAPS, 2 mM EDTA with 7 M urea. The run temperature was 55 °C. Samples were injected electrokinetically at 44 V/cm for 20 s. The field strength for the separation was 312 V/cm, with a current of 11 μ A per capillary. Each peak is labeled with the corresponding p53 locus and genotype.

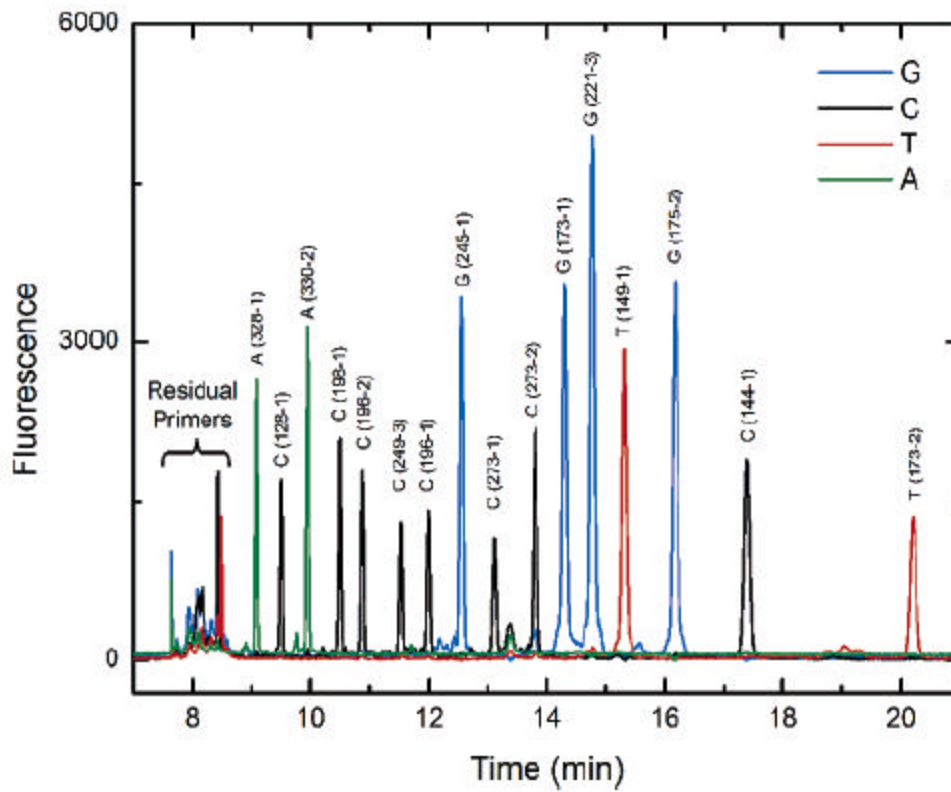
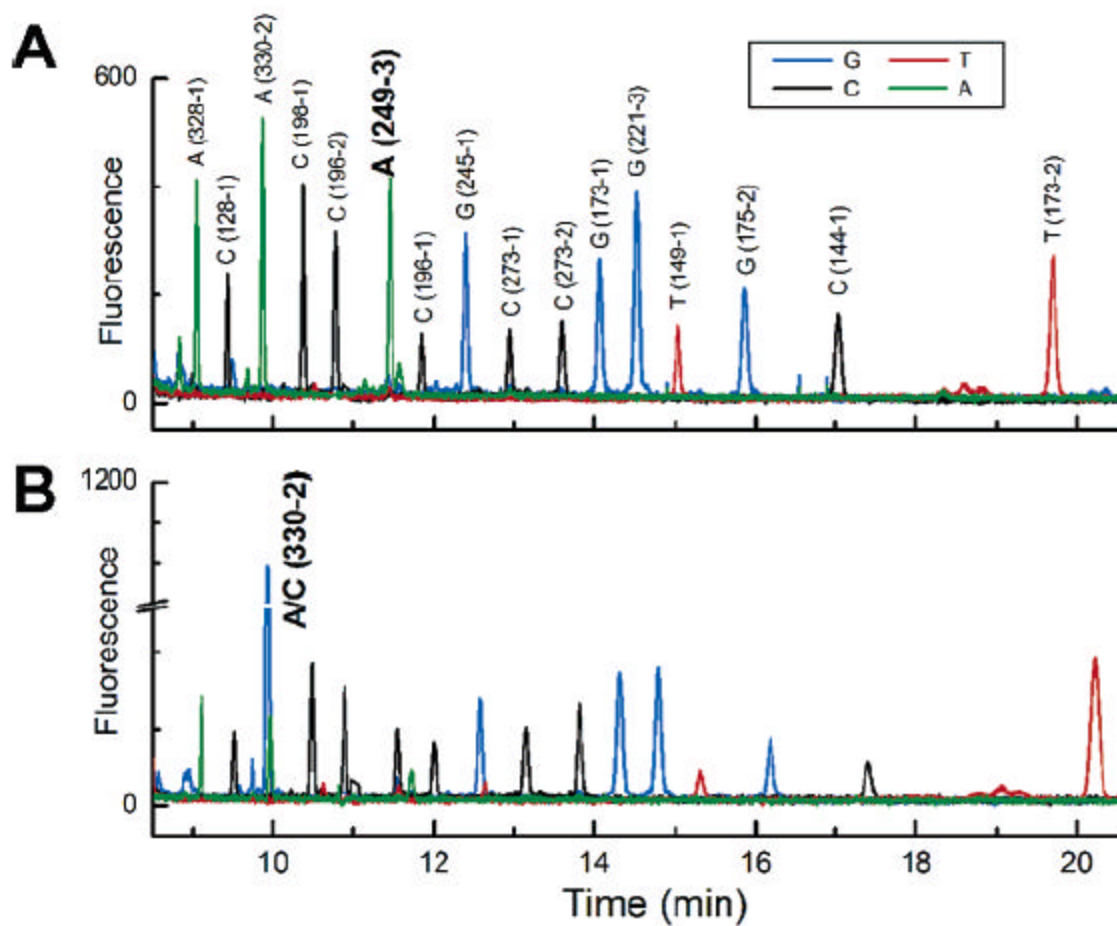


Figure 3.3. (A,B) Four-color FSCE electropherograms showing the analysis of 16plex SBE reactions using PCR amplicons of two different p53 variants as templates, with the mutated loci highlighted, including two heterozygotes confirmed by re-sequencing of the mutant template in (B). Separation conditions are the same as described for Figure 1.



3.4 Conclusions

In summary, branched, poly*N*meg-containing peptoids were successfully used for two fairly diverse electrophoretic applications. In one case, a branched peptoid-dsDNA conjugate exhibited superior separation and drag when dsDNA was doubly modified, and in the other, multiplexed genotyping was achieved with the use of this peptoid in combination with 15 others. In the latter study, the branched peptoid-DNA conjugate was utilized in both capillary array (separation in ~ 20 min) and microchannel (separation in ~ 70 s) electrophoresis. Therefore, this peptoid scaffold has proven to be a versatile, multifunctional molecular tool that enhances electrophoretic DNA-related separation results in several separate studies. The molecule's performance in these cases indicates a potential need for its use in many biologically relevant applications where chemical stability, high molecular weight, or monodispersity are strictly required.

Chapter 4. ELFSE DNA sequencing using a chemically synthesized drag-tag

A monodisperse poly-*N*-substituted glycine (polypeptoid) was evaluated as a synthetic drag-tag for capillary-based DNA sequencing using end-labeled free solution electrophoresis (ELFSE), where a read length of 100 bases in 16 minutes was achieved. ELFSE enables rapid separation of DNA sequencing fragments with single-base resolution, without a polymeric sieving matrix. Protein-based drag-tags previously used in ELFSE sequencing suffer from heterogeneity and charge-based band broadening, which significantly decreases the ability to obtain single-base resolution. The 11 kDa, 70 monomer unit peptoid drag-tag in this study was predominantly composed of poly-*N*-methoxyethylglycine (*N*meg), resulting in a hydrophilic, polyethylene glycol (PEG)-like molecule. This proof-of-concept study demonstrates the first instance of DNA sequencing using a synthetic drag-tag, and indicates that high molecular weight variants would be ideal molecules to reach a commercially competitive number of sequenced bases.

4.1 Introduction

4.1.1 Background

Capillary- and microchip-based electrophoresis techniques have significantly advanced high throughput DNA sequencing relative to the original slab gel methods [91-95]. Microchannel separations generally require viscous polymer matrices, which are

expensive and difficult to load, particularly into microfluidic chips [41, 66]. End-labeled free solution electrophoresis (ELFSE) is a matrix-free separation technique that relies on appending a mobility modifier or “drag-tag” to each DNA fragment [23, 25], resulting in size-based separation of DNA without a sieving matrix. While ELFSE has tremendous potential, most of the setbacks encountered thus far can be attributed to inferior molecular characteristics in the drag-tag [41, 47, 48, 96]. An ideal drag-tag would comprise the following: large size to provide adequate drag to separate long DNA fragments, monodispersity to ensure electropherograms can be interpreted easily, and charge neutrality to prevent non-specific interactions with the microchannel wall [26, 41, 42, 97, 98].

Both native and expressed proteins have been previously utilized as drag-tags for ELFSE sequencing. Typically, the globular nature, charged residues, and polydispersity of these proteins result in band broadening and a decrease in single base resolution of DNA sequencing data [48], although rationally designed protein polymers have recently been demonstrated for high-resolution sequencing [96]. Synthetic polymers such as PEG are generally unsuitable as drag-tags, due to polydispersity of size, even for so-called “monodisperse” preparations [89]. Poly-*N*-substituted glycines (peptoids) have been investigated as drag-tags due to their highly tunable properties, facile solid-phase synthesis, and stability [41, 65, 87, 89]. One perceived limitation of peptoids, however, is the difficulty of using solid-phase techniques to directly synthesize molecules larger than about 50 monomers for long read-length DNA sequencing.

In a previous study, we investigated the effect of peptoid architecture on hydrodynamic drag. A comb-like *N*-(methoxyethyl)glycine (*N*meg)-containing peptoid,

with 70 monomers total, was presented as the highest molecular weight example [41]; the structure of this branched molecule is illustrated in Table 1. Importantly, the amount of drag generated by the branched drag-tags scaled linearly with molecular weight, indicating that large drag could be obtained without the difficulty of synthesizing large, totally monodisperse linear polymer molecules.

4.1.2 Theoretical analysis

The amount of drag created by the drag-tag can be characterized in terms of the effective friction coefficient ζ , which is the hydrodynamic drag of the tag, relative to the drag generated by a single base of ssDNA [25] [99]. The drag parameter ζ can be estimated from the mobility μ of a drag-tag modified DNA fragment of M_c bases, relative to the free-solution mobility of DNA, μ_0 , as shown in Equation (1):

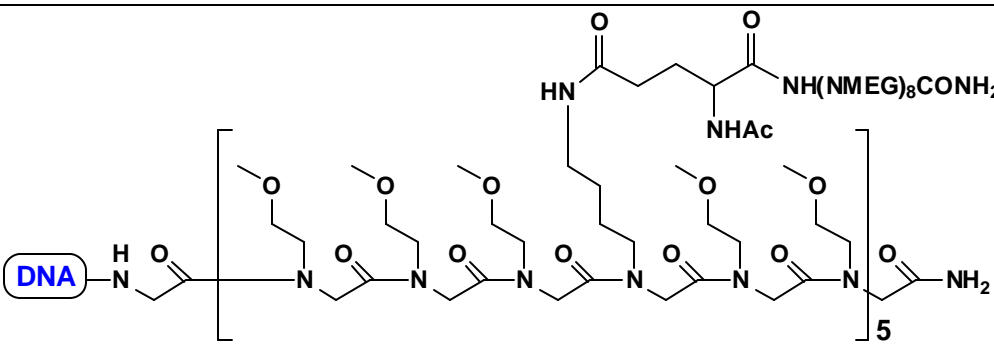
$$\frac{\zeta}{\zeta_0} = \frac{N}{N_0} \quad (1)$$

In previous work, the 70mer branched drag-tag was conjugated to 20mer and 30mer DNA oligonucleotides, and to single-stranded PCR products up to 150 bases in length; in these experiments we found ζ to be 17.2 [41]. The resolution R for diffusion-limited ELFSE sequencing is given by Equation (2) [83], and the read length for a drag-tag with a friction of ζ can be predicted by solving this equation for M_c at a resolution of $R = 1$.

$$R \approx R_0 \frac{M_c^{1/2} (M_c \tau)^{5/4}}{\tau} \quad (2)$$

In this equation, R_0 is an experimental parameter, which we estimate at about 5.3×10^{-3} for our experimental conditions. For an overall τ of 17.2, Equation (2) predicts a read length of 90 bases at an applied field of 313 V/cm. Thus, we expected the synthetic 70mer drag tag to produce a short but significant read length, of the same order of magnitude as obtained previously with streptavidin [48] or our 127mer protein polymer [96], which provided read lengths of 110-120 bases.

Table 4.1. Peptoid drag-tag structure and properties including the experimental sequencing results and theoretical prediction using Equation (2). In the branch portion of the drag-tag chemical structure, *N*-(methoxyethyl)glycine peptoid residues are abbreviated as “NMEG.”

Octamer-branched 30mer drag-tag structure	Mass (kDa)	Calculated a	Theoretical read length	Observed read length
	11.09	18.0	92	80-100

4.2 Experimental procedures

4.2.1 Drag-tag-DNA conjugation

The synthesis and purification of the 70mer Nmeg drag-tag used in this study has been described in detail elsewhere [41]. Briefly, a linear 30mer peptoid “backbone” was constructed by solid-phase ‘submonomer’ synthesis [10, 12, 52, 53, 100], and then octamer Nmeg branches were grafted onto the backbone *via* solution-phase coupling. It was subsequently purified by RP-HPLC to > 99% homogeneity, and the molecular weight was confirmed *via* MALDI-TOF/MS. The *N*-terminal primary amine of the drag-tag was conjugated to a reduced, 5’ thiolated, M13mp18 (-40) sequencing primer [5’-X₁GTTTTCCCAGTCACGAC-3’ where X₁ is a C6-thiol modification] using the heterobifunctional linker Sulfo-SMCC.

4.2.2 Sequencing reaction

The ABI SNaPshot kit, intended for single base extension genotyping, was used to achieve four-color sequencing, with small amounts of dNTPs added to generate small sequencing fragments (<200 bases). 5 µL of the SNaPshot premix was mixed with 3 pmol of the drag-tag linked primer, 0.12 µg of M13mp18 control template, and 200 nmol of each dNTP in a total volume of 10 µL. The mixture was subjected to 25 cycles of denaturation at 96 °C for 10 seconds, annealing at 50 °C for 5 seconds, and extension at 60 °C for 30 seconds. Sequencing reactions were purified by gel filtration with a Centri-sep column (Princeton Separations), and were denatured in formamide prior to analysis by capillary electrophoresis (CE).

The sequencing products were analyzed by free solution electrophoresis with 4-color LIF detection using an Applied Biosystems Prism 3100 capillary array instrument (Applied Biosystems, Foster City, CA), with standard sequencing protocols modified to allow loading of buffer rather than polymer into the capillary array. The capillary array had an effective length of 36 cm (total length of 47 cm). The running buffer was 50 mM Tris, 50 mM TAPS, 2 mM EDTA, and 7 M urea, pH = 8.5, with a 3% (v/v) dilution of POP-5 polymer as a dynamic coating agent to suppress electroosmotic flow (this low concentration of polymer does not lead to sieving behavior). Separations were carried out at 14.7 kV total potential (313 V/cm) at 55 °C.

4.3 Results and discussion

4.3.1 Capillary electrophoresis

The resulting four-color sequencing electropherograms are shown in Figures 1-2. Besides a simple scaling of the four channels and smoothing to improve the noisy baseline, this is a raw sequencing trace, without the customary data processing typically used for matrix-based sequencing. Manual alignment of the peaks to the known M13mp18 control sequence suggests a read length between 80 and 100 well-resolved bases. This result is impressive, considering that this drag-tag consists of only 70 monomers. Each dye terminator causes a slightly different mobility shift, which causes peaks to shift slightly out of their expected position, and overlap with (or even reverse position with) adjacent peaks. The resolution is also seemingly lower for the G-terminated fragments than for the other terminators; *e.g.*, the GG pairs at 71-72 and 80-81

bases show lower resolution than CCCC peaks at 75-78 bases. The G peak at 51 bases also appears to be split into two poorly resolved peaks, for an unknown reason, as there is only a single "G" in this position in the M13mp18 sequence. The AA pair at 100-101 bases shows two distinct peaks, but beyond this, repeated bases are run together. This

Figure 4.1 Four-color DNA sequencing performed using an M13 sequencing primer linked to the octamer-branched polypeptoid drag-tag. The ABI SNaPshot kit was used, with different amounts of dNTPs added to generate different sequencing read lengths. In (A), no dNTPs were added, giving a single-base extension. In (B) and (C), 20 μM and 200 μM of each dNTP were used, generating a short (B) or longer (C) read. Separations were performed with the ABI 3100, with injections performed at 1 kV for 10 or 30 seconds.

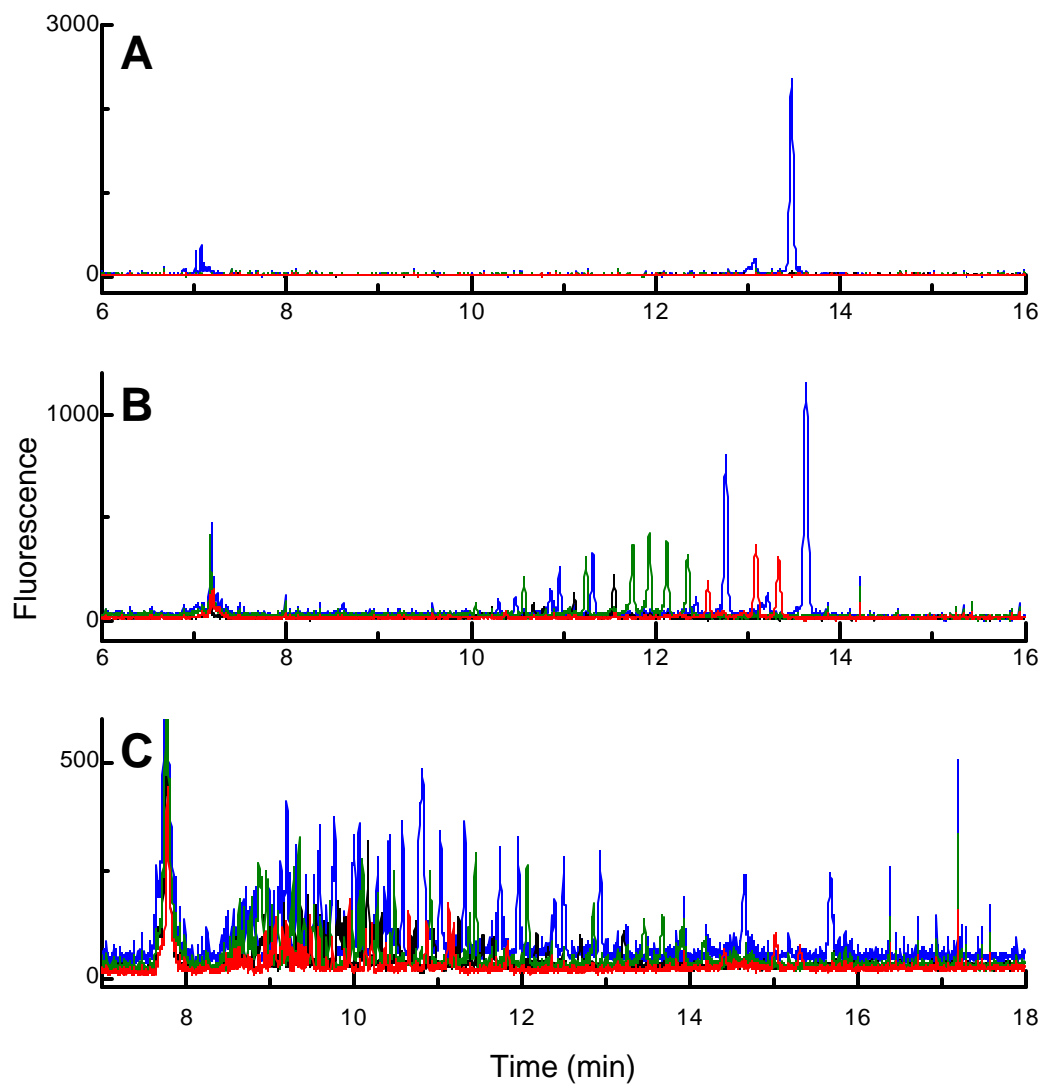
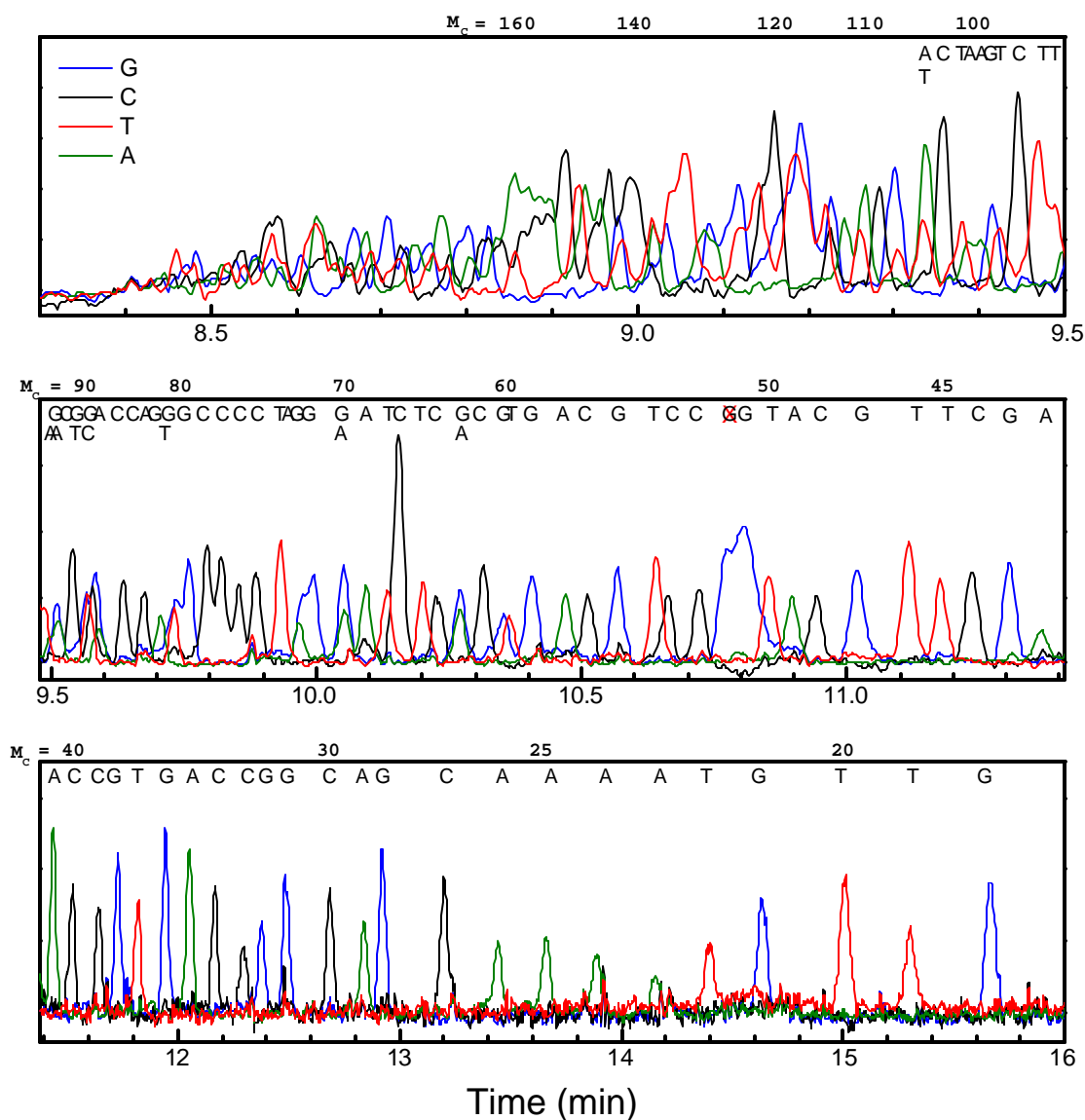


Figure 4.2 4-color sequencing electropherogram obtained with 70mer branched drag-tag, with manual base calls of the M13mp18 sequence. The DNA fragment sizes (M_c) are shown at the top of each panel, and a red “X” around $M_c = 52$ bases marks an unexpected “G” peak. For purposes of presentation, the “C” and “T” signals have been scaled by a factor of 2 to give peak heights comparable to the “G” and “C” traces, and the data has been smoothed to reduce high-frequency noise, possibly due to a small bubble in the fluid path.



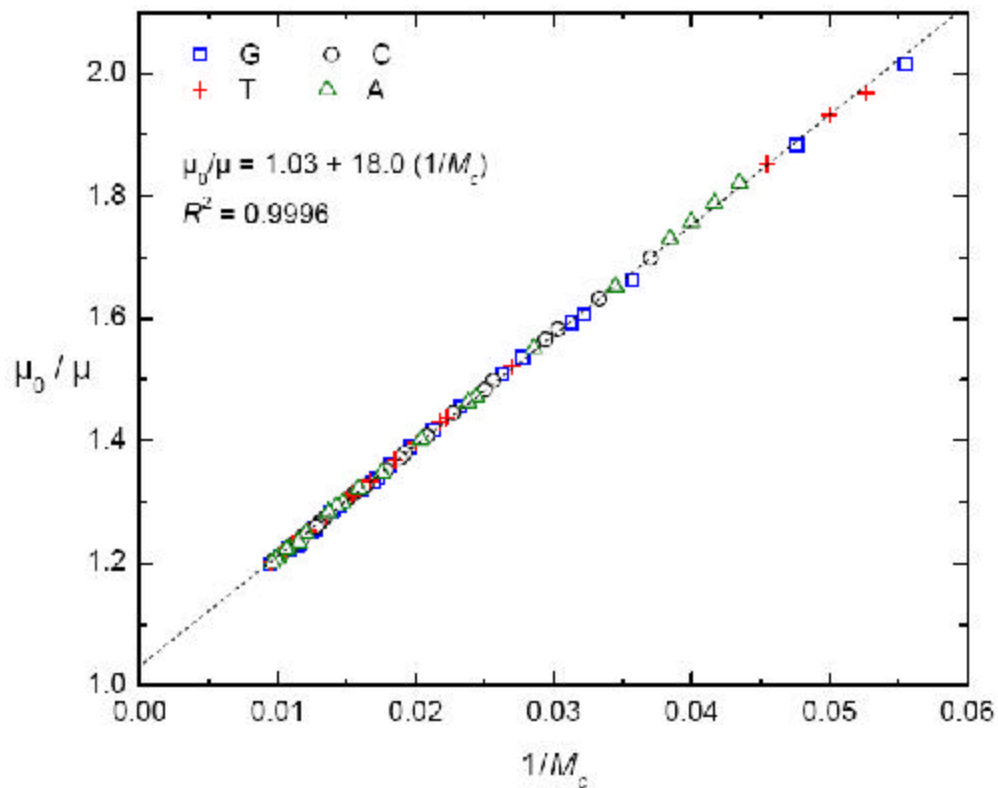
suggests that an upper limit for the read length is about 100 bases, although the resolution was not calculated due to a noisy baseline during all runs. We note that the shifting of peaks, and decreased resolution for “G” terminations also appeared when ELFSE sequencing was performed with a protein polymer drag-tag [96], and these may be features of the particular dye terminator chemistry we used (dichlororhodamine terminators, for the SNaPshot kit). It is also noteworthy that the bulky, branched polypeptoid attached to the sequencing primer does not seem to interfere with the DNA polymerase used in the Sanger sequencing reaction.

4.3.2 Calculation of λ

A linearized plot of mobility versus migration time is shown in Figure 3. The experimental data fits well with the simple model presented in Equation (1). In this case, we find $\lambda = 18.0$, which is quite similar to the value of 17.2 we had observed previously [41]. The sequencing read length we observed of 80-100 bases is comparable to the prediction of ~90 bases from Equation (2). While this is short compared to common matrix-based sequencing reads, it is impressive considering that the drag-tag consists of only 70 monomers and is 11 kDa in molecular weight. In comparison, streptavidin consists of more than 600 amino acids with a molecular weight of 53 kDa, but provided only a slightly longer read length of about 110 bases [48]. We have previously found that, for branched polypeptoid drag-tags, λ scales linearly with molecular weight (as opposed to roughly the 1/3 power of molecular weight for globular proteins), and thus we

expect that a branched drag-tag of molecular weight similar to streptavidin would provide dramatically better sequencing performance.

Figure 4.3 A fit of experimentally measured mobilities (μ_0/μ) versus DNA fragment size $1/M_c$, according to a rearranged version of Equation (1), with a slope of $\gamma = 18.0$ for the octamer-branched drag-tag. Different symbols are used to represent fragments with G, C, A, or T terminations, which reveals no terminator-specific deviation from model behavior.



4.4 Conclusions

In summary, there is great potential for high read length ELFSE sequencing using synthetic drag-tags, provided that higher molecular weight peptoid sequences can be successfully synthesized while simultaneously adhering to strict purity requirements. Using peptoids offers the advantages of facile sequence design and synthesis, and the ability to readily incorporate multivalency *via* the submonomer approach [12]. The synthesis of comblike, branched peptoids that are reasonably large has verified that guided sequence design and further optimization puts this goal within reach.

Chapter 5. Multivalent, high relaxivity magnetic resonance imaging (MRI) contrast agents

DOTA and DO3A have long been used as Gd(III) MRI contrast agent chelators, and their derivatives are well-characterized and easily accessible by efficient syntheses. In this study, we use a peptide-bond forming strategy to attach a DO3A derivative, wherein the fourth arm is pentanoic acid, to free amines displayed along a polypeptoid backbone consisting mainly of *N*-(methoxyethyl)glycine, or *N*meg, side-chains. This conjugation resulted in a relaxivity value per Gd(III) metal center equal to approximately three times the value of DO3A chelator conjugates alone. Up to eight chelators were successfully attached to the 30-mer peptoid backbone in good yield. Data revealed a relaxivity of $10.7 \text{ mM}^{-1}\text{s}^{-1}$ per Gd(III) center, indicating that the peptoid containing 8 Gd(III) sites has a relaxivity of $\sim 86 \text{ mM}^{-1}\text{s}^{-1}$ “*per molecule.*” This relaxivity value is one of the highest reported for an isolated structure.

5.1 Magnetic resonance imaging (MRI)

5.1.1 Background, contrast, and relaxivity

Magnetic resonance imaging (MRI) is a widely used diagnostic tool in radiology that generates high resolution images of living tissue. This non-invasive technique thus allows for three-dimensional visualization of the body’s biological structures, processes, and functions at cellular resolution [29-31]. MRI relies on the NMR signal of protons of

mostly water, and signal intensity in a given volume element is therefore a function of water concentration and proton relaxation times. The resulting signal intensity variations generate image contrast, permitting differentiation between various tissue types and stages of disease. High contrast is very desirable for imaging, as it increases the diagnostic capabilities of MRI in the clinical environment. There are many different mechanisms for creating contrast in an image, where an imaging sequence can be weighted to display differences in proton relaxation rates, chemical shifts, water diffusion, blood flow effects, or magnetization transfer techniques [32].

MRI signal intensity is derived from the local value of the longitudinal relaxation rate of water protons, $1/T_1$, and the transverse rate, $1/T_2$. Signal tends to positively correlate with $1/T_1$ and inversely correlate with $1/T_2$. T_1 -weighted pulse sequences are hence those that emphasize changes in $1/T_1$, and oppositely for T_2 -weighted scans. In T_1 -weighted imaging, a more intense signal is observed in regions where the longitudinal relaxation rate $1/T_1$ is fast, *i.e.*, where T_1 is short. The longitudinal relaxation rate of water protons can be further enhanced by the addition of paramagnetic metal complexes. These complexes, termed MRI contrast agents [33], afford increased image contrast in regions where the complex localizes.

Thus, the administration of MRI contrast agents in patients significantly expands the scope of imaging capabilities available to doctors and researchers. Several compounds are currently approved for clinical use, and more are undergoing clinical trials. Initial contrast agents were developed to distribute to plasma and extracellular space [34], while later efforts focused on targeting the liver and bodily fluids [35]. The

current, pre-clinical development of contrast agents hones in on improvements in “molecular imaging” [36].

Exogenous contrast agents employ paramagnetic metal ions, and most function by shortening the local T_1 , or increasing $1/T_1$, of solvent water protons, thus providing increased contrast. Depending on their nature and the applied magnetic field, contrast agents increase both $1/T_1$ and $1/T_2$ to varying extents. Agents such as gadolinium in its +3 oxidation state, Gd(III), increase both $1/T_2$ and $1/T_1$. Because the long electron spin relaxation time and high magnetic moment of Gd(III) make it an efficient perturbant of T_1 , this agent is best visualized using T_1 -weighted images, as the percentage change in $1/T_1$ in tissue is much greater than that in $1/T_2$. Advances in MRI have primarily favored T_1 agents, thus the widespread use of Gd(III) [33].

Relaxivity is defined as the ability of a complex to enhance the relaxation rate of the solvent, denoted r , (Equation 1), with units of $\text{mM}^{-1}\text{s}^{-1}$, where $\Delta 1/T_1$ is the change in the solvent relaxation rate after contrast agent addition at metal concentration $[M]$:

$$r = \frac{\Delta 1/T_1}{M} \quad (1)$$

High relaxivity thus translates to the increased ability of the contrast agent to be detected at lower concentrations, which may allow the imaging of low concentration molecular targets. Highly paramagnetic metal ions with a large spin number, S , are preferred, provided that electronic relaxation is slow. Therefore, again, complexes of Gd(III) [37] are commonly used as contrast agents because the metal center has seven unpaired electrons. However, current clinically used contrast agents have low relaxivities (3–7

$\text{mM}^{-1}\text{s}^{-1}$) and must be used at high concentrations for the MRI signal enhancement to be useful [38].

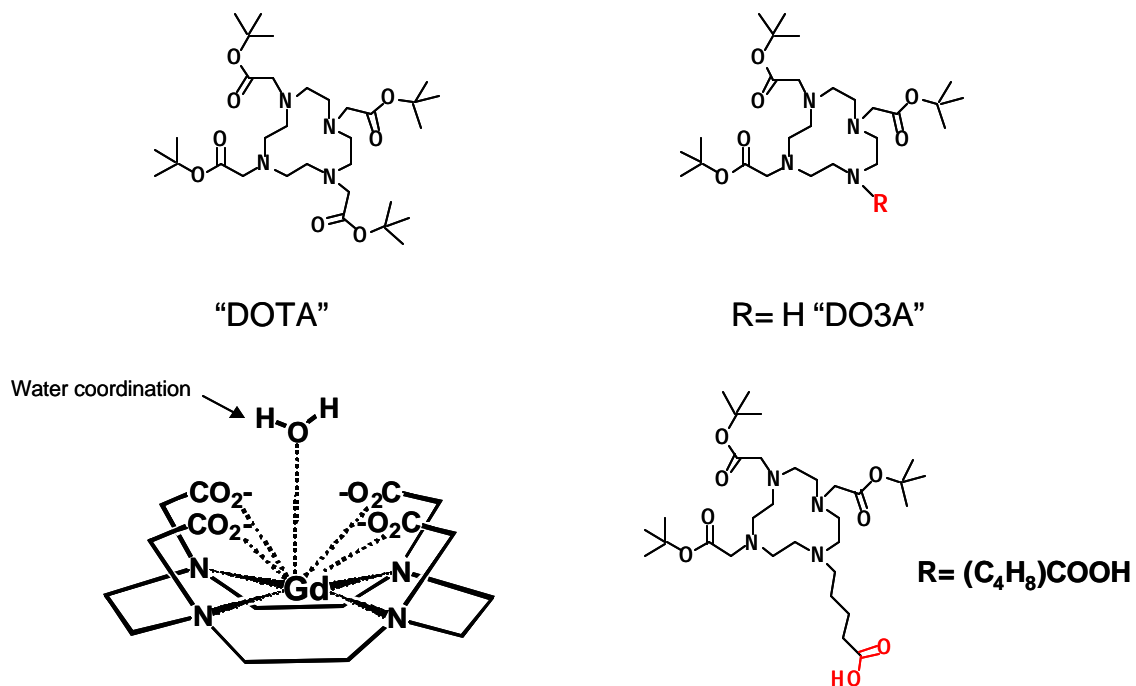
5.1.2 Gadolinium-based (GdIII) contrast agents – parameters for optimization

Since the approval of $[\text{Gd}(\text{DTPA})(\text{H}_2\text{O})]^{2-}$ (brand name Magnevist[®]) in 1988, it has been estimated that over 30 metric tons of Gd(III) have been administered worldwide to millions of patients [33]. Approximately 30% of current MRI exams include the use of contrast agents, and this percentage is expected to increase as new agents and applications become available. Though these contrast agents are used clinically with success, there is a tremendous opportunity for improvement and optimization of these molecules from chemistry and molecular biology standpoints. The efficacy of a contrast agent is evaluated by three parameters: q , the number of coordinated water molecules; t_m , the residence lifetime; and t_R , the rotational correlation time [101]. Notably, the current small-molecule contrast agents used clinically are limited by their fast (low) t_R , resulting in an undesirable lower relaxivity. Because of this, MRI contrast agents are traditionally used in high concentrations to enhance the signal. However, if contrast agents with higher relaxivity values were developed, lower concentrations could be used. The research and development efforts in the field of high relaxivity contrast agents are ongoing as evidenced by the many hundreds of articles published each year in the field. The additional benefits in imaging reaped when higher relaxivity contrast agents are

employed continue to spur academic and industrial efforts into new contrast agent molecular architectures.

Through these endeavors, it was discovered that macromolecular multivalent contrast agent designs are advantageous over their small-molecule counterparts because they increase r_1 , Gd(III) concentration, and contrast agent retention *in vivo* [33]. Multivalent scaffolds aim to optimize r_1 , but the simultaneous optimization of r_m , and q , or a combination of these parameters is of utmost importance to obtaining high contrast using T_1 imaging. The most popular method to increase the r_1 value of a contrast agent is to associate it with a macromolecule or induce monomer self-assembly into supramolecular structures. These strategies are effective at increasing relaxivity, but are limited in their versatility of other important aspects to include in contrast agents, such as targeting or fluorescent abilities. The number of water molecules q in contact with the paramagnetic center is another parameter that is typically independently varied. By increasing q , relaxivity is sometimes increased, but at the expense of Gd(III) stability inside the chelator, typically DOTA (Figure 1). Gd(III) stability in these contrast agents is vital due to its toxic nature; the chelation of the Gd(III) aqua ion using various ligands minimizes these toxic effects [102-104]. The final parameter to be modified is r_m , which has been manipulated by varying the chelating agent's conformation.

Figure 5.1 Gd(III) chelators DOTA and DO3A, where DO3A allows for the chelator to be attached to a macromolecular structure as a pendant group.



5.1.3 Current status of multivalent Gd(III) contrast agents

As examples, small-molecule contrast agents have been attached *via* covalent or non-covalent interactions to a number of macromolecules, including albumin [33], carbohydrates [105], linear polymers such as polylysine [106], dendrimers [107], viral capsids [108], liposomes [109], and other supramolecular structures. Multiple Gd(III) containing ligands have been attached to macromolecular scaffolds such as dextran, resulting in a highly polydisperse conjugate referred to as “GRID” [102-104, 110]. Dextran is a complex branched polysaccharide comprising many glucose molecules joined in chains of varying lengths with an enormously wide mass range of ~10-150 kDa. The synthesis of “GRID” involved the attachment of a six-carbon linker 1,6-diaminohexane to dextran, to which a carboxylate-terminated Gd(III) ligand was attached *via* a peptide bond. A more recent example of this type of conjugate involved the use of a genetically expressed “protein polymer” [111] that had evenly spaced lysine amino groups which acted as attachment points for Gd(III) moieties. Both this and the dextran example resulted in an increased relaxivity value per Gd(III) ion and overall high total-molecule relaxivity. In GRID examples, the increased relaxivity per Gd(III) ion was typically very modest; alternatively, in the protein polymer example, the relaxivity per Gd(III) ion increased markedly. It was proposed that the regular spacing intervals and the close proximity of chelator molecules along the protein polymer backbone was a leading factor in why the relaxivity values per Gd(III) ion were so high in this case.

Macromolecular contrast agents that possess a multitude of functionalities offer many improvements over intravascular or “blood-pool” gadolinium-based contrast

agents. A multivalent high-relaxivity contrast agent could potentially be used in low concentrations while simultaneously providing magnetic information. However, many developed macromolecular contrast agents do not provide high relaxivities, have limited biocompatibility, and/or do not have a structure that is readily modifiable to tailor to particular applications. Several known examples of macromolecular contrast agents fail in possessing unique attachment points that allow for multiple functionalities, including accurate quantification of concentration as well as multivalent capabilities such as attachment points for cell-penetrating moieties or targeting groups.

5.1.4 Multivalent Gd(III) contrast agents based on peptoid scaffold architectures

The multifunctional uses of comb-like, monodisperse, high molecular weight, polyNmeg-containing peptoid scaffolds in electrophoretic applications begged the question as to whether a similar construct could function as a high relaxivity multivalent contrast agent for MRI. The ease of synthesis, near monodispersity, high chemical stability, and facile inclusion of multiple attachment points for diverse pendant groups on one molecule fits quite well with the demands for a macromolecular Gd(III) contrast agent. After the initial synthesis of the DO3A derivative with a single pentanoic arm for attachment to primary amino groups, a test grafting onto a simple peptoid molecule with two attachment sites was performed. A 30mer scaffold containing eight branching points for Gd(III) ligands was then successfully synthesized, DO3A grafted on then deprotected, then metallated, and finally relaxivity experiments were performed.

5.2 Experimental

5.2.1 Materials

Peptoids or poly-*N*-substituted glycines used in this work were efficiently synthesized by the “sub-monomer” method, which has been described previously [10, 12, 53]. All peptoid backbone syntheses were carried out on an ABI 433A automated peptide synthesizer (Applied Biosystems, Foster City, CA). All reagents used were purchased from Aldrich (Milwaukee, WI), unless stated otherwise. The mass spectra were recorded by MALDI-TOF. (Voyager Pro DE, Perseptive Biosystems, Framingham, MA) and ESI/MS (Waters Micromass Quattro II, Milford, MA).

5.2.2 Reversed-phase high-performance liquid chromatography (RP-HPLC)

Analytical RP-HPLC was performed on a column with C18 packing (Vydac, 5 μm , 300 \AA , 2.1 x 250 mm). The following conditions were employed, unless otherwise stated: a linear gradient of 10-40 % B in A was run over 50 min at a flow rate of 0.5 mL/min (solvent A = 0.1 % TFA in water, solvent B = 0.1 % TFA in acetonitrile) at 58 $^{\circ}\text{C}$; analytes were detected by UV absorbance at 220 nm and/or 260 nm. Preparative HPLC was performed on a Vydac C18 column (Vydac, 15 μm , 300 \AA , 22 x 250 mm) using the same solvent and detection systems; analytes were eluted with a linear gradient of 10-40 % B in A over 50 min at 12 mL/min.

5.2.3 Synthesis of Gd(III) chelating ligand: pentanoic acid DO3A

(Compound 1)

5.2.3.1 Synthesis of 5-bromopentanoate

In a dry round bottom flask was combined 5-bromo valeric acid (2.00 g, 11 mmol), DTSP (3.56 g, 12.1 mmol), DIPC (1.81 g, 14.3 mmol) and DCM (200 mL). The solution was stirred for 5 minutes and a solution of benzyl alcohol (1.79 g, 16.6 mmol) and DCM (10 mL) was added dropwise. The reaction proceeded overnight then was diluted in DCM and washed with H₂O three times, dried over MgSO₄, and then the solvent was removed by rotary evaporation. Flash chromatography was performed using 5/95 MeOH/DCM to afford a clear liquid (2.82 g, 95% yield). ¹H NMR (500 MHz, CDCl₃) δ 7.36 (bs, 5H), 5.14 (s, 2H), 3.43 (t, $J=7$ Hz, 2H), 2.41 (t, $J=7$ Hz, 2H), 1.90 (q, $J=7$ Hz, $J=14$ Hz, 2H), 1.83 (q, $J=7$ Hz, $J=14$ Hz, 2H); ¹³C (125 MHz, CDCl₃) δ 173.19, 136.19, 128.86, 128.54, 128.51, 66.55, 33.53, 33.33, 32.21, 23.74. ESI/MS (methanol) Calculated:found 270.03:271.23 M+H.

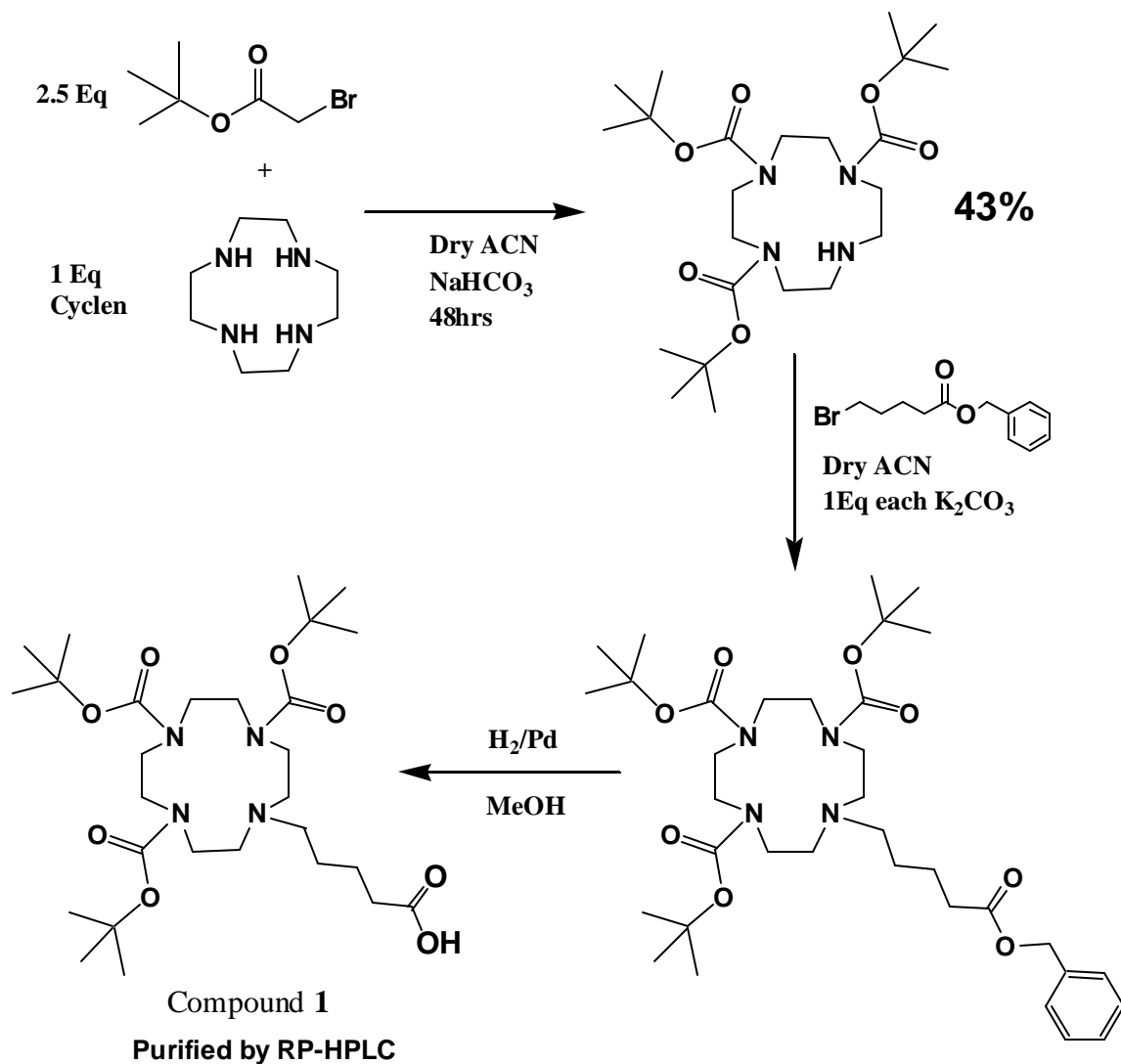
5.2.3.2 Synthesis of DO3A (Compound 1)

As shown in Figure 1, typical Gd(III) chelators are DOTA and DO3A, where DO3A allows for the chelator to be attached to a macromolecular structure as a pendant group [33]. Thus, the synthesis of Gd(III) chelator pentanoic acid DO3A (Compound 1) is shown in Scheme 1. DO3A was synthesized using a hydrogenation-labile protection scheme with tert-butyl 2-bromoacetate and benzyl 5-bromopentanoate as the chelating arms of the macrocycle (Scheme 1). The addition of three tert-butyl 2-bromoacetate arms

to cyclen was followed by the addition of benzyl 5-bromopentanoate. Deprotection by hydrogenation of the chelator and subsequent metalation with GdCl_3 afforded **1** (see Appendix A for MALDI-TOF/MS and structure).

Synthesis details: in a dry round bottom flask was combined cyclen, 2.5 molar equivalents of tert-butyl 2-bromoacetate, and sodium bicarbonate, in dry acetonitrile. The solution was stirred under nitrogen for 48 hours and then the solvent was removed by rotary evaporation. Flash chromatography was performed on silica gel to afford the three-armed DO3A intermediate in 43% as the major product. ESI and ^1H proton and ^{13}C NMR were performed and the desired mass and structure was confirmed before progressing to the next step of the synthesis. The addition of the five-carbon spacer was attained by alkylating the tert-butyl protected DO3A species with benzyl 5-bromopentanoate in 1:1 molar amounts, with potassium carbonate as the base and dry acetonitrile as the solvent. This alkylation reaction was performed under rigorous air-free conditions using flame-dried glassware, and delivery of reagents *via* cannula transfer. The benzyl 5-bromopentanoate spacer arm contained a terminal carboxylate group that was deprotected using hydrogenation techniques. This final step of the synthesis of **1** was performed using a Parr apparatus in methanol solution using Pd/C and a H_2 at 50 psi. Deprotection was performed to reveal the reactive carboxylic acid group for further reaction with amino groups on multivalent peptoid scaffolds. Once grafting was complete, the acid-labile tert-butyl groups were removed, allowing for Gd(III) chelation.

Scheme 5.1 Synthesis of Gd(III) Chelator pentanoic acid DO3A (Compound 1). Hydrogenation-labile deprotection was used to reveal the reactive carboxylic acid group for further reaction with amino groups on multivalent scaffolds. Once grafting is complete the acid-labile tert-butyl groups can be removed allowing for Gd(III) chelation.



5.2.4 Polypeptoid “backbone” synthesis (Compounds 2 and 4)

Synthesis details: Fmoc-Rink amide resin (Nova Biochem, San Diego CA. 0.30 mmol scale) was deprotected by treatment with piperidine in dimethylformamide (DMF) (20 % v/v; 2 x 7 mL) in two consecutive 15-min treatments. The oligomer chain was then assembled with alternating cycles of the bromoacetylation step and amine displacement of the alkyl bromide moiety. Bromoacetylation was achieved by mixing the resin with bromoacetic acid (BAA) (1.2 M; 4.3 mL) in DMF and diisopropylcarbodiimide (DIC) (1 mL; 9.9 mmol). The mixture was vortexed for 45 min, the liquid drained, and the resin rinsed with DMF (4 x 7 mL). The resin was then mixed and vortexed (45 min) with either methoxyethylamine (1.0 M; 4 mL) or mono-Boc protected diaminobutane (1.0 M; 4 mL) [55] in *N*-methylpyrrolidone (NMP) to introduce the *N*-(methoxyethyl)glycine (*N*meg) or *N*-amino(ethyl)glycine (*N*abg) side chain moieties. The liquid was drained, and the resin rinsed with DMF (4 x 7 mL). These two reaction cycles were alternated until the polypeptoid was of the desired sequence and length. Finally, an Fmoc protecting group was installed on the amine terminus while the polypeptoid was still on the resin. This was achieved by adding Fmoc-Glycine and DIC under the same conditions as used for the bromoacetylation step.

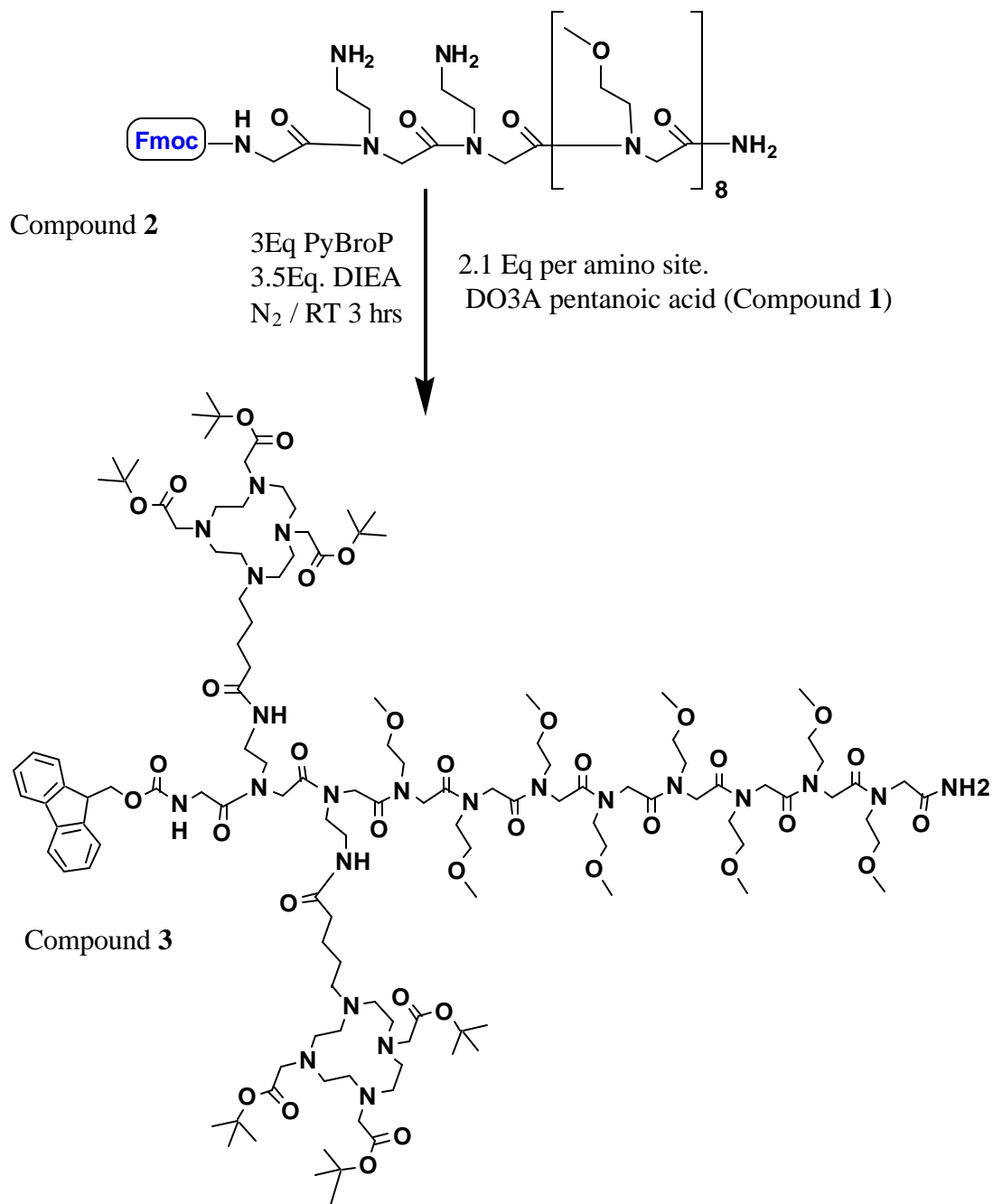
Finally, the polypeptoid was cleaved from the solid support by treatment with 95:2.5:2.5 trifluoroacetic acid (TFA):triisopropylsilane (TIS):water for 10 min. The polypeptoid was filtered through a fritted glass vessel to remove the solid support, diluted with water (50 mL), frozen (-80 °C) and then lyophilized. The product of the solid-phase synthesis was evaluated by analytical reverse-phase high performance liquid

chromatography (RP-HPLC). Preparative RP-HPLC was subsequently performed and appropriate fractions were combined to afford the desired product in pure preparation.

5.2.5 Grafting reactions (Compounds 3 and 5)

The coupling reaction between the amino groups of the peptoid backbone and the carboxylate groups of the DO3A Gd(III) ligand was performed under rigorously dry and air-free conditions (Scheme 2). An excess of peptoid (2.1 equivalents per amino site) was combined with peptide bond-forming reagents PyBrop and diisopropylethyl amine (DIEA) in *N*-methylpyrrolidone (NMP) as the solvent. The NMP was dried over activated 4Å molecular sieves to remove any water that might be present. Unlike previous strategies [111], we chose not to premetallate the DO3A chelators so that the grafting reactions would proceed in organic solution and the most efficient peptide coupling reagents could be used. RP-HPLC and MALDI-TOF/MS (see Appendix A) analysis of the conjugate confirmed that the reaction proceeded in near quantitative yield.

Scheme 5 2. To test the possibility of densely grafting DO3A pentanoic acid chelators onto a polyNmeg peptoid scaffold, Compound 2 was synthesized. 2.1 Equivalents of Compound 1 were used along with 2.5 Eq PyBroP and DIEA in dry NMP.



5.2.6 Deprotection and metallation with GdCl_3 (Compound 6)

The tert-butyl groups on the DO3A pendant groups were then removed using 95:5 trifluoroacetic acid:water. This deprotection proceeded in quantitative yield within an hour, as monitored by RP-HPLC. The MRI contrast agents were metallated using a solution of GdCl_3 in buffer at 60 °C. In a falcon tube was placed DO3A-peptoid conjugate (0.165 g, 0.37 mmol), millipore H_2O (4 mL), and GdCl_3 (0.151 g, 0.4 mmol). The pH was adjusted to 6.5 using ammonium hydroxide and the solution was stirred for 2 days. The solution was then brought up to pH 10, the precipitate was centrifuged at 4000 rpm for 10 minutes, and the liquid decanted. The water was removed by lyophilization yielding a white powder, of which the mass and yield were inaccurate due to NaOH salt in the final product from the pH adjustment. ESI/MS (negative mode, methanol) confirmed the mass.

5.2.7 Relaxivity determination

Relaxivity measurements were recorded in triplicate using a Bruker mq60 NMR Analyzer (Bruker Canada, Milton, Ont., Canada) at 37 °C. Inductively coupled plasma mass spectrometry (ICP-MS) was used to determine Gd(III) concentration. The contrast agent displayed a relaxivity of $10.7 \text{ mM}^{-1}\text{s}^{-1}$ per Gd(III) ion and $\sim 86 \text{ mM}^{-1}\text{s}^{-1}$ per conjugated molecule complex, a product of the number of Gd(III) chelators per peptoid scaffold backbone multiplied by the relaxivity per Gd(III).

5.3 Results and Discussion

5.3.1 Initial scaffold with two DO3A attachment sites

Initially, **2** was designed and synthesized as a preliminary test in an attempt to densely graft DO3A pentanoic acid chelators onto a polyNmeg peptoid scaffold. It was possible that DO3A would not append itself to such a large backbone, especially at adjacent *N*-substituted sites. The structure of the DO3A attachment sites were designed to be spatially close to the backbone, hence containing *N*-(aminoethyl)glycine (*Naeg*) side chains instead of the *N*-(aminobutyl)glycine (*Nabg*) side chains previously used in polyNmeg peptoid scaffolds [41]. The purpose of this substitution was to increase the ‘tightness’ of the backbone, resulting in slower tumbling, increased τ_r , and thus higher relaxivity values. Therefore, **2** served as a proof of concept example whereby the grafting of a bulky Gd(III) chelator could be optimized and evaluated. It was further useful to evaluate deprotection conditions as well as requirements for complete metalation of the pendant chelators.

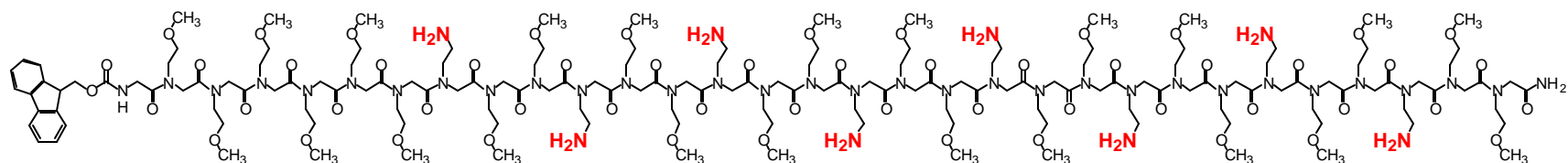
Compound **1** was then successfully coupled to the active sites on **2** to yield **3** (Scheme 2) using similar conditions to previous examples, although fewer equivalents of branch molecule and coupling reagents were used in this case. In order to conserve the chelator, it was proposed to use fewer equivalents of **1** in the grafting reactions. Compound **3** was successfully synthesized using only 2.1 equivalents of **1** per amino-attachment site. This was almost an 80% reduction in the amount of branching material needed over amounts used in previous grafting protocols [41]. Compound **2** possesses two attachment points, and so, to this end, an overall molar excess of 4.2 equivalents of **1**

was used in the grafting protocol. Compound **3** was then purified by RP-HPLC and lyophilized. The tert-butyl groups on the Gd(III) chelator ligands were then deprotected by dissolving in 95% trifluoroacetic acid, and then the subsequent metallation was completed using $GdCl_3$ to afford **3**.

5.3.2 Subsequent 8-site 30mer scaffold design

The successful synthesis of **2** with two proximally close Gd(III) chelator attachment sites indicated that a larger molecule with multiple closely spaced attachment sites would be a viable design for a high-relaxivity multivalent contrast agent. The design and synthesis of a 30mer peptoid backbone with five branching sites used in a previous study for electrophoretic applications was thus expanded to an 8-site, 30mer backbone, **4** (Scheme 3). In addition, as was the case for the test compound **2**, the branching sites were designed to be spatially close to the backbone, hence containing *Naeg* instead of the previously used *Nabg*. The coupling of the pentanoic acid-armed DO3A chelator onto the scaffold was accomplished to yield **5**, and subsequent deprotection and metallation with $GdCl_3$ led to **6** (Scheme 4). Relaxivity measurements were then obtained for **6** using NMR and ICP techniques.

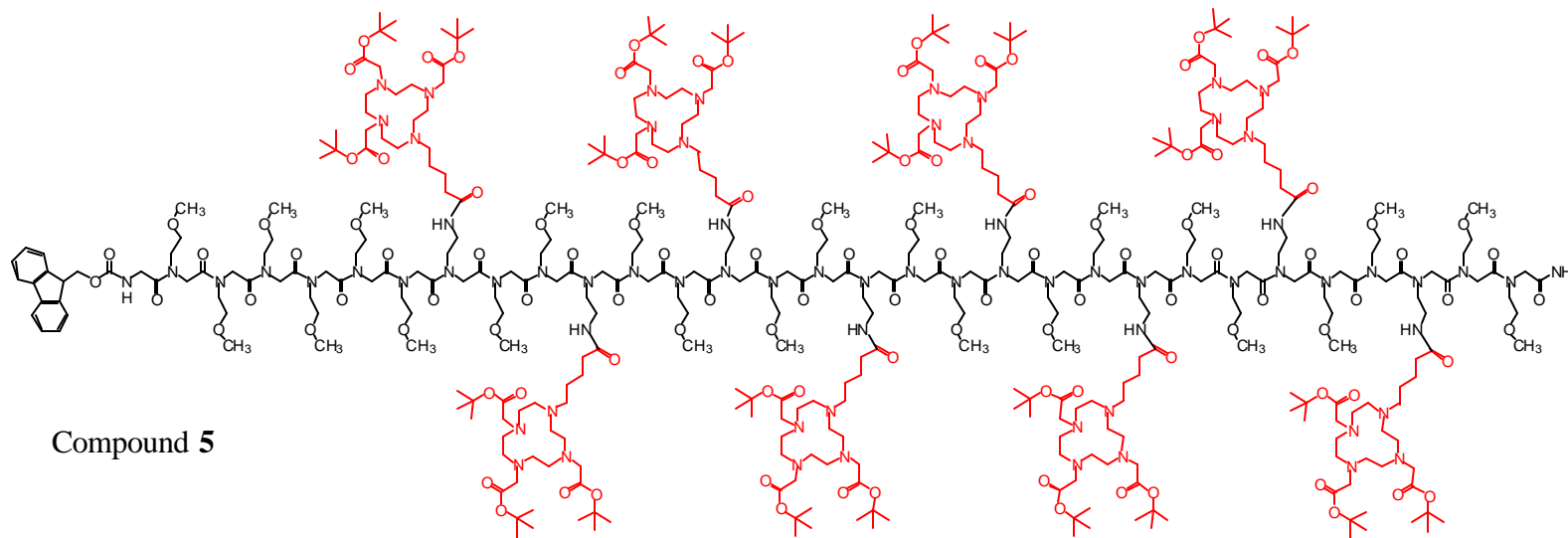
Scheme 5.3 Modified version of previously published grafting protocol.



Compound 4

3Eq PyBroP
3.5Eq. DIEA
N₂ / RT 3 hrs

2.3 Eq per amino site.
DO3A pentanoic acid (Compound 1)

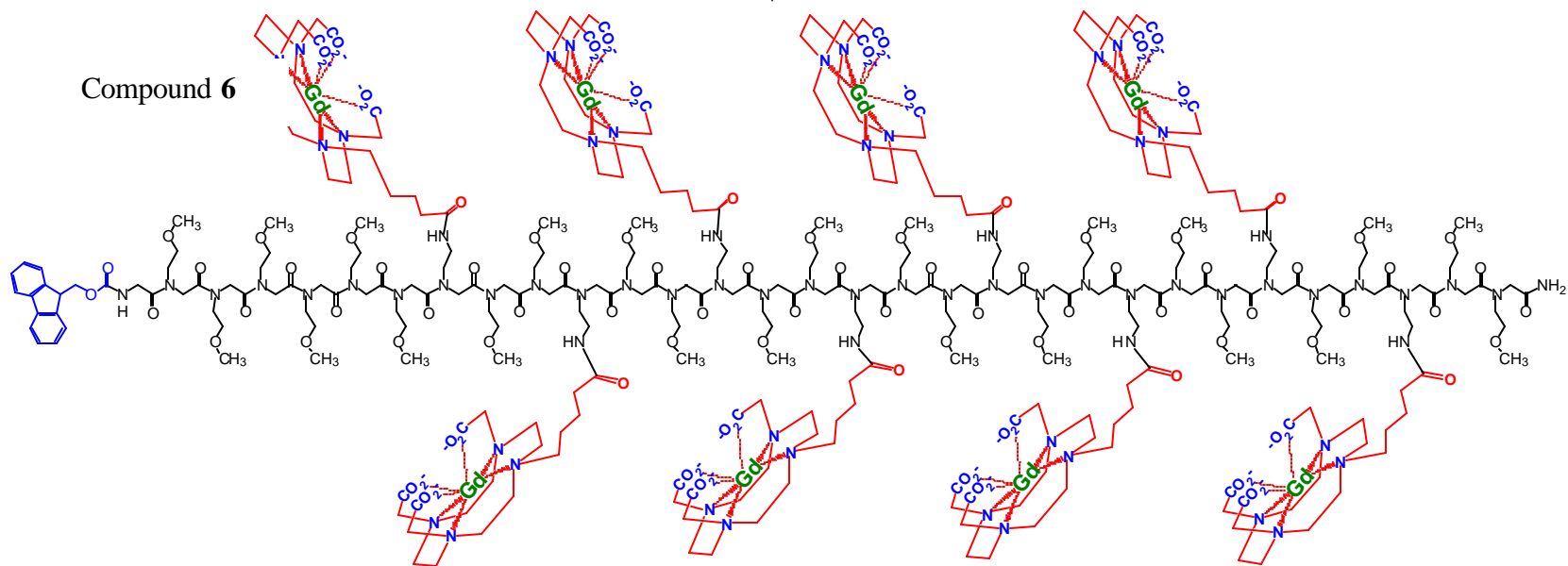


Compound 5

Scheme 5.4 Deprotection of the DO3A side-chains followed by metalation using GdCl₃.

5mg Compound 5
RP-HPLC purified

1. 95:5 Trifluoroacetic acid:water
2. GdCl₃ stir for 2 days at 60 °C
3. Precipitation to remove excess Gd(III)



5.3.3 Relaxivity data

The peptoid oligomer backbone was synthesized on the solid phase in high yield. The Gd(III) chelator (DO3A derivative) that was then attached to the backbone was also a clinically administered drug, giving good confidence in the stability of the Gd(III) in this structure. The relaxivity increase we observed for the grafted species over the chelate monomer is thought to arise from an increase in τ_r . As an explanation for the high relaxivity, it was proposed that perhaps $q > 1$; however, initial experimental results showed that q in fact appeared to be equal to one, despite the DO3A derivatives commonly exhibiting $q = 2$.

The relaxivity value per gadolinium ion (Gd III) was $10.7 \text{ mM}^{-1}\text{s}^{-1}$ at 60 MHz, as indicated by inductively coupled plasma (ICP), which corresponds to a relaxivity of $86 \text{ mM}^{-1}\text{s}^{-1}$ per fully derivatized molecule. This relatively high relaxivity value is impressive, especially given that the multivalency of the molecule will allow for the inclusion of additional functionalities that may make the contrast agent even more useful. This is not the case for synthetic polymers, such as metallostar-based and metallofullerenes, that exhibit moderate relaxivities of $\sim 33 \text{ mM}^{-1}\text{s}^{-1}$ [112] and $\sim 60 \text{ mM}^{-1}\text{s}^{-1}$ [113], respectively. Similarly, dendrimeric constructs are typically on the order of $\sim 35 \text{ mM}^{-1}\text{s}^{-1}$ [114]. In addition, there are some natural, protein-based contrast agents that demonstrate high molecular relaxivities, such as cowpea chlorotic mottle virus, $\sim 200\text{--}400 \text{ mM}^{-1} \text{ s}^{-1}$ per viral conjugate [115], apoferritin, $\sim 800 \text{ mM}^{-1}\text{s}^{-1}$ per protein complex [116], and MS2 viral capsid, $\sim 7200 \text{ mM}^{-1}\text{s}^{-1}$ [108]. However, our novel

contrast agents based on a peptoid scaffold circumvent various disadvantages associated with using these other types of macromolecules.

Namely, peptoid sequences are extremely stable under typical conditions of acidic or basic solutions [9, 100], and are protease-resistant [17], two characteristics that are problems for peptide- or protein-based contrast agents. Although the *in vivo* circulation time and mode of excretion in peptoids are not yet known, enzyme-cleavable peptide side chains can be easily incorporated into the sequence during regular solid-phase peptide/peptoid synthesis. Ultimately, the unique advantage of the peptoid scaffold is the extremely high ability to tune and modify the molecular structure using diverse, appended chemical groups that could possess multiple functions. Length, number of various side chains, number of attachment sites (Gd(III) centers), and spacing between centers can all be precisely controlled and adjusted at will for the particular application. This inherent multifunctionality is the pinnacle of multivalent contrast design, where targeting, fluorescence, *and* high contrast could all be achieved using a single scaffold. Particularly, the *N*-terminus *Fmoc*-protected amine can be modified to attach translocation molecules, fluorophores, DNA, proteins, or a large variety of functional groups. The flexibility and versatile of this novel class of molecules encompasses ideal contrast agents for MRI use.

5.4 Conclusions

Here, we report the design, synthesis, and characterization of a novel, multivalent, macromolecular contrast agent based on a poly-*N*-substituted glycine (peptoid) backbone

comprising 30 monomer units in length. There were eight reactive primary amines (ϵ -amino groups) that were available for derivatization. The 3.63 kDa peptoid scaffold Compound **4** is water-soluble and can be produced in high yield. The macrocyclic chelate that coordinates the Gd(III) ion is a chemically synthesized derivative of 1,4,7,10-tetraazacyclododecane-1,4,7,10-tetraacetic acid (DOTA) [117]. The three acetate arms chelate the Gd(III), while the carboxylate group on the 5-carbon arm is used for covalent attachment to the primary amine of the lysine residues *via* amide bond formation.

In conclusion, solution-phase and solid-phase chemical methods have been used to create a high-contrast, multivalent, peptoid-based MRI contrast agent. A convergent synthetic strategy was successfully employed to produce milligram quantities and is amenable to scale-up. We have demonstrated a reliable synthetic protocol that allows conjugates to be characterized by MALDI and provides high relaxivity results, both per molecule and per Gd(III). At this time, some concerns remain with regards to reproducing the metallation step, whereby the procedures used for metallating the final peptoid construct were inconsistent, making it difficult to discern which step resulted in supposed peptoid insolubility. Architectural improvements that are intended to overcome the problems encountered concerning the contrast agent's solubility in aqueous solution with the initial peptoid scaffold design have been incorporated into new molecules and synthesized.

Chapter 6. Additional drag-tag designs, progress, and future directions

6.1 Hydroxy drag-tags

6.1.1 Rationale for use of a new, extremely hydrophilic drag-tag side chain in peptoid scaffold sequences

The comparison of poly-*N*-(methoxyethyl)glycine (*N*meg) drag-tags to protein polymer analogues of the same molecular mass and presumably similar random-coil secondary structure led to the observation that poly-*N*meg peptoids caused a higher degree of electrophoretic friction, *i.e.*, drag, per monomer unit than protein polymers. The reason for this increase likely related to the beneficial properties of poly-*N*meg drag-tags, most notably the abundant, highly water-soluble PEG-like *N*meg side chain chemistry. By replacing the methyl ester group of *N*meg with a “free” hydroxyl group, the hydrophilicity of the side-chain would be incrementally increased without introducing charge. An excess of cationic charge on drag-tags is known to have potentially negative effects, including non-specific adsorptive interactions with the capillary wall. Inclusion of hydroxyl groups in the sequences instead would allow participation in hydrogen bonding in aqueous buffer without these negative interactions.

Depending on how η or “drag” scales with molecular weight for a drag-tag containing hydroxy-terminated *N*-substituted side chains, this work could potentially result in more efficient sequencing *via* improved drag-tag sequence design, and would

also be of interest to theoretical physicists that study fundamental aspects of ELFSE separations.

6.1.2 Hydroxy side chain design and synthesis

A new peptoid submonomer was designed and influenced by feasibility, *i.e.*, the commercial availability of chemicals and ease of synthesis. The peptoid submonomer was designed as a PEG-like side chain that, when cleaved from the solid support, would reveal a terminal hydroxyl group at each side chain end. Therefore, 2-(2-aminoethoxy)ethanol (Compound **1**, see Scheme 1) was purchased from Sigma Aldrich (Milwaukee, WI) at a modest price, on the same order as the *N*meg submonomer, 2-methoxyethylamine, or *N*-(methoxyethyl)glycine. The hydroxyl group would feasibly interfere with the synthetic steps for peptoid synthesis *via* the submonomer method, and a protecting group for the hydroxyl moiety was researched and evaluated.

From the literature, it was found that tert-butyl dimethyl silyl (TBS) would be a good candidate for a protecting group, as it is easily cleaved using strong acid and can be removed efficiently from Rink amide solid-phase resin. The hydrophobic portion of this protecting group would also facilitate purification as the desired product could be isolated into organic solvent, thereby easily removing other reagents present in the reaction mixture. The chemical used to generate a TBS-protected hydroxyl group was tert-butyldimethylsilyl chloride (TBDMSCl) (Compound **2**).

Following literature procedures, the desired submonomer was synthesized and isolated in 82% yield (Scheme 1). To a flame-dried 100mL round bottom flask 2-(2-aminoethoxy)ethanol (1.8 mL, 16.6 mmol), tert-butyldimethylsilyl chloride (2.74 g, 18.2

mmol), and triethylamine (1.31 mL, 18.2 mmol) were dissolved in CH_2Cl_2 (50 mL) and 4-dimethylaminopyridine (DMAP) was added (cat.). The reaction mixture was then allowed to stir for 18 h. The solution was then diluted with water (50 mL), and the organic layer was washed with water (25 mL) and brine (25 mL). The organic layer was subsequently dried (MgSO_4) and concentrated. The TBS-protected 2-(2-aminoethoxy)ethanol was used as a peptoid submonomer for peptoid synthesis on the Applied Biosystems 433A automated peptide synthesizer without need for further purification. Standard peptoid synthesis conditions and methods were used as published previously [41, 65]. The cleaved peptoid was purified by RP-HPLC using a C18 column, and mass was confirmed with MALDI-TOF/MS. This molecule has yet to be conjugated to a DNA primer and evaluated as a drag-tag. The value of ζ that is obtained for this drag-tag will provide interesting information concerning the scaling of ζ in terms of how chemical composition, specifically that of the side chain, and hydrophobicity affects drag.

Scheme 6.1. Synthesis of 22-mer polyN/meg/hydr oxy drag-tag using TBS-protected 2-(2-Aminoethoxy)ethanol as a peptoid submonomer.

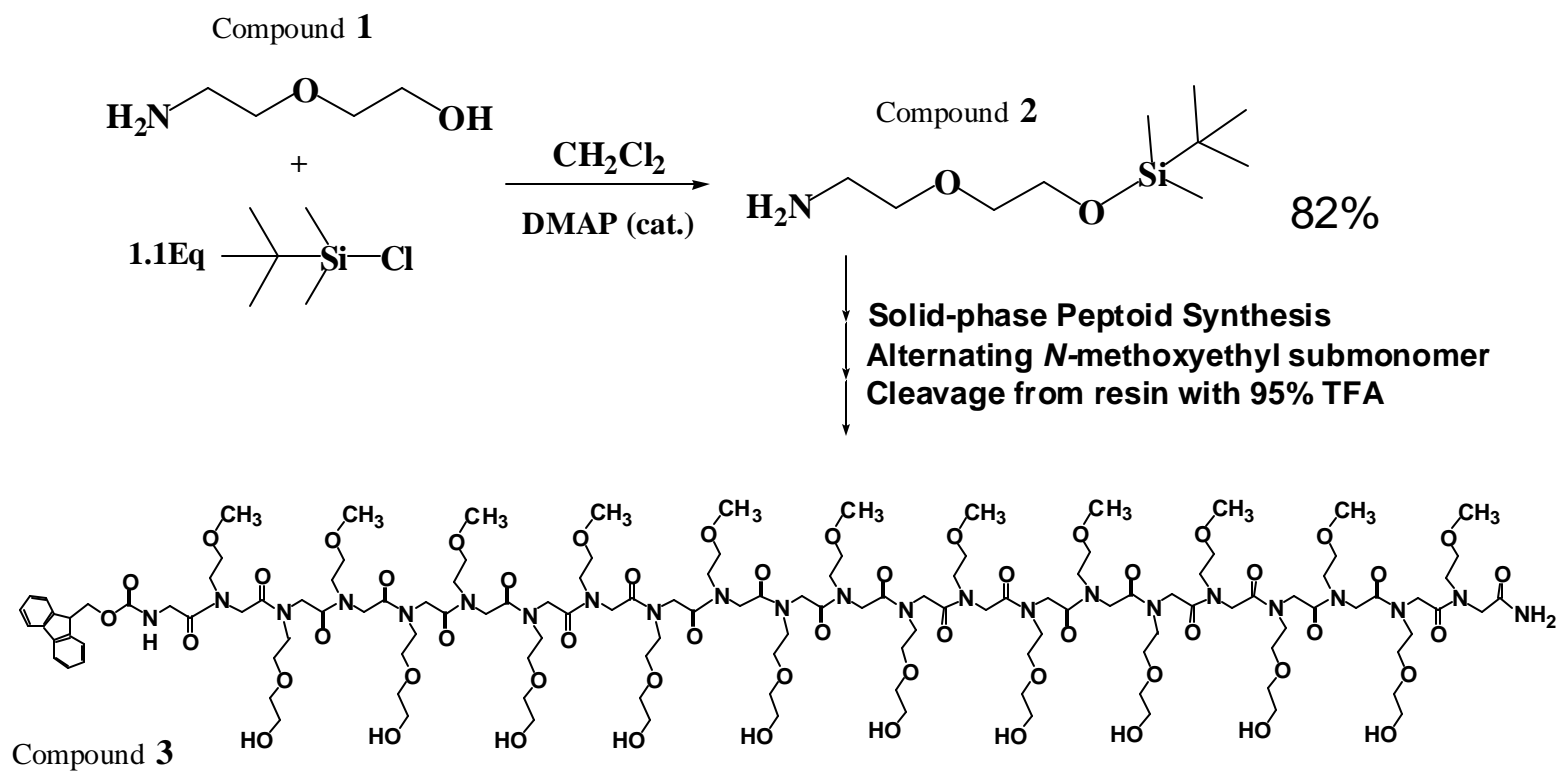
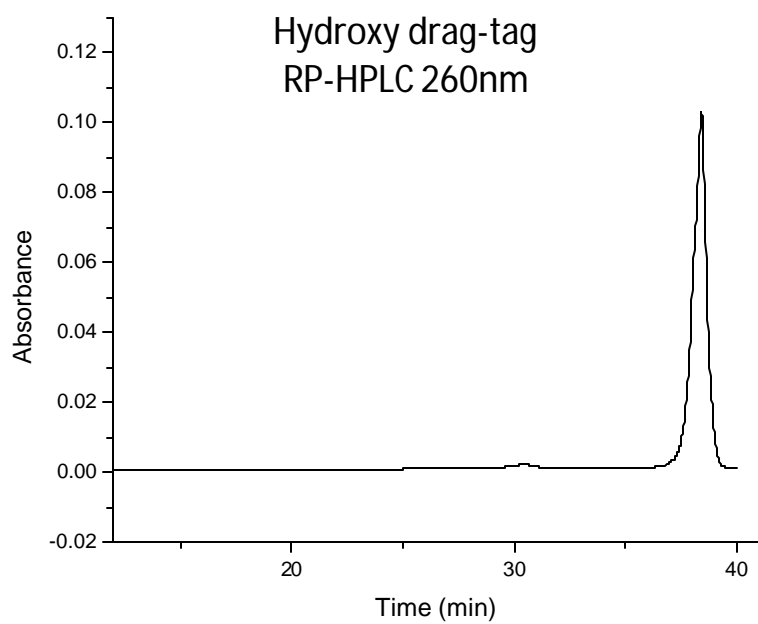
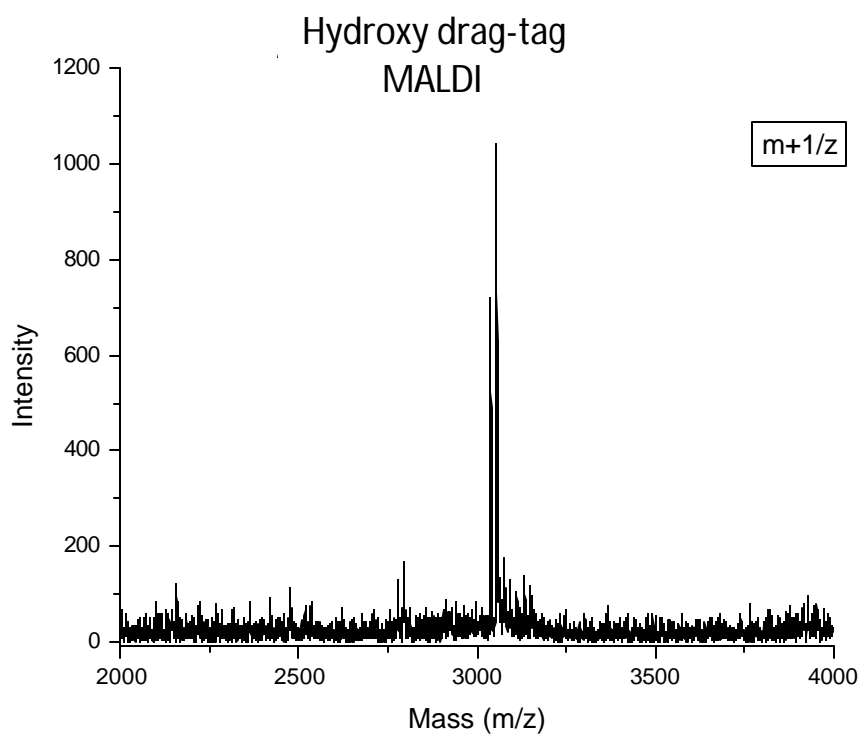


Figure 6.1 MALDI-TOF/MS and analytical RP-HPLC trace of Compound 3.

6.2 Positively-charged drag-tags

6.2.1 Rationale for including charge in drag-tag design

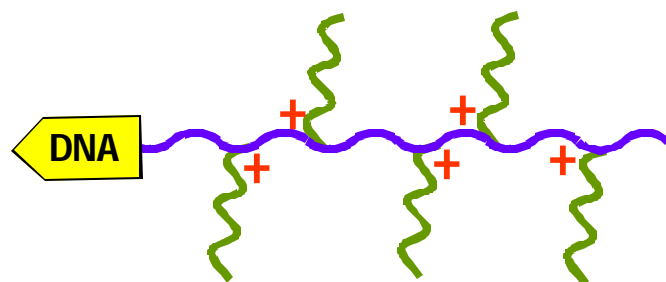
Professor Gary Slater is one of the pioneers in ELFSE research, having presented the first example of ELFSE DNA sequencing, together with his coworker, Ren [48]. During a research meeting with the Slater and Barron groups, Professor Slater suggested the possibility of including positive charges in a drag-tag while simultaneously using sequence design to minimize potential negative effects in the resulting molecule. This suggestion stemmed from recent work in the Barron laboratory that involved the use of a protein polymer drag-tag which serendipitously ended up possessing a positively charged Arg group [96]. This occurred during the use of a technique called “controlled cloning” [84], wherein an artificial gene was created that encoded for a repetitive protein polymer with the sequence (GAGTGSA)₁₈G. This sequence became (GAGTGSA)₄-GAGTGRA-(GAGTGSA)₇-GAGTGRA-(GAGTGSA)₅-G after an unexpected mutation arose in the *E. coli* cell line used for expression of the protein polymer. The mutation, which was discovered by DNA sequencing of the insert, yielded a drag-tag with a net charge of +1 following conjugation to DNA at the *N*-terminus.

With this result in mind, an idea burgeoned to place cationic charges near the junction between the backbone and the branches of these poly*N*meg structures. The intent was to sterically shield the positive charges with the branches, and hence prevent unwanted interactions with the capillary inner surfaces. The overall hypothesis was that judicious placement of charge in a poly*N*meg peptoid drag-tag would allow us to garner a significant increase in drag (?) without the adverse effects normally associated with the inclusion of charged species in drag-tags.

6.2.2 Drag-tag synthesis and preliminary results

The basic design premise is illustrated in Figure 2. Expanding on the aforementioned idea, a suitable “branch” molecule (Compound 4) was designed and is presented in Figure 3. This conjugate design would possess a total of five positively charged side chains along the branch, each positioned close to the attachment point of the scaffold backbone. Standard peptoid synthesis conditions and methods were used as published previously [41, 65].

Figure 6.2. Schematic representation of 30-mer drag-tag design with five octamer branches containing positive charges near to the branching junction on the peptoid scaffold backbone.



However, an unforeseen problem arose concerning the integrity of one of the reagents used in the synthesis of **4**. Poor quality acetic anhydride was unknowingly used in the final step in the synthesis, and the routine “capping” at the *N*-terminus with an acetyl group was therefore not achieved in complete yield. Instead, both the desired product and an additional product with two free-amine groups instead of one were isolated after preparative RP-HPLC. The two cleaved peptoids were purified by RP-HPLC using a C18 column, and mass was confirmed with MALDI-TOF/MS.

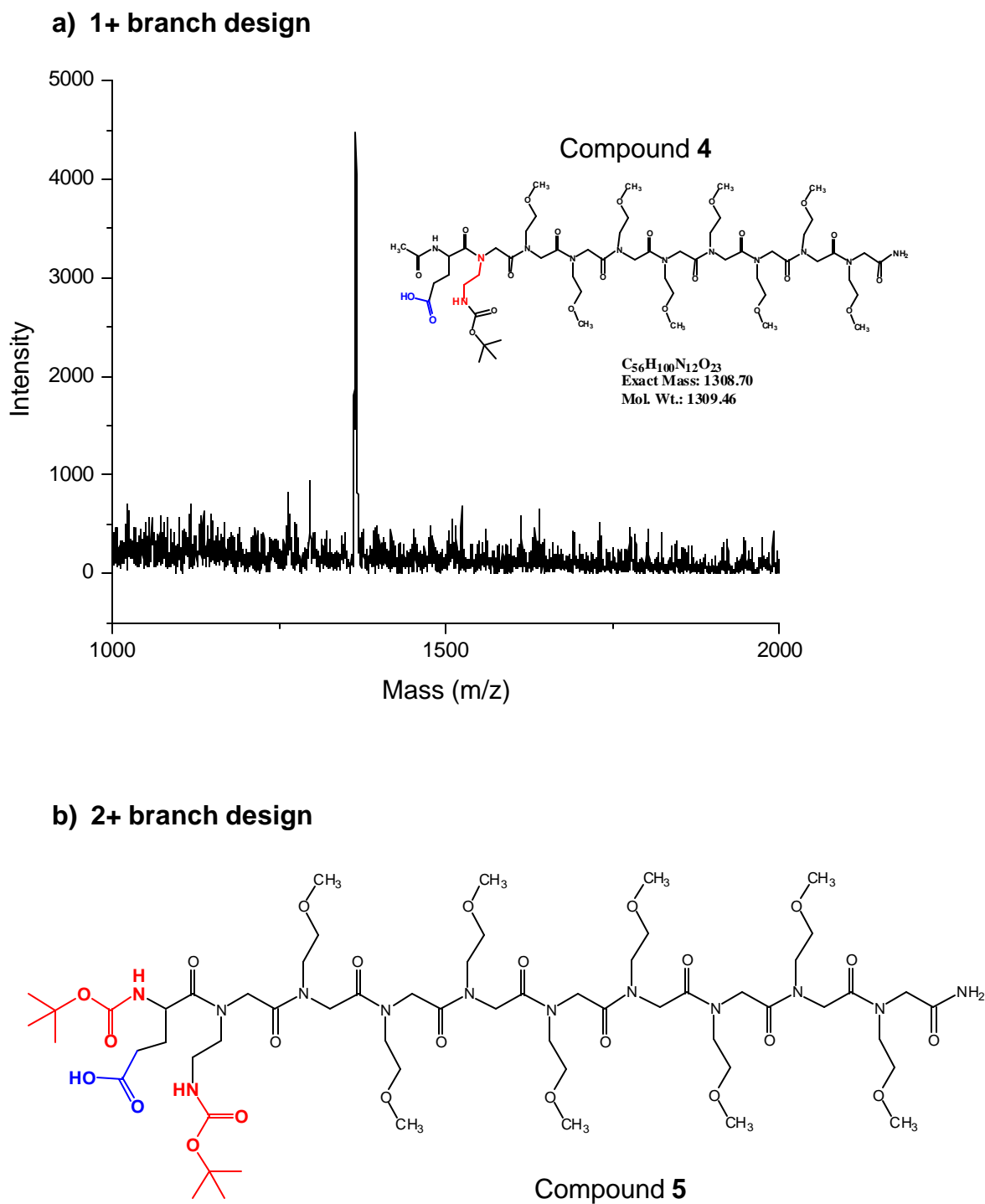
These molecules were then Boc-protected, followed by an additional preparative HPLC purification, resulting in the isolation of compounds **4** and **5** (Figure 3). Having obtained sufficient quantities of both **4** and **5** at this stage, a grafting reaction was performed using established techniques from previous work [41]. The peptoid scaffold backbone used was of the same design as that in the cited study, with five amino groups for attachment to carboxylate-containing branches. Scheme 2 shows the reagents and protocol used for the grafting reaction of the two branches (compounds **4** and **5**) to the backbone, and Figure 4 presents the desired molecules (**6** and **7**) that were isolated and mass confirmed by MALDI-TOF/MS.

Compounds **6** and **7** were then reacted with sulfo-SMCC and re-purified by RP-HPLC. These molecules were then conjugated to 20- and 30-base 5' thiolated DNA primers, followed by free solution electrophoresis analysis using an ABI Prism 3100 instrument with a 36-cm long capillary array (55 mm i.d. capillaries) at 55 °C.

The resulting CE data showed inconclusive results, but it appeared as though the high positive charge density of the drag-tags was associating with the DNA primers. It was proposed that the drag-tag was effectively “condensing” DNA, thereby eliminating

any possibility of evaluating the electrophoretic drag for such a positively charged species. This study showed that future designs for positively charged drag-tags must take into account the possibility for destructive charge interactions with the negatively charged, conjugated DNA.

Figure 6.3 a) Compound 4 is a positively charged octamer “branch.” The design included a Boc-protected short ethylamino group (in red) and was acetylated at the *N*-terminus. The terminal glutamic acid residue had an unprotected carboxylate group (in blue) that served as the peptide bond-forming functionality. b) Compound 5 represents the molecule that was actually isolated due to poor quality acetic anhydride that was used in the penultimate synthesis step prior to cleavage from the solid-phase resin.



Scheme 6.2. Synthesis of a 5+ and 10+ branched drag-tag following literature grafting procedures.

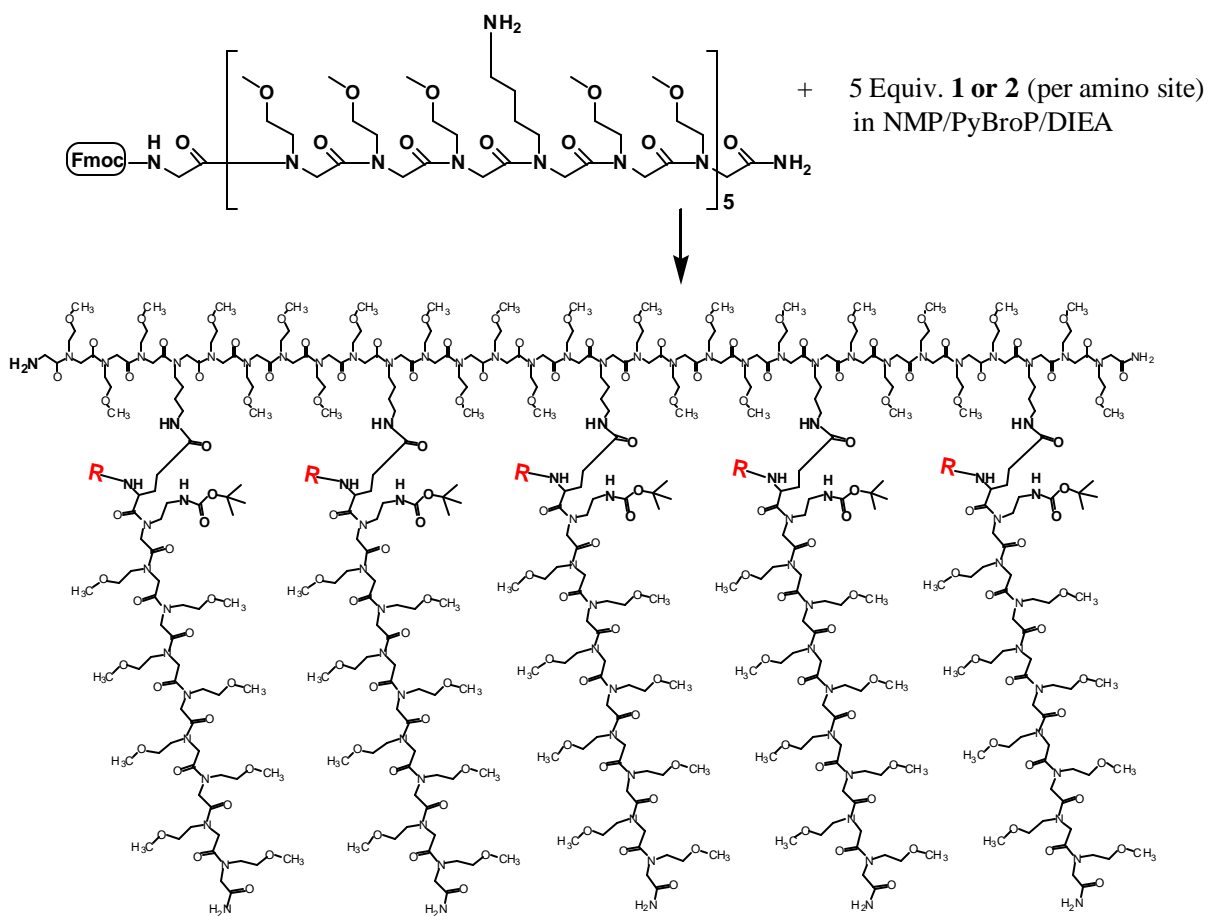
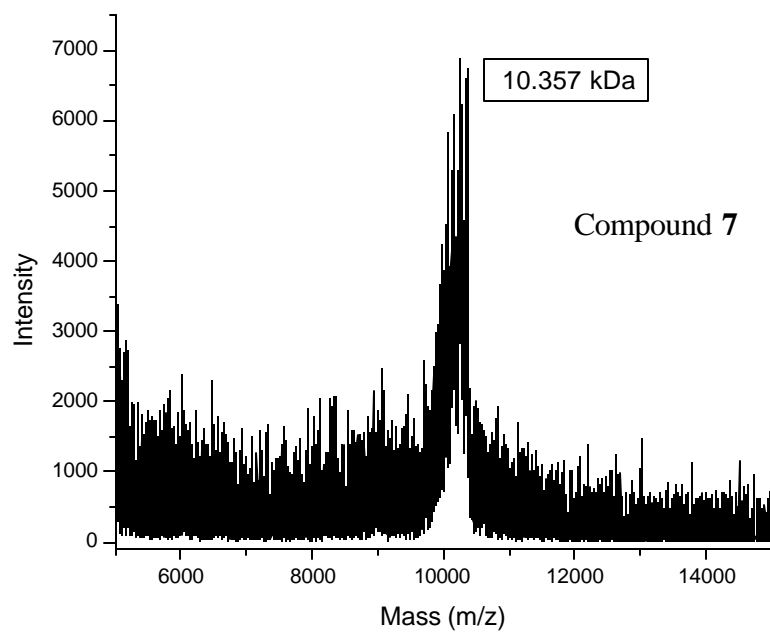
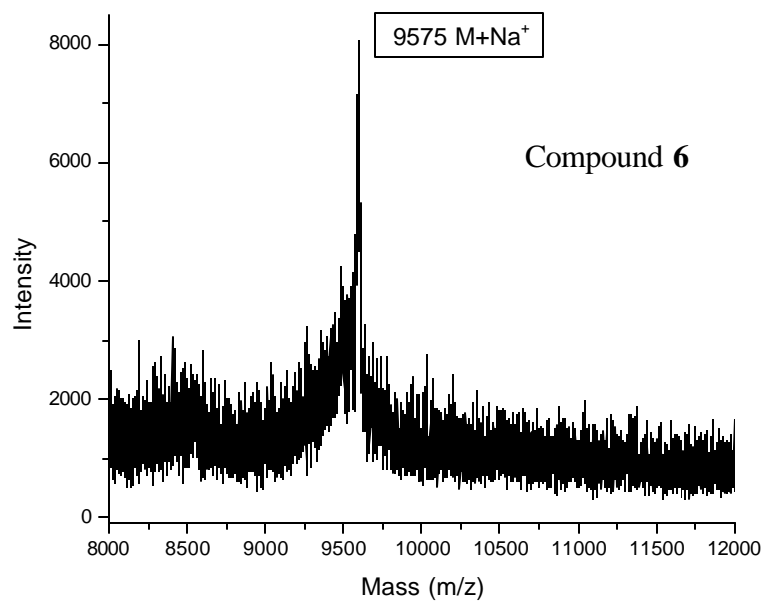


Figure 6.4 MALDI-TOF/MS spectra of Compounds 5 and 6. The trifluoroacetic acid in the MALDI matrix solution resulted in varying degrees of the acid-labile Boc-protecting group deprotection.



6.3 Larger drag-tag designs

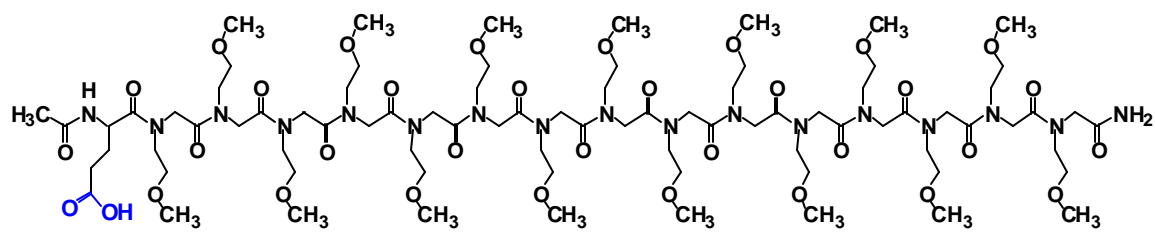
6.3.1 Doubling the size of the octamer-branched drag-tag

Previous work with branched peptoid scaffolds has shown that electrophoretic drag, or ζ , scaled somewhat linearly with molecular weight for these polyNmeg drag-tags [41]. The largest of this class of molecules was a 30-mer polyNmeg peptoid with five branching points, to which octamer polyNmeg arms were appended. This yielded a total molecular mass of ~ 11 kDa, with 70 monomers in length. Since that study, a new scaffold, discussed in Chapter 5, has been synthesized, comprising eight branching points. Results have now shown that, despite the relatively dense spacing needed to fit this number of reactive sites along the backbone of the scaffold, it was still possible to achieve complete derivatization using relatively large and bulky appendages like DOTA-like gadolinium(III) chelators.

Due to the successful synthesis and application of large peptoid scaffolds with densely spaced branching sites for the MRI contrast agent study, it was suggested that we attach up to eight 15mer polyNmeg branches, longer than the current octamer branches previously used, in hopes of attaining both high molecular weight and increased drag. As discussed at length in the branched drag-tag article from *Bioconjugate Chemistry* (Chapter 2), ζ (drag) was shown to scale linearly with increasing molecular mass. It would therefore be of interest to determine if this result continued to hold true when the mass was doubly increased. By appending eight 15-mer polyNmeg branches onto the 30-mer polyNmeg scaffold described in Chapter 5, a two-fold increase in molecular mass over the octamer-branched drag-tag (presented in Chapters 2-4) would be attained.

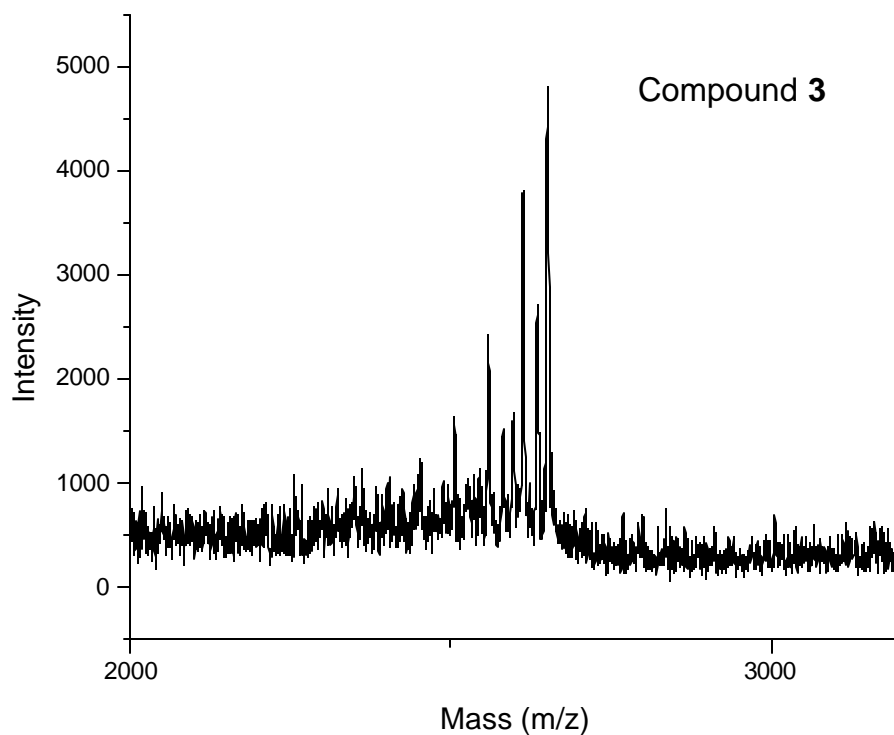
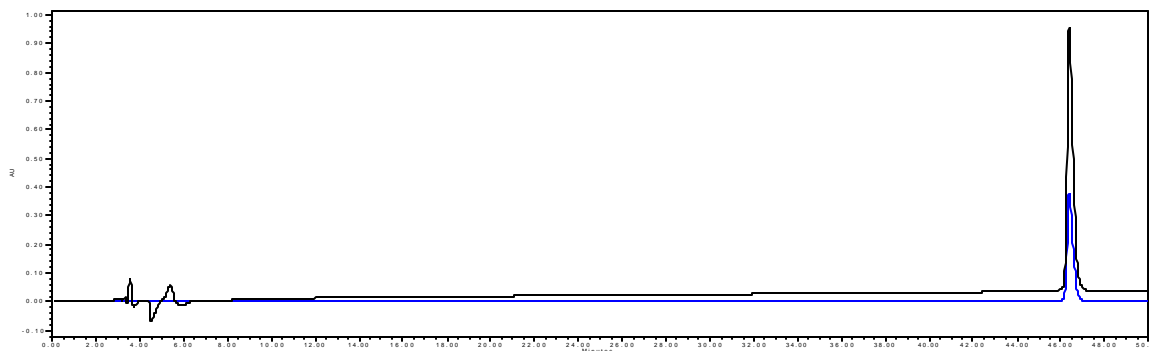
Figure 5 shows the drag-tag branch (Compound 7) designed for the attachment to the 8-site 30mer polyNmeg scaffold. Standard peptoid synthesis conditions and methods were used as published previously [41, 65]. The cleaved peptoid was purified by RP-HPLC using a C18 column, and mass was confirmed with MALDI-TOF/MS. Figure 6 shows the characterization of this branch molecule by RP-HPLC and MALDI-MS. Purification was completed on a Phenomenex Jupiter analytical (150 mm × 2 mm, 5 μm, 300 Å) C18 column, conditions: 5-40% Acetonitrile/water (0.1% TFA) over 50 minutes. So far, 300mg of this pure material has been amassed for further attachment to a 30mer polyNmeg scaffold.

Figure 6.5. Structure of 15mer polyNmeg “branch” for attachment to an 8-site 30mer scaffold.



Compound 7

Figure 6.6 Analytical RP-HPLC trace of 15mer polyNmeg “branch.” So far 300mg of this pure material has been amassed for further attachment to 30mer polyNmeg scaffold. Phenomenex Jupiter analytical (150 mm × 2 mm, 5 μm, 300 Å) C18 column, conditions: 5-40% Acetonitrile/water (0.1% TFA) over 50minutes. Black trace is 220nm absorbance and blue trace is 260nm.



References

1. Choi, S.-k. (2004). *Synthetic multivalent molecules : concepts and biomedical applications* (Hoboken, N.J.: Wiley).
2. Gellman, S.H. (1998). Foldamers: A manifesto. *Accounts of Chemical Research* 31, 173-180.
3. Patch, J.A., and Barron, A.E. (2002). Mimicry of bioactive peptides via non-natural, sequence-specific peptidomimetic oligomers. *Current Opinion in Chemical Biology* 6, 872-877.
4. Stigers, K.D., Soth, M.J., and Nowick, J.S. (1999). Designed molecules that fold to mimic protein secondary structures. *Current Opinion in Chemical Biology* 3, 714-723.
5. Burkoth, T.S., Beausoleil, E., Kaur, S., Tang, D.Z., Cohen, F.E., and Zuckermann, R.N. (2002). Toward the synthesis of artificial proteins: The discovery of an amphiphilic helical peptoid assembly. *Chemistry & Biology* 9, 647-654.
6. Haag, R., and Kratz, F. (2006). *Polymer therapeutics: Concepts and applications*. *Angewandte Chemie-International Edition* 45, 1198-1215.
7. Barron, A.E., and Zuckermann, R.N. (1999). Bioinspired polymeric materials: in-between proteins and plastics. *Current Opinion in Chemical Biology* 3, 681-687.
8. Kirshenbaum, K., Zuckermann, R.N., and Dill, K.A. (1999). Designing polymers that mimic biomolecules. *Current Opinion in Structural Biology* 9.
9. Kirshenbaum, K., Barron, A.E., Goldsmith, R.A., Armand, P., Bradley, E.K., Truong, K.T.V., Dill, K.A., Cohen, F.E., and Zuckermann, R.N. (1998). Sequence-specific polypeptoids: A diverse family of heteropolymers with stable secondary structure. *Proceedings of the National Academy of Sciences of the United States of America* 95, 4303-4308.
10. Simon, R.J., Kania, R.S., Zuckermann, R.N., Huebner, V.D., Jewell, D.A., Banville, S., Ng, S., Wang, L., Rosenberg, S., Marlowe, C.K., Spellmeyer, D.C., Tan, R.Y., Frankel, A.D., Santi, D.V., Cohen, F.E., and Bartlett, P.A. (1992). Peptoids - a Modular Approach to Drug Discovery. *Proceedings of the National Academy of Sciences of the United States of America* 89, 9367-9371.

11. Patch, J.A., Zuckermann, R.N., and Barron, A.E. (2004). Structure-activity relationships in magainin-mimetic antibacterial peptoids. *Biophysical Journal* *86*, 309A-309A.
12. Zuckermann, R.N., Kerr, J.M., Kent, S.B.H., and Moos, W.H. (1992). Efficient Method for the Preparation of Peptoids Oligo(N-Substituted Glycines) by Submonomer Solid-Phase Synthesis. *Journal of the American Chemical Society* *114*, 10646-10647.
13. Patch, J.A., and Barron, A.E. (2003). Helical peptoid mimics of magainin-2 amide. *Journal of the American Chemical Society* *125*, 12092-12093.
14. Seurnynck, S.L., Patch, J.A., and Barron, A.E. (2005). Simple, helical peptoid analogs of lung surfactant protein B. *Chemistry & Biology* *12*, 77-88.
15. Wu, C.W., Kirshenbaum, K., Sanborn, T.J., Patch, J.A., Huang, K., Dill, K.A., Zuckermann, R.N., and Barron, A.E. (2003). Structural and spectroscopic studies of peptoid oligomers with alpha-chiral aliphatic side chains. *Journal of the American Chemical Society* *125*, 13525-13530.
16. Soth, M.J., and Nowick, J.S. (1997). Unnatural oligomers and unnatural oligomer libraries. *Current Opinion in Chemical Biology* *1*, 120-129.
17. Murphy, J.E., Uno, T., Hamer, J.D., Cohen, F.E., Dwarki, V., and Zuckermann, R.N. (1998). A combinatorial approach to the discovery of efficient cationic peptoid reagents for gene delivery. *Proceedings of the National Academy of Sciences of the United States of America* *95*, 1517-1522.
18. Kruijtzter, J.A.W., Hofmeyer, L.J.F., Heerma, W., Versluis, C., and Liskamp, R.M.J. (1998). Solid-phase syntheses of peptoids using Fmoc-protected N-substituted glycines: the synthesis of (retro)peptoids of leu-enkephalin and substance P. *Chemistry--A European Journal* *4*, 1570-1580.
19. Merrifield, B. (1986). Solid-Phase Synthesis. *Science* *232*, 341-347.
20. Merrifield, R.B. (1963). Solid Phase Peptide Synthesis. I. The Synthesis of a Tetrapeptide. *Journal of the American Chemical Society* *85*, 2149-2154.
21. Simon, R.J., Kania, R.S., Zuckermann, R.N., Huebner, V.D., Jewell, D.A., Banville, S., Ng, S., Wang, L., Rosenberg, S., and et al. (1992). Peptoids: a modular approach to drug discovery. *Proceedings of the National Academy of Sciences of the United States of America* *89*, 9367-9371.
22. Armand, P., Kirshenbaum, K., Goldsmith, R.A., Farr-Jones, S., Barron, A.E., Truong, K.T.V., Dill, K.A., Mierke, D.F., Cohen, F.E., Zuckermann, R.N., and Bradley, E.K. (1998). NMR determination of the major solution conformation of

a peptoid pentamer with chiral side chains. *Proceedings of the National Academy of Sciences of the United States of America* *95*, 4309-4314.

23. Noolandi, J. (1992). A New Concept for Sequencing DNA by Capillary Electrophoresis. *Electrophoresis* *13*, 394-395.
24. Sanger, F., Nicklen, S., and Coulson, A.R. (1977). DNA Sequencing with Chain-Terminating Inhibitors. *Proceedings of the National Academy of Sciences of the United States of America* *74*, 5463-5467.
25. Mayer, P., Slater, G.W., and Drouin, G. (1994). Theory of DNA-Sequencing Using Free-Solution Electrophoresis of Protein-DNA Complexes. *Analytical Chemistry* *66*, 1777-1780.
26. Long, D., Dobrynin, A.V., Rubinstein, M., and Ajdari, A. (1998). Electrophoresis of polyampholytes. *Journal of Chemical Physics* *108*, 1234-1244.
27. Saariaho, M., Subbotin, A., Ikkala, O., and ten Brinke, G. (2000). Comb copolymer cylindrical brushes containing semiflexible side chains: a Monte Carlo study. *Macromolecular Rapid Communications* *21*, 110-115.
28. Saariaho, M., Subbotin, A., Szleifer, I., Ikkala, O., and ten Brinke, G. (1999). Effect of side chain rigidity on the elasticity of comb copolymer cylindrical brushes: A Monte Carlo simulation study. *Macromolecules* *32*, 4439-4443.
29. Bowtell, R.W., Peters, A., Sharp, J.C., Mansfield, P., Hsu, E.W., Aiken, N., Horsman, A., and Blackband, S.J. (1995). NMR microscopy of single neurons using spin-echo and line narrowed 2D FT imaging. *Magnetic Resonance in Medicine* *33*, 790-794.
30. Kayyem, J.F., Kumar, R.M., Fraser, S.E., and Meade, T.J. (1995). Receptor-targeted cotransport of DNA and magnetic-resonance contrast agents. *Chemistry & Biology* *2*, 615-620.
31. Moats, R.A., Fraser, S.E., and Meade, T.J. (1997). A "smart" magnetic resonance imaging agent that reports on specific enzymatic activity. *Angewandte Chemie-International Edition in English* *36*, 726-728.
32. Edelman, R.R., Hesselink, J.R., and Zlatkin, M.B. (1996). *MRI : clinical magnetic resonance imaging*, 2nd Edition (Philadelphia: Saunders).
33. Caravan, P., Ellison, J.J., McMurry, T.J., and Lauffer, R.B. (1999). Gadolinium(III) chelates as MRI contrast agents: Structure, dynamics, and applications. *Chemical Reviews* *99*, 2293-2352.

34. Gries, H. (2002). Extracellular MRI contrast agents based on gadolinium. In *Contrast Agents I*, Volume 221. pp. 1-24.
35. Weinmann, H.J., Ebert, W., Misselwitz, B., and Schmitt-Willich, H. (2003). Tissue-specific MR contrast agents. *European Journal of Radiology* 46, 33-44.
36. Weissleder, R., and Mahmood, U. (2001). Molecular imaging. *Radiology* 219, 316-333.
37. Lauffer, R.B. (1987). Paramagnetic metal-complexes as water proton relaxation agents for NMR imaging - theory and design. *Chemical Reviews* 87, 901-927.
38. Artemov, D., Bhujwala, Z.M., and Bulte, J.W.M. (2004). Magnetic resonance imaging of cell surface receptors using targeted contrast agents. *Current Pharmaceutical Biotechnology* 5, 485-494.
39. Olivera, B.M., Baine, P., and Davidson, N. (1964). Electrophoresis of the Nucleic Acids. *Biopolymers* 2, 245-257.
40. Grossman, P.D.F., S.; Menchen, S. M.; Woo, S. L.; Winn-Deen, E. S. (1993). Distinguishing different polynucleotide(s) in non-sieving medium - useful in DNA sequencing and target detection in sample, World Patent.
41. Haynes, R.D., Meagher, R.J., Won, J.I., Bogdan, F.M., and Barron, A.E. (2005). Comblike, monodisperse polypeptoid drag-tags for DNA separations by end-labeled free-solution electrophoresis (ELFSE). *Bioconjugate Chemistry* 16, 929-938.
42. McCormick, L.C., Slater, G.W., Karger, A.E., Vreeland, W.N., Barron, A.E., Desruisseaux, C., and Drouin, G. (2001). Capillary electrophoretic separation of uncharged polymers using polyelectrolyte engines - Theoretical model. *Journal of Chromatography A* 924, 43-52.
43. Volkel, A.R., and Noolandi, J. (1995). Mobilities of Labeled and Unlabeled Single-Stranded-DNA in Free Solution Electrophoresis. *Macromolecules* 28, 8182-8189.
44. Heller, C., Slater, G.W., Mayer, P., Dovichi, N., Pinto, D., Viovy, J.L., and Drouin, G. (1998). Free-solution electrophoresis of DNA. *Journal of Chromatography A* 806, 113-121.
45. Sundberg, S., Kopf-Sill, A., Nagle, R., Gallagher, S., Chow, C., Wada, G., Nikiforov, T., and Parce, J.W. (1998). Laboratory on a chip: A new experimentation format. *American Laboratory* 30, 22.

46. Desruisseaux, C., Drouin, G., and Slater, G.W. (2001). Electrophoresis of composite molecular objects. 2. Competition between sieving and frictional effects in polymer solutions. *Macromolecules* 34, 5280-5286.
47. Won, J.I., Meagher, R.J., and Barron, A.E. (2004). Characterization of glutamine deamidation in a long, repetitive protein polymer via bioconjugate capillary electrophoresis. *Biomacromolecules* 5, 618-627.
48. Ren, H., Karger, A.E., Oaks, F., Menchen, S., Slater, G.W., and Drouin, G. (1999). Separating DNA sequencing fragments without a sieving matrix. *Electrophoresis* 20, 2501-2509.
49. Hendrickson, W.A., Pahler, A., Smith, J.L., Satow, Y., Merritt, E.A., and Phizackerley, R.P. (1989). Crystal-Structure of Core Streptavidin Determined from Multiwavelength Anomalous Diffraction of Synchrotron Radiation. *Proceedings of the National Academy of Sciences of the United States of America* 86, 2190-2194.
50. Buckland, R.M. (1986). Strong Signals from Streptavidin Biotin. *Nature* 320, 557-558.
51. Kramer, R.H., and Karpen, J.W. (1998). Spanning binding sites on allosteric proteins with polymer-linked ligand dimers. *Nature* 395, 710-713.
52. Burkoth, T.S., Fafarman, A.T., Charych, D.H., Connolly, M.D., and Zuckermann, R.N. (2003). Incorporation of unprotected heterocyclic side chains into peptoid oligomers via solid-phase submonomer synthesis. *Journal of the American Chemical Society* 125, 8841-8845.
53. Uno, T., Beausoleil, E., Goldsmith, R.A., Levine, B.H., and Zuckermann, R.N. (1999). New submonomers for poly N-substituted glycines (peptoids). *Tetrahedron Letters* 40, 1475-1478.
54. Vreeland, W.N., Meagher, R.J., and Barron, A.E. (2002). Multiplexed, high-throughput genotyping by single-base extension and end-labeled free-solution electrophoresis. *Analytical Chemistry* 74, 4328-4333.
55. Krapcho, A.P., and Kuell, C.S. (1990). Mono-Protected Diamines - N-Tert-Butoxycarbonyl-Alpha,Omega-Alkanediamines from Alpha,Omega-Alkanediamines. *Synthetic Communications* 20, 2559-2564.
56. Helms, B.M., J. L.; Hawker, C.J.; Frechet, M.J. (2004). Dendronized Linear Polymers via "Click Chemistry". *Journal of the American Chemical Society*.
57. Bogdan, F.M. (Unpublished results).

58. Ostuni, E., Chapman, R.G., Holmlin, R.E., Takayama, S., and Whitesides, G.M. (2001). A survey of structure-property relationships of surfaces that resist the adsorption of protein. *Langmuir* *17*, 5605-5620.
59. Carpino, L.A. (1993). 1-Hydroxy-7-Azabenzotriazole - an Efficient Peptide Coupling Additive. *Journal of the American Chemical Society* *115*, 4397-4398.
60. Frerot, E., Coste, J., Pantaloni, A., Dufour, M.N., and Jouin, P. (1991). Pybop and Pybrop - 2 Reagents for the Difficult Coupling of the Alpha,Alpha-Dialkyl Amino-Acid, *Aib. Tetrahedron* *47*, 259-270.
61. Dourtoglou, V., Ziegler, J.C., and Gross, B. (1978). Hexafluorophosphate of O-Benzotriazole-N, N-Tetramethurea - New and Effective Reagent of Coupling Peptide. *Tetrahedron Letters*, 1269-1272.
62. Tyagarajan, K., Pretzer, E., and Wiktorowicz, J.E. (2003). Thiol-reactive dyes for fluorescence labeling of proteomic samples. *Electrophoresis* *24*, 2348-2358.
63. Shafer, D.E., Inman, J.K., and Lees, A. (2000). Reaction of tris(2-carboxyethyl)phosphine (TCEP) with maleimide and alpha-haloacyl groups: Anomalous elution of TCEP by gel filtration. *Analytical Biochemistry* *282*, 161-164.
64. Getz, E.B., Xiao, M., Chakrabarty, T., Cooke, R., and Selvin, P.R. (1999). A comparison between the sulfhydryl reductants tris(2-carboxyethyl)phosphine and dithiothreitol for use in protein biochemistry. *Analytical Biochemistry* *273*, 73-80.
65. Meagher, R.J., Coyne, J.A., Hestekin, C.N., Chiesl, T.N., Haynes, R.D., Won, J.I., and Barron, A.E. (2007). Multiplexed p53 mutation detection by free-solution conjugate microchannel electrophoresis with polyamide drag-tags. *Analytical Chemistry* *79*, 1848-1854.
66. Meagher, R.J., McCormick, L.C., Haynes, R.D., Won, J.I., Lin, J.S., Slater, G.W., and Barron, A.E. (2006). Free-solution electrophoresis of DNA modified with drag-tags at both ends. *Electrophoresis* *27*, 1702-1712.
67. McCormick, L.C., and Slater, G.W. (2005). The molecular end effect and its critical impact on the behavior of charged-uncharged polymer conjugates during free-solution electrophoresis. *Electrophoresis* *26*, 1659-1667.
68. Viovy, J.L. (2000). Electrophoresis of DNA and other polyelectrolytes: Physical mechanisms. *Reviews of Modern Physics* *72*, 813-872.
69. Slater, G.W., Kenward, M., McCormick, L.C., and Gauthier, M.G. (2003). The theory of DNA separation by capillary electrophoresis. *Current Opinion in Biotechnology* *14*, 58-64.

70. Meistermann, L., and Tinland, B. (1998). Band broadening in gel electrophoresis of DNA: Measurements of longitudinal and transverse dispersion coefficients. *Physical Review E* 58, 4801-4806.
71. Pluen, A., Tinland, B., Sturm, J., and Weill, G. (1998). Migration of single-stranded DNA in polyacrylamide gels during electrophoresis. *Electrophoresis* 19, 1548-1559.
72. Chiesl, T.N., Shi, W., and Barron, A.E. (2005). Poly(acrylamide-co-alkylacrylamides) for electrophoretic DNA purification in microchannels. *Analytical Chemistry* 77, 772-779.
73. Giordano, B.C., Ferrance, J., Swedberg, S., Huhmer, A.F.R., and Landers, J.P. (2001). Polymerase chain reaction in polymeric microchips: DNA amplification in less than 240 seconds. *Analytical Biochemistry* 291, 124-132.
74. Medintz, I.L., Paegel, B.M., and Mathies, R.A. (2001). Microfabricated capillary array electrophoresis DNA analysis systems. *Journal of Chromatography A* 924, 265-270.
75. Woolley, A.T., and Mathies, R.A. (1994). Ultra-high-speed DNA fragment separations using microfabricated capillary array electrophoresis chips. *Proceedings of the National Academy of Sciences of the United States of America* 91, 11348-11352.
76. Woolley, A.T., and Mathies, R.A. (1995). Ultra-high-speed DNA-sequencing using capillary electrophoresis chips. *Analytical Chemistry* 67, 3676-3680.
77. Slater, G.W., Desrulsseaux, C., Hubert, S.J., Mercier, J.F., Labrie, J., Boileau, J., Tessier, F., and Pepin, M.P. (2000). Theory of DNA electrophoresis: A look at some current challenges. *Electrophoresis* 21, 3873-3887.
78. Han, J., and Craighead, H.G. (2000). Separation of long DNA molecules in a microfabricated entropic trap array. *Science* 288, 1026-1029.
79. Han, J.Y., and Craighead, H.G. (2002). Characterization and optimization of an entropic trap for DNA separation. *Analytical Chemistry* 74, 394-401.
80. Barron, A.E., Soane, D.S., and Blanch, H.W. (1993). Capillary electrophoresis of DNA in uncross-linked polymer solutions. *Journal of Chromatography A* 652, 3-16.

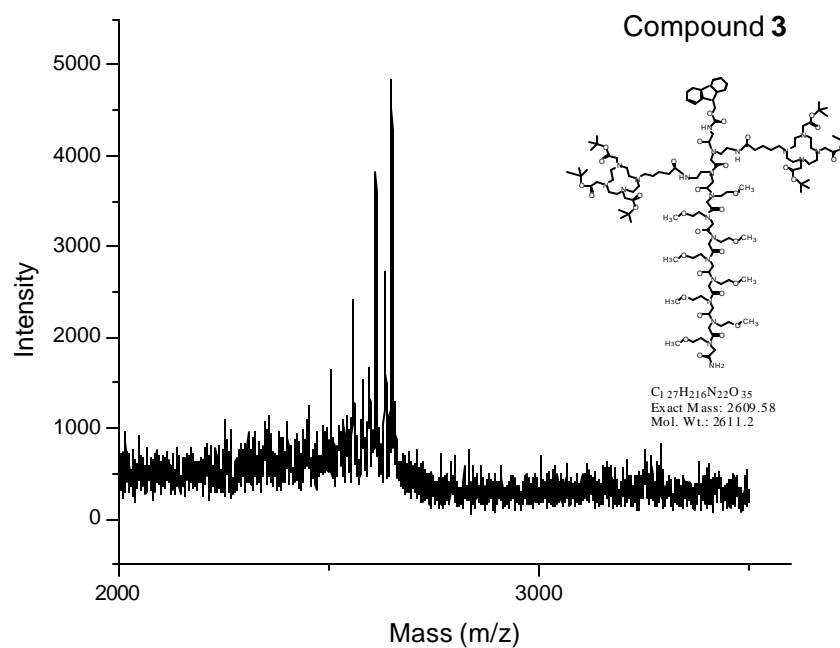
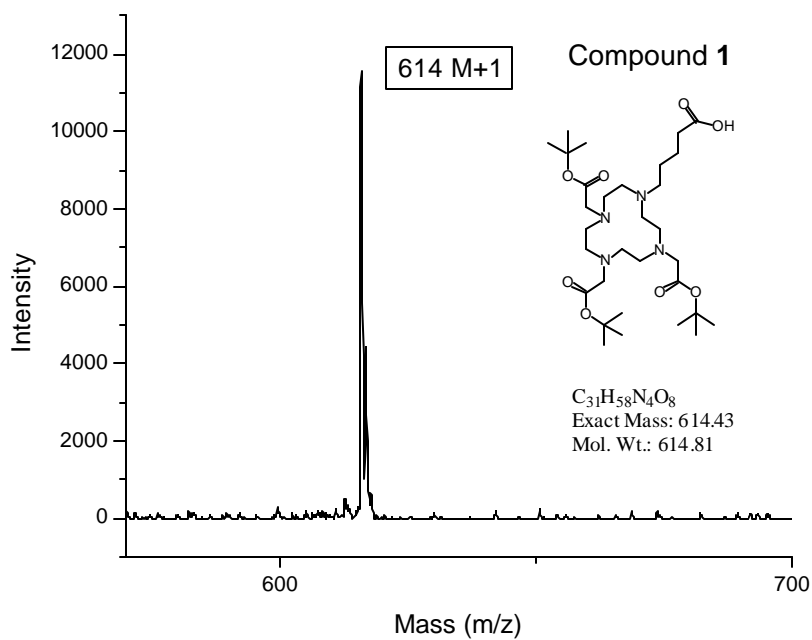
81. Chou, C.F., Austin, R.H., Bakajin, O., Tegenfeldt, J.O., Castelino, J.A., Chan, S.S., Cox, E.C., Craighead, H., Darnton, N., Duke, T., Han, J.Y., and Turner, S. (2000). Sorting biomolecules with microdevices. *Electrophoresis* 21, 81-90.
82. Volkmuth, W.D., and Austin, R.H. (1992). DNA electrophoresis in microlithographic arrays. *Nature* 358, 600-602.
83. Meagher, R.J., Won, J.I., McCormick, L.C., Nedelcu, S., Bertrand, M.M., Bertram, J.L., Drouin, G., Barron, A.E., and Slater, G.W. (2005). End-labeled free-solution electrophoresis of DNA. *Electrophoresis* 26, 331-350.
84. Won, J.I., and Barron, A.E. (2002). A new cloning method for the preparation of long repetitive polypeptides without a sequence requirement. *Macromolecules* 35, 8281-8287.
85. Won, J.I., Meagher, R.J., and Barron, A.E. (2005). Protein polymer drag-tags for DNA separations by end-labeled free-solution electrophoresis. *Electrophoresis* 26, 2138-2148.
86. Vreeland, W.N., and Barron, A.E. (2000). Free-solution capillary electrophoresis of polypeptoid-oligonucleotide conjugates. *Abstracts of Papers of the American Chemical Society* 219, U449-U449.
87. Vreeland, W.N., Slater, G.W., and Barron, A.E. (2002). Profiling solid-phase synthesis products by free-solution conjugate capillary electrophoresis. *Bioconjugate Chemistry* 13, 663-670.
88. McCormick, L.C., and Slater, G.W. (2006). A theoretical study of the possible use of electroosmotic flow to extend the read length of DNA sequencing by end-labeled free solution electrophoresis. *Electrophoresis* 27, 1693-1701.
89. Vreeland, W.N., Desruisseaux, C., Karger, A.E., Drouin, G., Slater, G.W., and Barron, A.E. (2001). Molar mass profiling of synthetic polymers by free-solution capillary electrophoresis of DNA-polymer conjugates. *Analytical Chemistry* 73, 1795-1803.
90. Doherty, E.A.S., Berglund, K.D., Buchholz, B.A., Kourkine, I.V., Przybycien, T.M., Tilton, R.D., and Barron, A.E. (2002). Critical factors for high-performance physically adsorbed (dynamic) polymeric wall coatings for capillary electrophoresis of DNA. *Electrophoresis* 23, 2766-2776.
91. Liolios, K., Mavromatis, K., Tavernarakis, N., and Kyrpides, N.C. (2008). The Genomes On Line Database (GOLD) in 2007: status of genomic and metagenomic projects and their associated metadata. *Nucleic Acids Research* 36, D475-D479.

92. Shendure, J., Mitra, R.D., Varma, C., and Church, G.M. (2004). Advanced sequencing technologies: Methods and goals. *Nature Reviews Genetics* 5, 335-344.
93. Zhang, K., Martiny, A.C., Reppas, N.B., Barry, K.W., Malek, J., Chisholm, S.W., and Church, G.M. (2006). Sequencing genomes from single cells by polymerase cloning. *Nature Biotechnology* 24, 680-686.
94. Fredlake, C.P., Hert, D.G., Kan, C.W., Chiesl, T.N., Root, B.E., Forster, R.E., and Barron, A.E. (2008). Ultrafast DNA sequencing on a microchip by a hybrid separation mechanism that gives 600 bases in 6.5 minutes. *Proceedings of the National Academy of Sciences of the United States of America* 105, 476-481.
95. Kan, C.W., Fredlake, C.P., Doherty, E.A.S., and Barron, A.E. (2004). DNA sequencing and genotyping in miniaturized electrophoresis systems. *Electrophoresis* 25, 3564-3588.
96. Meagher, R.J., Won, J.I., Coyne, J.A., Lin, J., and Barron, A.E. (2008). Sequencing of DNA by Free-Solution Capillary Electrophoresis Using a Genetically Engineered Protein Polymer Drag-Tag. *Anal. Chem.* 80, 2842-2848.
97. Long, D., and Ajdari, A. (1996). Electrophoretic mobility of composite objects in free solution: Application to DNA separation. *Electrophoresis* 17, 1161-1166.
98. Nedelcu, S., Meagher, R.J., Barron, A.E., and Slater, G.W. (2007). Electric and hydrodynamic stretching of DNA-polymer conjugates in free-solution electrophoresis. *Journal of Chemical Physics* 126.
99. Desruisseaux, C., Long, D., Drouin, G., and Slater, G.W. (2001). Electrophoresis of composite molecular objects. 1. Relation between friction, charge, and ionic strength in free solution. *Macromolecules* 34, 44-52.
100. Horn, T., Lee, B.C., Dill, K.A., and Zuckermann, R.N. (2004). Incorporation of chemoselective functionalities into peptoids via solid-phase submonomer synthesis. *Bioconjugate Chemistry* 15, 428-435.
101. Merbach, A.E., and Toth, E. (2001). *The Chemistry of Contrast Agents in Medical Magnetic Resonance Imaging*, John Wiley & Sons, Inc., West Sussex, England.
102. Alexander, V. (1995). Design and synthesis of macrocyclic ligands and their complex of lanthanides. *Chemical Reviews* 95, 273-342.

103. Jacques, V., Gilsoul, D., Comblin, V., and Desreux, J.F. (1997). Rigidified macrocyclic lanthanide chelates for magnetic resonance imaging. *Journal of Alloys and Compounds* 249, 173-177.
104. Kumar, K., and Tweedle, M.F. (1993). Macrocyclic Polyaminocarboxylate Complexes of Lanthanides as Magnetic-Resonance-Imaging Contrast Agents. *Pure and Applied Chemistry* 65, 515-520.
105. Sirlin, C.B., Vera, D.R., Corbeil, J.A., Caballero, M.B., Buxton, R.B., and Mattrey, R.F. (2004). Gadolinium-DTPA-dextran: A macromolecular MR blood pool contrast agent. *Academic Radiology* 11, 1361-1369.
106. Opsahl, L.R., Uzgiris, E.E., and Vera, D.R. (1995). Tumor imaging with a macromolecular paramagnetic contrast agent - gadopentate dimeglumine-polylysine. *Academic Radiology* 2, 762-767.
107. Langereis, S., de Lussanet, Q.G., van Genderen, M.H.P., Meijer, E.W., Beets-Tan, R.G.H., Griffioen, A.W., van Engelshoven, J.M.A., and Backes, W.H. (2006). Evaluation of Gd(III)DTPA-terminated poly(propylene imine) dendrimers as contrast agents for MR imaging. *Nmr in Biomedicine* 19, 133-141.
108. Anderson, E.A., Isaacman, S., Peabody, D.S., Wang, E.Y., Canary, J.W., and Kirshenbaum, K. (2006). Viral nanoparticles donning a paramagnetic coat: Conjugation of MRI contrast agents to the MS2 capsid. *Nano Letters* 6, 1160-1164.
109. Strijkers, G.J., Mulder, W.J.M., van Heeswijk, R.B., Frederik, P.M., Bomans, P., Magusin, P., and Nicolay, K. (2005). Relaxivity of liposomal paramagnetic MRI contrast agents. *Magnetic Resonance Materials in Physics Biology and Medicine* 18, 186-192.
110. Aime, S., Botta, M., Fasano, M., Marques, M.P.M., Geraldes, C., Pubanz, D., and Merbach, A.E. (1997). Conformational and coordination equilibria on DOTA complexes of lanthanide metal ions in aqueous solution studied by H-1-NMR spectroscopy. *Inorganic Chemistry* 36, 2059-2068.
111. Karfeld, L.S., Bull, S.R., Davis, N.E., Meade, T.J., and Barron, A.E. (2007). Use of a genetically engineered protein for the design of a multivalent MRI contrast agent. *Bioconjugate Chemistry* 18, 1697-1700.
112. Livramento, J.B., Toth, E., Sour, A., Borel, A., Merbach, A.E., and Ruloff, R. (2005). High relaxivity confined to a small molecular space: A metallostar-based, potential MRI contrast agent. *Angewandte Chemie-International Edition* 44, 1480-1484.

113. Mikawa, M., Kato, H., Okumura, M., Narazaki, M., Kanazawa, Y., Miwa, N., and Shinohara, H. (2001). Paramagnetic water-soluble metallofullerenes having the highest relaxivity for MRI contrast agents. *Bioconjugate Chemistry* 12, 510-514.
114. Kobayashi, H., and Brechbiel, M.W. (2004). Dendrimer-based nanosized MRI contrast agents. *Current Pharmaceutical Biotechnology* 5, 539-549.
115. Allen, M., Bulte, J.W.M., Liepold, L., Basu, G., Zywicke, H.A., Frank, J.A., Young, M., and Douglas, T. (2005). Paramagnetic viral nanoparticles as potential high-relaxivity magnetic resonance contrast agents. *Magnetic Resonance in Medicine* 54, 807-812.
116. Aime, S., Frullano, L., and Crich, S.G. (2002). Compartmentalization of a gadolinium complex in the apoferritin cavity: A route to obtain high relaxivity contrast agents for magnetic resonance imaging. *Angewandte Chemie-International Edition* 41, 1017.
117. Artemov, D., Mori, N., Okollie, B., and Bhujwala, Z.M. (2003). MR molecular imaging of the Her-2/neu receptor in breast cancer cells using targeted iron oxide nanoparticles. *Magnetic Resonance in Medicine* 49, 403-408.

Appendix A



Vita

Russell Dean Haynes was born in Winston-Salem, NC on January 5th, 1976, the son of Dean and Kathryn Haynes. After receiving his G.C.S.E.'s from Mossley Hollins High School in 1992, he attended Ashton Sixth Form College where he completed A levels in Chemistry, Geology, Physics and General Studies. Russell completed his Bachelor's of science degree in Chemistry in 1999 at Northeastern Illinois University, in Chicago, IL. After obtaining an undergraduate degree, Russell worked as a synthetic chemist at Great Lakes Fine Chemicals in Mount Prospect Illinois with Dr. Scott Laneman. In 2001, he entered the Chemistry Ph.D program at Northwestern University in Evanston, IL. Initially advised by Professor Daniel H. Appella, he earned a Master's degree in Organic Chemistry in May 2002. The thesis title was: "Design and Synthesis of Novel Conformationally Constrained Peptide Nucleic Acids (PNA) for Selective Binding to Complementary RNA." In June 2002 Russell joined Professor Annelise Barron's research group and has authored and co-authored the following publications:

Haynes, R. D., R. J. Meagher, et al. (2005). "Combllike, monodisperse polypeptoid drag-tags for DNA separations by end-labeled free-solution electrophoresis (ELFSE)." *Bioconjugate Chemistry* 16(4): 929-938;

Meagher, R. J., Coyne, J. A., Hestekin, C. N., Chiesl, T. N., **Haynes, R. D.,** Won, J. I., Barron, A. E. (2007). "Multiplexed p53 mutation detection by free-solution conjugate microchannel electrophoresis with polyamide drag-tags." *Analytical Chemistry* 79(5): 1848-1854.

Meagher, R. J., McCormick, L. C., **Haynes, R. D.,** Won, J. I., Lin, J. S., Slater, G. W., Barron, A. E. (2006). "Free-solution electrophoresis of DNA modified with drag-tags at both ends." *Electrophoresis* 27(9): 1702-1712.

Myers, M. C., Witschi, M. A., Larionova, N. V., Franck, J. M., **Haynes, R. D.** Hara, T., Grajkowski, A., Appella, D. H. (2003). "A cyclopentane conformational restraint for a peptide nucleic acid: Design, asymmetric synthesis, and improved binding affinity to DNA and RNA." *Organic Letters* 5(15): 2695-2698.

Statement of contribution of others

All capillary electrophoresis experiments that are presented in this work were completed by Dr. Robert J. Meagher and Jennifer A. Coyne. DO3A synthesis and relaxivity experiments presented in Chapter 5 were performed by Dr. Steve Bull.